UNIVERSITY OF CALIFORNIA SAN DIEGO

Zooglider reveals the importance of marine snow, small particles, and body size to planktonic trophic interactions

A dissertation submitted in partial satisfaction of the requirements for the degree Doctor of Philosophy

in

Oceanography

by

Benjamin Michael Whitmore

Committee in charge:

Professor Mark D. Ohman, Chair
Professor Peter J.S. Franks
Professor Michael R. Landry
Professor Daniel L. Rudnick
Professor Jonathan B. Shurin

2019

The Dissertation of Benjamin Michael Whitmore is approved, and it is acceptable in quality and form for publication on microfilm and electronically:

_____

_____

_____

_____

_____

Chair

University of California San Diego

2019

DEDICATION

To my family and friends, thank you for always pushing me to succeed.

TABLE OF CONTENTS

LIST OF TABLES

Chapter 1

Chapter 3

Chapter 4

LIST OF FIGURES

Chapter 1

Chapter 2

Chapter 3

Chapter 4

ACKNOWLEDGEMENTS

I want to thank my family, friends, lab mates, the 2013 SIO and BO cohorts, the Instrument Development Group, the SIO community, and my committee members for helping me through this process. I would not have been able to accomplish this without all of your help and support along the way.

Mark, thank you for introducing me to the world of biology and for taking a chance on an engineer so many years ago.

Chapter 2, in full, is a reprint of the material as it appears in **Whitmore, B.M.,** Nickels, C.F. and Ohman, M.D., 2019. A comparison between *Zooglider* and shipboard net and acoustic mesozooplankton sensing systems. *Journal of Plankton Research*, 41(4), pp.521-533. The dissertation author was the primary author on this paper.

Chapter 3, in full, is currently being prepared for submission for publication of the material. **Whitmore, B.M.** and Ohman, M.D. The influences of the prey field and water column stability on the fine-scale vertical distributions of zooplankton. The dissertation author was the primary author on this paper.

Chapter 4, in part, is currently being prepared for submission for publication of the material. **Whitmore, B.M.** and Ohman, M.D. Size-dependent predator-prey encounters in the zooplankton. The dissertation author was the primary author on this paper.

VITA

2013	Bachelor of Sciences, Environmental Engineering, Florida Gulf Coast University
2013	Bachelor of Sciences, Civil Engineering, Florida Gulf Coast University
2015	Master of Sciences, Marine Biology, Scripps Institution of Oceanography, University of California San Diego
2019	Doctor of Philosophy, Oceanography, Scripps Institution of Oceanography, University of California San Diego

PUBLICATIONS

Whitmore, B.M., Nickels, C.F. and Ohman, M.D., 2019. A comparison between *Zooglider* and shipboard net and acoustic mesozooplankton sensing systems. *Journal of Plankton Research*, 41(4), pp.521-533.

Ohman, M.D., Davis, R.E., Sherman, J.T., Grindley, K.R., **Whitmore, B.M.,** Nickels, C.F. and Ellen, J.S., 2018. *Zooglider*: An autonomous vehicle for optical and acoustic sensing of zooplankton. *Limnology and Oceanography: Methods*, 17(1), pp.69-86.

Whitmore, B.M., White, C.F., Gleiss, A.C. and Whitney, N.M., 2016. A float-release package for recovering data-loggers from wild sharks. *Journal of Experimental Marine Biology and Ecology*, 475, pp.49-53.

Pickett, M.T., **Whitmore, B.M.,** Komisar, S.J. and Falk, T.C., 2015. Anaerobic Degradation of Cadaver Waste Using an Attached Growth Recycle System. *Journal of Hazardous, Toxic, and Radioactive Waste*, 20(2), pp. 040150221-040150226

Everham III E. M., Ceilley D. W., Croshaw D.A., Firth J., Gunnels C., Hanson D. D., Mariolan S., Spear R. J., Thomas B., Van Norman D. E., **Whitmore B. M.,** and J. R. Cassani. 2013. Ten Years of the Southwest Florida Frog Monitoring Network: Natural Cycles and Human Driven Changes. *Florida Scientist*, 76(2), pp. 138-149.

ABSTRACT OF THE DISSERTATION

Zooglider reveals the importance of marine snow, small particles, and body size to planktonic trophic interactions

by

Benjamin Michael Whitmore

Doctor of Philosophy in Oceanography

University of California San Diego, 2019

Professor Mark D. Ohman, Chair

Conventional sampling systems (nets, pumps, acoustics, and most optical imaging systems) are inadequate to study planktonic trophic interactions. However, *Zooglider*, a novel endurance zooplankton sensing glider, is shown here to be uniquely capable of resolving planktonic trophic interactions at 5 cm vertical resolution.

In March 2017, *Zooglider's* optical (Zoocam) and acoustic backscatter (Zonar) systems were compared against conventional ship-based nets (MOCNESS) and acoustics (EK80). Zoocam observed similar abundances of robust organisms (chaetognaths, euphausiids, and nauplii) and greater abundances of both smaller and more delicate zooplankton. Compared to

the MOCNESS, Zoocam observed significantly more smaller appendicularia and copepods, while simultaneously observing significantly more larger gelatinous predators (ctenophora and hydromedusae) and mineralized protists (foraminifera, phaeodaria, and mostly acantharia). Furthermore, Zoocam revealed *in situ* local maxima in organismal abundances that were not resolvable by the coarser net resolution. Zonar matched the relative distributions and magnitude of ship-based acoustics, without the disadvantage of reduced signal-to-noise ratios in deeper depths.

From seven deployments spanning 15 months, *Zooglider* revealed the limitations of solely using chlorophyll-*a* fluorescence (Chl-*a*) as a proxy for herbivorous zooplankton prey. Zoocam observed that marine snow, small particles, and many zooplankton taxa, i.e., appendicularians, copepods, and large mineralized protists (primarily acantharia), have bilinear and nonlinear relationships with Chl-*a* concentrations. In most cases, zooplankton showed improved overlap with distributions of small suspended particles than with Chl-*a*. Furthermore, marine snow and small particles were determined to be the primary explanatory variables for zooplankton abundances, whereas Chl-*a* was either secondary or insignificant. No relationship was found between maximum water column stability and zooplankton or prey abundances.

Zooglider also detected size-dependent zooplankton predator-prey interactions. Size-dependent vertical distributions were found for three prey taxa and five predatory taxa and differential size-dependent diel vertical migration behavior was detected for copepods and chaetognaths. Zoocam images showed *in situ* predator-prey encounters (co-occurrence of predator and prey within a 250 mL sample volume). Analysis of these encounters revealed that abundances of smaller predatory zooplankton (chaetognaths, ctenophores, siphonophores, and

trachymedusae) have stronger relationships with abundances of smaller prey and that smaller predators have greater observed probabilities of encountering smaller prey.

CHAPTER 1: Introduction

1.1 Planktonic Patchiness:

Patchiness is the aggregated (nonrandom) distribution of individuals per unit of habitat (Haury et al. 1978). Patchiness can be broken down into several components (i.e., patch size, intensity, spacing, composition, and longevity; Haury et al., 1978). The differences in these components between patches can have significant ecological consequences. For example, if the distance between patches is large and the intensity of the patch is small, then predators must expend much energy for minimal returns. If patches have different predator to prey ratios, each patch will have different survival potential (Haury et al. 1978). Patches can also enhance productivity of systems. Rovinsky et al. (1997) modeled how patchiness affects phytoplankton and zooplankton populations and found that in patchy states productivity was enhanced by factors of 20 (phytoplankton) and 2 (zooplankton) compared to homogeneous states.

It is easy to observe that organisms exhibit patchiness in both terrestrial and littoral habitats. However, patchiness is difficult to observe in the pelagic ocean, in particular with planktonic ecosystems, as it must be measured in a dynamic marine environment and at micro (<1 m) to fine (1-10 m) scales (Haury et al., 1978). The micro scale is important as the size of many planktonic organisms is on the order of μm's to mm's and as such these organisms interact on scales much less than 1 m. The fine scale is important as many planktonic patches have been shown to have a vertical extent of under 5 m (Dekshenieks et al. 2001). Furthermore, planktonic patchiness within the ocean exists in both the horizontal and vertical dimensions (Omori and Hamner, 1982). For this dissertation, I will focus specifically on the vertical micro-scale distributions (vertical microstructure) of mesozooplankton, zooplankton with body sizes ranging from 0.5 to 20 mm, and how they relate to other biotic and physical properties within the ocean water column.

1.2 Sampling Mesozooplankton vertical microstructure:

Zooplankton vertical microstructure data are typically gathered in one of three ways: physical collection, acoustic backscatter, or optical imaging (Wiebe and Benfield, 2003). Each method has unique benefits and limitations. Net tows and pumps physically retain the organism, allow for species level classification, and with proper preservation, samples can be examined long after initial collection. All types of physical collection have financial limitations (e.g., ship-time, sample collection, processing, preservation, and maintenance), which severely limit the number of samples and replicates that can be collected. Pump systems (e.g., CALPS and CUFES) are often mounted to the ship hull and sample at a fixed depth (Pitois et al., 2016; Checkley et al., 1997). Opening-closing nets are similar to conventional open nets in that they are usually towed obliquely (MOCNESS; Wiebe et al., 1985) or vertically (Mulit-net; Weikert and John, 1981) through the water and thus give a sample integrated over the entire tow distance (Wiebe and Benfield, 2003). However, opening-closing nets also have the added capability of being able to sample discrete depths. Typically the smallest vertical resolution of opening-closing nets is ~10 m, which is too coarse to resolve the fine and micro scales of planktonic patchiness and predator-prey interactions (Möller et al., 2012). Additionally, evidence has also shown that some planktonic organisms exhibit net avoidance (Brinton, 1967; Wiebe et al., 1982) and more delicate organisms (e.g., hydromedusae, ctenophores, phaeodaria, foraminifera acantharia) are damaged during net collection (Biard and Ohman 2019 in review; Hamner et al., 1975; Omori and Hamner, 1982; Shiota et al., 2012; Stemmann et al., 2012;) or preservation (Beers and Stewart, 1970; Michaels et al., 1995), and are thus underrepresented in samples.

In addition to physical collection methods, acoustic backscatter (ABS) and optical imaging systems are also widely used. The principle behind bioacoustic methods is that a sound wave is transmitted by a transducer. The wave propagates through the medium where attenuation and scattering occur. When the wave encounters a target, a proportion of the initial sound is reflected to the receiver. This proportion of reflected sound to incident sound is known as the target strength (Jurvelius et al., 2008). Systems that utilize ABS to estimate biomass are less susceptible to organismal avoidance and can sample great volumes quickly. However, the acoustic sensing of zooplankton is complicated by several factors (e.g., target composition, acoustic frequency, and target orientation) and the specific identity of the target is unable to be discerned from acoustic sampling alone (Griffithes et al., 2002; McGehee et al., 1998).

Optical imaging systems use a light source to illuminate a sample volume, which is later captured as an image by an array of photo diodes or cameras. The image resolution, capture rate, and sample volume can vary widely by system (as described in the following section), however, some similarities still exist with respect to lighting and image capture techniques (Wiebe and Benfield, 2003). Particle sensing techniques rely on the targets to block a portion of the light source (e.g., Herman et al., 2004), thus impeding the light from being registered on the photo diode. These systems generate rough shape profiles of the targets within the sample volume, but are unable to be definitively assigned to taxa (Jackson and Checkley, 2011).

Two-dimensional systems use a high-speed camera to record an image of the entire sample volume. Typically, these systems have the resolution to determine composition and resolve the two-dimensional spatial position of the targets within the sample volume. However, the third dimension is obscured. As these optical imaging systems capture targets across a depth of field, unequal magnification and illumination across the depth of field become problematic.

Typically, these discrepancies in magnification and illumination are remedied using a collimated light field and a shadowgraph camera. This imaging technique results in an evenly illuminated shadowgraph image (Arnold and Nuttall-Smith, 1974) that has uniform magnification across the sample volume (i.e., a telecentric image).

Alternatively, three-dimensional systems (e.g., particle image velocimetry and holography) can resolve the velocities and 3-D orientation patterns of planktonic organisms, within relatively small sample volumes (~1 mL). 3-D systems have high-power and memory consumption which limit their use to ship-based operations, whereas the small sample volume of these instruments makes it difficult to observe rare organisms (Malkiel et al., 2006; Sheng et al., 2003). Optical imaging systems can have a range of sample volumes depending on tow speed, image resolution, and image capture rate, but in general are limited to ship-mounted or towed instrument platforms due to high-power consumption rates (Wiebe and Benfield, 2003).

I will now discuss the primary instrument used for data acquisition in this dissertation: *Zooglider*, a novel low-power acoustic and optical mesozooplankton sensing glider, in greater detail (Fig. 1.1).

Zooglider, was developed by the Ohman lab and the Instrument Development Group at the Scripps Institution of Oceanography, UCSD. *Zooglider* is an autonomous underwater vehicle (AUV) known as a *Spray* glider (Sherman et al., 2001) that has been modified specifically to sample mesozooplankton. *Zooglider* has a front mounted camera (Zoocam, Fig. 1.2) and downward-facing dual frequency acoustics (200 and 1000kHz, Zonar). Zoocam utilizes a red (620-630 nm) LED light (Cree XPE2) to illuminate a 250 mL sample volume. A point source of light is expanded by a lens, collimated, and redirected across the sample volume by a pair of mirrors before being recorded by a camera, ultimately resulting in a telecentric image. Each

image has a resolution of 40 µm and is ~1.2 MB in size (1280 x 960 pixels) and is internally written to either a 512 Gb universal serial bus drive or a 200 Gb solid-state drive memory card (Ohman et al., 2018). Images are captured using a Chameleon CMLB-1352M camera (Point Grey) that captures shadowgraph images at 1.875 Hz, while *Zooglider* ascends at ~10 cm s^{-1}, thereby yielding a vertical resolution of ~5 cm. In addition to its optical and acoustic sensing capabilities, *Zooglider* concurrently records CTD (Conductivity, Temperature, and Depth) and chlorophyll-*a* fluorescence (Chl-*a*) data at 8 s intervals (Ohman et al., 2018). A comparison of *Zooglider* with other imaging systems used for measuring planktonic distributions may be seen in Table 1.1.

The LOPC, VPR, UVP, and *IS*IIS sample much greater volumes than other imaging systems, depending on the tow speed, but also have their own limitations. The LOPC is unable to resolve the identity of objects and has an image resolution of only 1 mm, whereas the VPR, UCP, and *IS*IIS all have high-power requirements and thus require mounting to ship-based rosettes or towed instrument platforms. *Zooglider* is unique in relation to these other imaging systems in that it is low-power and completely autonomous. The autonomy of the *Zooglider* allows it to be deployed for extended missions (~50-day battery capacity), repeatedly sample an area, and/or sample many different areas of interest. Furthermore, its two-way communications (via Iridium) allow for near-realtime data acquisition and adaptive sampling from remote locations. For a complete description of *Zooglider* engineering specifications and capabilities, see Ohman et al. (2018).

The autonomy provided by gliders can allow for a vastly greater sampling effort than otherwise previously attained. For example, Powell and Ohman (2015) used *Spray* gliders to conduct ~23,000 vertical profiles over the course of 6 years. In addition to the benefits of

autonomy, the endurance and vertical resolution (~5 cm) of *Zooglider* allow for multiple trophic levels of mesozooplankton, potential prey sources (i.e., chlorophyll-*a* fluorescence, marine snow, and small particles), and physical variables to be measured.

1.3 Mesozooplankton Vertical Microstructure:

When data are gathered at fine- to mico-scale vertical resolution, it is possible to observe that many mesozooplankton and their prey can concentrate in layers of heightened local abundances that are less than 5 m in vertical height (Moller et al., 2012; Fig. 1.3). Layers with this small vertical extent have been shown to be composed of phytoplankton (Dekshenieks et al., 2001; McManus et al., 2008; Ryan et al., 2008; Sullivan et al., 2010), zooplankton (Cheriton et al., 2007), planktivorous fish (Benoit-Bird, 2009; Clay et al., 2004), bacteria, viruses, and marine snow (Alldredge et al., 2002; McManus et al., 2003).

Furthermore, if these layers are spatially and temporally persistent (i.e., identifiable in multiple profiles) and their maximum concentration exceeds certain thresholds (e.g., three times the ambient concentration) they are often referred to as “thin layers” (Cullen, 2015; Dekshenieks et al., 2001; Durham and Stocker, 2012; Fig. 1.4).

1.4 Mesozooplankton Vertical Microstructure and Physical Conditions:

Such fine-scale layers of organisms and particles are often associated with abrupt changes in water column properties, e.g., thermoclines (Steinbuck et al., 2009), haloclines (Möller et al., 2012; Rines et al., 2002), and pycnoclines (Dekshenieks et al., 2001). However, there are conflicting hypotheses about the role of water column stability in maintaining these layers of heightened concentrations. For instance, Lasker (1975) showed that a storm effectively diluted

dinoflagellate concentrations to levels that were unable to sustain first-feeding anchovy larvae. These results led to the Lasker Stable Ocean Hypothesis, which states that the survival of larval fishes requires the cooccurrence of larval patches with elevated prey concentrations, and that these conditions can only persist in stable ocean conditions (Lasker, 1981). In contrast, Rothschild and Osborn (1988) argued that higher encounter rates are expected during mixing events and more turbulent conditions.

1.5 Mesozooplankton Vertical Microstructure and Prey Associations:

Mesozooplankton layers have also been found to be associated with particle and phytoplankton distributions (i.e., prey sources). Zooplankton layers were found to be associated with phytoplankton layers only when the phytoplankton within the layer accounted for greater than 18% of the integrated water column chlorophyll fluorescence (Benoit-Bird et al., 2010). Biard and Ohman (2019, in review) found that the depth of the Chl-*a* maximum and temperature were the best explanatory variables for acantharians ($R^2 = 0.43$). Other work has found Chl-*a* distributions and water column stability to be the main environmental factors influencing appendicularia vertical microstructure **(**Capitanio and Esnal, 1998; Kodama et al., 2018; Spinelli et al., 2013, 2015; Tomita et al., 2003**).**

Chl-*a* distributions are often measured *in situ* using *in vivo* chlorophyll-*a* fluorescence and these distributions have long been used as a proxy for the vertical structure of phytoplankton within the water column (Cullen, 2015). The depth of the Chl-*a* maximum sometimes corresponds to the depth of the phytoplankton biomass maximum (Cullen, 1981). However, there are several uncertainties associated with use of Chl-*a* fluorescence as a proxy for the available phytoplankton prey field, e.g., non-photochemical quenching (Cullen and Lewis 1995;

Omand et al., 2017), dark adaptation (Checkalyuk and Hafez, 2011; Falkowski and Kiefer, 1985), depth and nitracline dependent Carbon to Chl-*a* ratios (Taylor et al., 2011; Taylor et al., 2015), and the uncertainty of the fraction of phytoplankton that are readily ingestible to different zooplankton taxa (Calbet et al., 2000; Djeghri et al., 2018**;** Kruse et al., 2009; Ohman, 2019)

Mesozooplankton have also been found to be highly associated with particle distributions in the water column. Suspended detrital particles or aggregates greater than 0.5 mm equivalent circular diameter (ECD) within the ocean are classically referred to as marine snow (Alldredge and Silver, 1988; Silver et al., 1978). Marine snow can be composed of abiotic (e.g. silt, clay, sediment, and trace metals; see references in Fowler and Knauer 1986) and biotic (e.g., planktonic remains, abandoned appendicularia houses, fecal pellets, molts; Alldredge and Silver 1988; Fowler and Knauer; 1986; Möller et al., 2012; Silver et al., 1978; Stemmann et al., 2012; Stoecker, 1984). As marine snow is abundant and ubiquitous within the water column, the sinking of marine snow is considered a primary method for surface material to be transported to the sea floor. Marine snow sinking rates can be highly variable, (ranging from 1 to 1,000 m day^{-1}). The sinking rate of marine snow is dependent upon a number of factors, e.g., particle size, shape, and density (Fowler and Knauer, 1986), fluid shear (Alldredge et al., 1990), bacteria decomposition (Cho and Azam, 1988), and interactions with zooplankton (Dilling and Alldredge, 2000; Goldthwait et al., 2004).

For example, Dilling and Alldredge (2000) showed that the size of marine snow aggregates decreased with increases in euphausiid abundance, suggesting that marine snow aggregations were being fragmented by the feeding action of euphausiids. This suggestion was quantified by Goldthwait et al. (2004) where the fluid stress generated around euphausiid swimming appendages was shown to be capable of fragmenting larger (>0.5 mm) particles into

smaller daughter particles. These smaller particles could theoretically have reduced sinking rates and thus remain longer in surface waters. Prairie et al. (2015) measured heightened microbial enzymatic activity, which initiates the remineralization of organic matter, on marine snow aggregates. This heightened enzymatic activity, in combination with a longer residence time in surface waters, would result in more remineralization within surface waters and less organic matter flux to the benthos (Prairie et al., 2015). Alternatively, some zooplankton repackage marine snow into more dense particles with greater sinking velocities which would enhance transport of material to the benthos (Wilson and Steinberg, 2010). Several studies have shown that many zooplankton taxa utilize marine snow as a viable prey source (Alldredge et al., 1972; Malkiel et al., 2006; Möller et al., 2012; Stukel et al., 2018; Stukel et al., 2019). Specifically, some imaging studies have allowed for the direct observation of potential feeding behavior by zooplankton on marine snow (Malkiel et al., 2006; Ohman 2019). Möller et al. (2012) found 5% of the images of coincident marine snow and copepods showed copepods directly attached to the marine snow, suggesting an active feeding behavior.

An additional feeding behavior, beyond the active feeding examples of zooplankton shown above is called ‘flux feeding’. Jackson (1993) argued that the mucous feeding web secreted by pteropods captured the flux of falling material within the water column. Jackson and Checkley (2011) deployed autonomous particle sensing floats that showed increasing particle size with depth. Below the vertical maximum in particle size there was an abrupt decrease in particle size that they attributed to particle consumption by zooplankton. Flux-feeding Phaeodaria and pteropods were found to account for between 10 and 20% of the total carbon flux attenuation at the base of the euphotic zone (Stukel et al., 2019).

1.6 Mesozooplankton Vertical Microstructure and Predator-Prey Associations:

Additionally, concentrated layers of mesozooplankton have also been shown to be associated with one another and with their predators. Benoit-Bird (2009) observed that in the absence of a copepod thin layer, fish (primarily Pacific sardine and northern anchovy) resided near the surface regardless of the time of day; however, in the presence of copepod thin layers only 25% of fish maintained this surface-keeping behavior. Furthermore, the fish that did not maintain this surface-keeping behavior were located within 2 m of the copepod thin layer 82% of the time. Greer et al. (2015) showed that fish larvae tended to overlap spatially with gelatinous zooplankton predators near the Georges Bank shelf edge, whereas copepods showed separation with gelatinous zooplankton predators in Monterey Bay (Greer, 2013).

The association of predator and prey within the same depth stratum significantly impacts the probability of predation events. Predation is the consequence of sequential events, i.e., encounter, attack, capture, and ingestion, and as such may be described by the independent probabilities of each event (Holling, 1966; Ohman, 1988). Each predation event can be mediated by a corresponding prey response (Table 1.2). For example, if the vertical distributions of predatory and herbivorous zooplankton do not overlap (spatial refugia), the probability of an encounter will be significantly decreased. The probability of a predator-prey encounter is a function of vertical overlap, predator-prey densities (Williamson and Stoeckel, 1990), relative organism velocities (Gerritsen and Strickler, 1977), and environmental turbulence conditions (Kiørboe and MacKenzie, 1995).

The vertical distributions of predatory and prey mesozooplankton can be greatly influenced by light variability (Ohman and Romagnan, 2016), organism size (De Robertis et al., 2000), life-stage (Huntley and Brooks, 1982), and the presence or absence of predators (Ohman

et al., 1983, Ohman, 1990). The influence of predator and prey velocities on the probability of encounter is dependent upon the predation method being utilized. Ambush predators, e.g., chaetognaths (Feigenbaum and Reeve, 1977), some lobate and cydippid ctenophores (Greene et al., 1986; Waggett and Costello, 1999), some cyclopoid copepods (Kiørboe, 2008; Kiørboe et al., 2009), colonial siphonophores, and trachymedusae (Costello et al., 2008), remain stationary and rely primarily on the velocity of their prey for an encounter to occur (Gerritsen and Strickler, 1977**;** Kiørboe, 2011). Conversely, cruise predators, e.g., some calanoid copepods (Kjellerup and Kiørboe, 2011), narcomedusae (Costello et al., 2008), and beroid ctenophores (Swanberg, 1974), swim continually and rely on their own velocity to initiate prey encounters (Gerritsen and Strickler, 1977; Kiørboe, 2011). Both ambush and cruise feeding have distinct advantages and disadvantages. Ambush feeders have reduced metabolic demand and decreased predation risk, but are limited to motile prey. Alternatively, cruise-feeders have substantially more energy requirements and have increased predation risk (compared to ambush feeders), but they are able to encounter both motile and non-motile prey (Visser, 2007; Kiørboe, 2011).

1.7 Summary:

When observed at fine and micro-scales, the vertical microstructure of the planktonic ecosystem is highly patchy. These patches can have significant ecological consequences (e.g., increased encounter rates, behavioral changes, enhanced water column productivity, differential grazing rates, altered carbon cycling). Many patchiness studies have primarily focused on bulk groups of organisms (e.g., phytoplankton [McManus et al., 2008; Ryan et al., 2008], zooplankton (Cheriton et al., 2007)). In more recent years technological advances have allowed for the study of organisms at finer taxonomic resolution and multiple trophic levels, together with physical

factors with heightened resolution (Benoit-Bird, 2009; Benoit-Bird et al., 2009; Greer, 2013; McManus et al., 2003; Pinel-Alloul and Ghadouani, 2007). The autonomy of *Zooglider* in combination with its ability to gather high optical resolution images in conjunction with physical data at 5 cm scales aides greatly in resolving questions pertaining to mesozooplankton trophic interactions.

In this dissertation, I first compare *Zooglider* against conventional ship-based zooplankton collection systems, to determine mesozooplankton measurement similarities or biases. I specifically address the question whether *Zooglider* detects the same abundances, vertical distributions, and size distributions of mesozooplankton as conventional net and acoustic systems (Chapter 2)? *Zooglider's* unique capability to measure *in situ* particle concentrations autonomously in tandem with micro-scale distributions of physical variables allows for the impact of particles and water column stability on omnivorous mesozooplankton abundances to be examined. This leads to the central question that I address in Chapter 3: Which prey resource best explains the spatial distributions of omnivorous mesozooplankton: phytoplankton (as measured by chlorophyll-*a* fluorescence), small suspended particles, or larger marine snow? I further address whether greater water column stability enhances mesozooplankton and prey concentrations? Finally, the small image volume, vertical resolution, and endurance of *Zooglider* enable the study of how zooplankton size impacts predator-prey vertical distributions and encounter rates. In Chapter 4, I ask whether vertical distributions of mesozooplankton and the co-occurrence of predators and prey are body size-dependent? Does body size alter the probability of encounter between mesozooplankton predators and prey in situ? Finally, in Chapter 5, I summarize the results of the dissertation.

1.8 Tables and Figures:

Table 1.1: A comparison of imaging systems and their sample volume under typical deployment conditions.

Optical imaging system	Image type	Deployment type	Image Resolution (µm)	Sampling volume (Ls^{-1})	Reference
LOPC	particle sensing	Rosette	>1000	59	Herman et al., 2004
VPR	2D	Rosette/towed	>100	2	Davis et al., 2005
ZOOVIS	2D	Rosette/towed	?	0.4-3.4	Trevorrow et al., 2005
UVP	2D	Rosette	>100	5	Picheral et al., 2010
LOKI	2D	Rosette/towed	<100	0.1	Schulz et al., 2010
*IS*IIS	2D	Towed	>100	70	Cowen and Guigand, 2008
Zooglider	2D	AUV	>100	0.5	Ohman et al., 2019
SPC	2D	Pier Mounted	<100	0.080	Roberts et al., 2014
Holography	3D	Rosette	<20	0.001	Sheng et al., 2003

Table 1.2. Zooplankton behavioral responses to specific components of the predation sequence, (Ohman, 1988).

Prey response	Component affected
Avoidance	Encounter
Spatial refugia	
Diel rhythms	
Seasonal refugia	
Locomotory behavior	
Escape	Attack, capture
Motility	
Passive evasion	
Aggregation	
Bioluminescence	
Defense	Ingestion
Chemical	
Inducible morphology	

Figure. 1.1. *Zooglider* on deployment off of Mission Bay, CA (Photo: B.M. Whitmore).

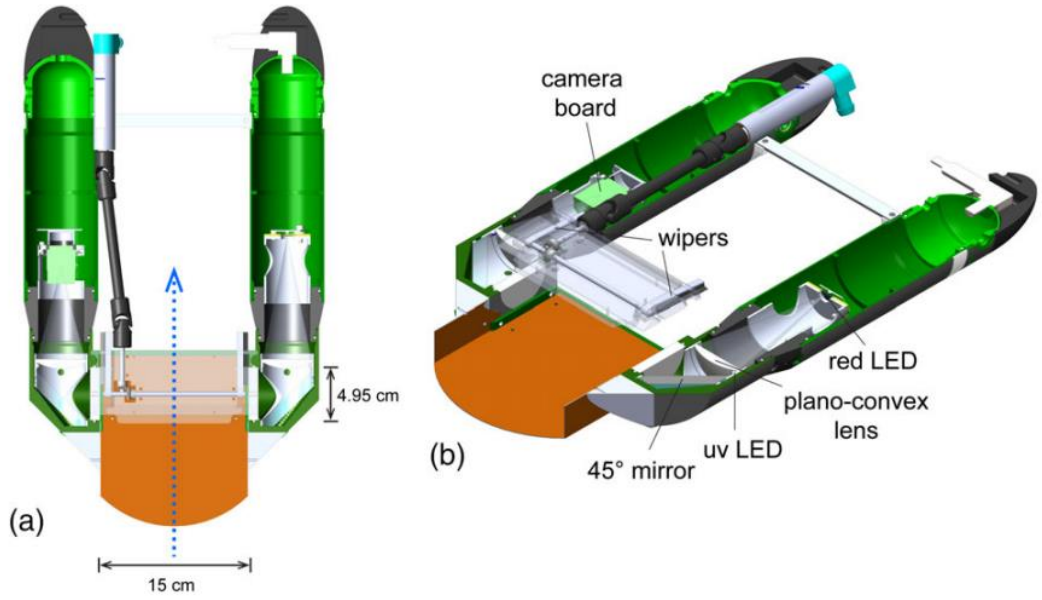

Figure 1.2. Schematic of Zoocam **(a)** plan view, with partial cutaway and **(b)** oblique view, cutaway showing imaging system components. Water flows unimpeded through the sampling tunnel (blue dotted arrow panel **a**). The red LED light source is collimated and directed across the sample volume (250 mL), by a pair of plano-convex lenses and angled mirrors, before it is captured by the camera (adapted from Ohman et al., 2018).

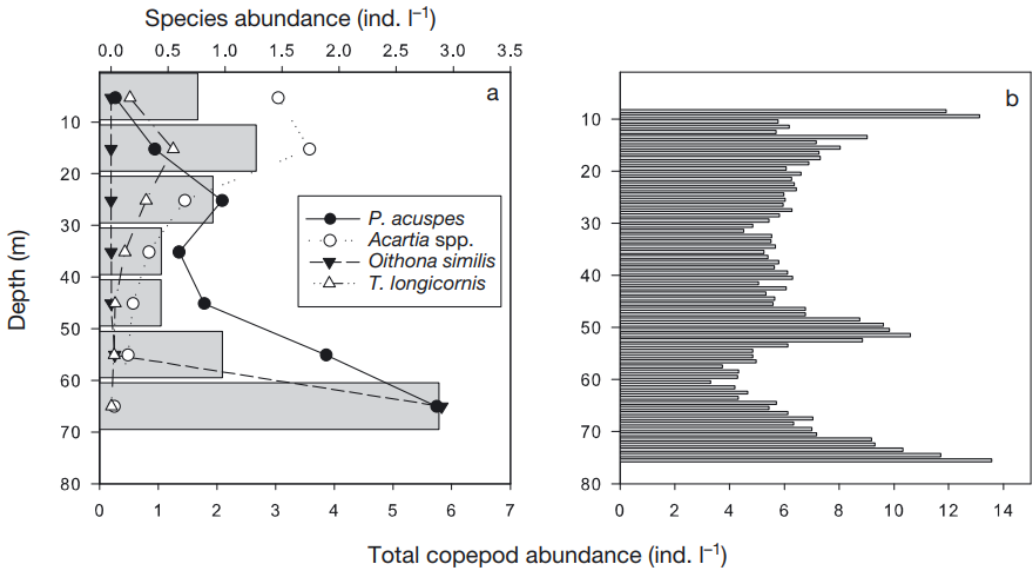

Figure 1.3. Vertical distributions of copepod abundances as sampled by (a) Multi-net with a 10 m resolution and (B) Video Plankton Recorder (VPR) with a 1 m resolution (Adapted from Möller et al., 2012).

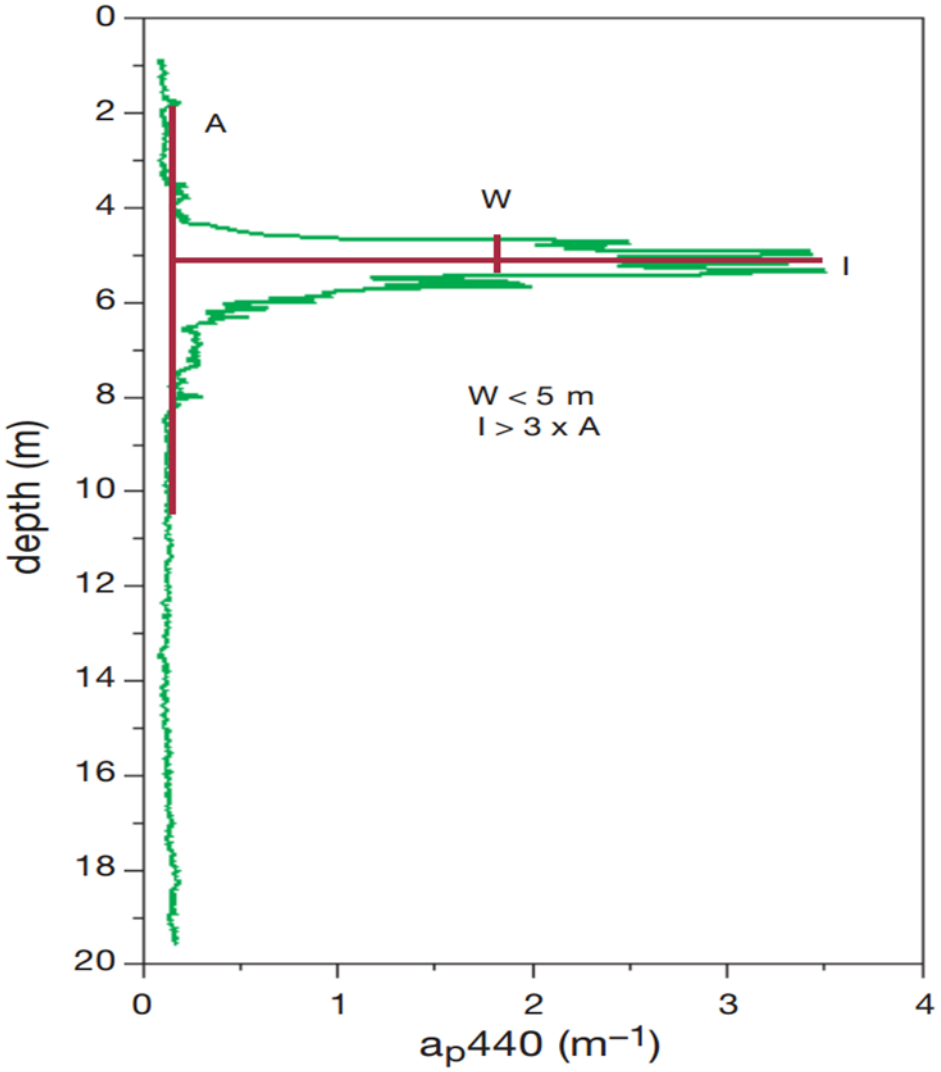

Figure 1.4. A thin layer of particulate adsorption of 440 nm light (a proxy for phytoplankton concentrations). The 'A' shows the ambient concentration, 'I' represents the intensity of the layer. 'W' represents the vertical extent of the layer (adapted from Dekshenieks et al., 2001).

1.9 References:

Alldredge, A.L., Cowles, T.J., MacIntyre, S., Rines, J.E., Donaghay, P.L., Greenlaw, C.F., Holliday, D., Dekshenieks, M.M., Sullivan, J.M., and Zaneveld, J.R.V., 2002, Occurrence and mechanisms of formation of a dramatic thin layer of marine snow in a shallow Pacific fjord: *Marine Ecology Progress Series*, 233, pp.1-12.

Alldredge, A.L., Granata, T.C., Gotschalk, C.C. and Dickey, T.D., 1990. The physical strength of marine snow and its implications for particle disaggregation in the ocean. *Limnology and Oceanography*, 35(7), pp.1415-1428.

Alldredge, A.L. and Silver, M.W., 1988. Characteristics, dynamics and significance of marine snow. *Progress in Oceanography*, 20(1), pp.41-82.

Alldredge, A.L., 1972. Abandoned larvacean houses: a unique food source in the pelagic environment. *Science*, 177(4052), pp.885-887.

Arnold, G.P. and Nuttall-Smith, P.B.N., 1974. Shadow cinematography of fish larvae. *Marine Biology*, 28(1), pp.51-53.

Benoit-Bird, K.J., Moline, M.A., Waluk, C.M. and Robbins, I.C., 2010. Integrated measurements of acoustical and optical thin layers I: Vertical scales of association. *Continental Shelf Research*, 30(1), pp.17-28.

Benoit-Bird, K.J., 2009. Dynamic 3-dimensional structure of thin zooplankton layers is impacted by foraging fish. *Marine Ecology Progress Series*, 396, pp.61-76.

Benoit-Bird, K.J., Cowles, T.J. and Wingard, C.E., 2009. Edge gradients provide evidence of ecological interactions in planktonic thin layers. *Limnology and Oceanography*, 54(4), pp.1382-1392.

Beers, J.R. and Stewart, G.L. (1970) The preservation of acantharians in fixed plankton samples. *Limnology and Oceanography*, 15, pp.825-827.

Brinton, E., 1967, Vertical migration and avoidance capability of euphausiids in the California Current. *Limnology and Oceanography*, 12, pp.451-483.

Calbet, A., Landry, M.R. and Scheinberg, R.D., 2000. Copepod grazing in a subtropical bay: species-specific responses to a midsummer increase in nanoplankton standing stock. *Marine Ecology Progress Series*, 193, pp.75-84.

Capitanio, F.L. and Esnal, G.B., 1998. Vertical distribution of maturity stages of *Oikopleura dioica* (Tunicata, Appendicularia) in the frontal system off Valdés Peninsula, Argentina. *Bulletin of Marine Science*, *63*(3), pp.531-539.

Checkley Jr, D.M., Ortner, P.B., Settle, L.R. and Cummings, S.R., 1997. A continuous, underway fish egg sampler. *Fisheries Oceanography*, 6(2), pp.58-73.

Cheriton, O.M., McManus, M.A., Holliday, D.V., Greenlaw, C.F., Donaghay, P.L. and Cowles, T.J., 2007. Effects of mesoscale physical processes on thin zooplankton layers at four sites along the west coast of the US. *Estuaries and Coasts*, 30(4), pp.575-590.

Chekalyuk, A. and Hafez, M., 2011. Photo-physiological variability in phytoplankton chlorophyll fluorescence and assessment of chlorophyll concentration. *Optics Express*, 19(23), pp.22643-22658.

Cho, B.C. and Azam, F., 1988. Major role of bacteria in biogeochemical fluxes in the ocean's interior. *Nature*, 332(6163), p.441.

Clay, T.W., Bollens, S.M., Bochdansky, A.B. and Ignoffo, T.R., 2004. The effects of thin layers on the vertical distribution of larval Pacific herring, *Clupea pallasi*. *Journal of Experimental Marine Biology and Ecology*, 305(2), pp.171-189.

Costello, J.H., Colin, S.P. and Dabiri, J.O., 2008. Medusan morphospace: phylogenetic constraints, biomechanical solutions, and ecological consequences. *Invertebrate Biology*, *127*(3), pp.265-290.

Cowen, R.K. and Guigand, C.M., 2008. *In situ* ichthyoplankton imaging system (*IS*IIS): system design and preliminary results. *Limnology and Oceanography: Methods*, 6(2), pp.126-132.

Cullen, J. J., 2015, Subsurface chlorophyll maximum layers: enduring enigma or mystery solved?. *Annual Review of Marine Science*, 7, pp. 207-239.

Cullen, J.J. and Lewis, M.R., 1995. Biological processes and optical measurements near the sea surface: Some issues relevant to remote sensing. *Journal of Geophysical Research*: Oceans, 100(C7), pp.13255-13266.

Davis, C.S., Thwaites, F.T., Gallager, S.M. and Hu, Q., 2005. A three-axis fast-tow digital Video Plankton Recorder for rapid surveys of plankton taxa and hydrography. *Limnology and Oceanography: Methods*, 3(2), pp.59-74.

Dekshenieks, M.M., Donaghay, P.L., Sullivan, J.M., Rines, J.E., Osborn, T.R. and Twardowski, M.S., 2001. Temporal and spatial occurrence of thin phytoplankton layers in relation to physical processes. *Marine Ecology Progress Series*, 223, pp.61-71.

De Robertis, A., Jaffe, J.S. and Ohman, M.D., 2000. Size-dependent visual predation risk and the timing of vertical migration in zooplankton. *Limnology and Oceanography*, 45(8), pp.1838-1844.

Dilling, L. and Alldredge, A.L., 2000. Fragmentation of marine snow by swimming macrozooplankton: A new process impacting carbon cycling in the sea. *Deep Sea Research Part I: Oceanographic Research Papers*, 47(7), pp.1227-1245.

Djeghri, N., Atkinson, A., Fileman, E.S., Harmer, R.A., Widdicombe, C.E., McEvoy, A.J., Cornwell, L. and Mayor, D.J., 2018. High prey-predator size ratios and unselective

feeding in copepods: A seasonal comparison of five species with contrasting feeding modes. *Progress in Oceanography*, 165, pp.63-74.

Durham, W.M. and Stocker, R., 2012. Thin phytoplankton layers: characteristics, mechanisms, and consequences. *Annual Review of Marine Science*, 4, pp.177-207.

Falkowski, P. and Kiefer, D.A., 1985. Chlorophyll *a* fluorescence in phytoplankton: relationship to photosynthesis and biomass. *Journal of Plankton Research*, 7(5), pp.715-731.

Feigenbaum D., and Reeve M.R., 1977. Prey detection in Chaetognatha: Response to a vibrating probe and experimental determination of attack distance in large aquaria. *Limnology and Oceanography*, 22, pp. 1052–1058.

Fowler, S.W., and Knauer, G.A., 1986, Role of large particles in the transport of elements and organic compounds through the oceanic water column: *Progress in Oceanography*, 16, pp.147-194.

Gerritsen, J. and Strickler, J.R., 1977. Encounter probabilities and community structure in zooplankton: a mathematical model. *Journal of the Fisheries Board of Canada*, 34(1), pp.73-82.

Goldthwait, S., Yen, J., Brown, J. and Alldredge, A., 2004. Quantification of marine snow fragmentation by swimming euphausiids. *Limnology and Oceanography*, 49(4), pp.940-952.

Greene, C.H., Landry, M.R. and Monger, B.C., 1986. Foraging behavior and prey selection by the ambush entangling predator *Pleurobrachia bachei*. *Ecology*, 67(6), pp.1493-1501.

Greer, A. T., 2013, Fine-scale Distributions of Plankton and Larval Fishes: Implications for Predator-prey Interactions near Coastal Oceanographic Features. *Open Access Dissertations*, University of Miami, Paper 1102.

Greer, A.T., Cowen, R.K., Guigand, C.M. and Hare, J.A., 2015. Fine-scale planktonic habitat partitioning at a shelf-slope front revealed by a high-resolution imaging system. *Journal of Marine Systems*, 142, pp.111-125.

Griffiths, G., Fielding, S., and Roe, H.S., 2002, Biological–physical–acoustical interactions: *The Sea*, 12, pp. 441-474.

Hamner, W.M., Madin, L.P., Alldredge, A.L., Gilmer, R.W. and Hamner, P.P., 1975. Underwater observations of gelatinous zooplankton: Sampling problems, feeding biology, and behavior 1. *Limnology and Oceanography*, *20*(6), pp.907-917.

Haury, L.R., McGowan, J.A. and Wiebe, P.H., 1978. Patterns and processes in the time-space scales of plankton distributions. In *Spatial pattern in plankton communities* (pp. 277-327). Springer, Boston, MA.

Herman, A.W., Beanlands, B. and Phillips, E.F., 2004. The next generation of optical plankton counter: the laser-OPC. *Journal of Plankton Research*, 26(10), pp.1135-1145.

Holling, C.S., 1966. The functional response of invertebrate predators to prey density. *The Memoirs of the Entomological Society of Canada*, 98(S48), pp.5-86.

Huntley, M. and Brooks, E.R., 1982. Effects of age and food availability on diel vertical migration of *Calanus pacificus. Marine Biology*, 71(1), pp.23-31.

Jackson, G.A. and Checkley Jr, D.M., 2011. Particle size distributions in the upper 100 m water column and their implications for animal feeding in the plankton. *Deep Sea Research Part I: Oceanographic Research Papers*, 58(3), pp.283-297.

Jackson, G.A., 1993. Flux feeding as a mechanism for zooplankton grazing and its implications for vertical particulate flux. *Limnology and Oceanography*, 38(6), pp.1328-1331.

Jurvelius, J., Knudsen, F.R., Balk, H., Marjomaki, T.J., Peltonen, H., Taskinen, J., Tuomaala, A. and Viljanen, M., 2008. Echo-sounding can discriminate between fish and macroinvertebrates in fresh water. *Freshwater Biology*, 53(5), pp.912-923.

Kiørboe, T., 2011. How zooplankton feed: mechanisms, traits and trade-offs. *Biological Reviews*, 86(2), pp.311-339.

Kiørboe, T., 2008. Optimal swimming strategies in mate-searching pelagic copepods. *Oecologia*, 155(1), pp.179-192.

Kiørboe, T., Andersen, A., Langlois, V.J., Jakobsen, H.H. and Bohr, T., 2009. Mechanisms and feasibility of prey capture in ambush-feeding zooplankton. *Proceedings of the National Academy of Sciences*, *106*(30), pp.12394-12399.

Kiørboe, T. and MacKenzie, B., 1995. Turbulence-enhanced prey encounter rates in larval fish: effects of spatial scale, larval behaviour and size. *Journal of Plankton Research*, 17(12), pp.2319-2331.

Kjellerup, S. and Kiørboe, T., 2011. Prey detection in a cruising copepod. *Biology Letters*, 8(3), pp.438-441.

Kodama, T., Iguchi, N., Tomita, M., Morimoto, H., Ota, T. and Ohshimo, S., 2018. Appendicularians in the southwestern Sea of Japan during the summer: abundance and role as secondary producers. *Journal of Plankton Research*, *40*(3), pp.269-283.

Kruse, S., Jansen, S., Krägefsky, S. and Bathmann, U., 2009. Gut content analyses of three dominant Antarctic copepod species during an induced phytoplankton bloom EIFEX (European iron fertilization experiment). *Marine Ecology*, 30(3), pp.301-312.

Lasker, R., 1981, The role of a stable ocean in larval fish survival and subsequent recruitment: *Marine fish larvae: morphology, ecology and relation to fisheries*, pp. 81-87.

Lasker, R., 1975, Field criteria for survival of anchovy larvae-relation between inshore chlorophyll maximum layers and successful 1st feeding. *Fishery Bulletin*, 73(3), pp. 453-462.

Malkiel, E., Abras, J.N., Widder, E.A. and Katz, J., 2006. On the spatial distribution and nearest neighbor distance between particles in the water column determined from *in situ* holographic measurements. *Journal of Plankton Research*, 28(2), pp.149-170.

McGehee, D.E., O'Driscoll, R.L. and Traykovski, L.M., 1998. Effects of orientation on acoustic scattering from Antarctic krill at 120 kHz. *Deep Sea Research Part II: Topical Studies in Oceanography*, 45(7), pp.1273-1294.

McManus, M.A., Kudela, R.M., Silver, M.W., Steward, G.F., Donaghay, P.L. and Sullivan, J.M., 2008. Cryptic blooms: are thin layers the missing connection?. *Estuaries and Coasts*, 31(2), pp.396-401.

McManus, M.A., Alldredge, A.L., Barnard, A.H., Boss, E., Case, J.F., Cowles, T.J., Donaghay, P.L., Eisner, L.B., Gifford, D.J., Greenlaw, C.F. and Herren, C.M., 2003. Characteristics, distribution and persistence of thin layers over a 48 hour period. *Marine Ecology Progress Series*, 261, pp.1-19.

Michaels, A.F., Caron, D.A., Swanberg, N.R., Howse, F.A. and Michaels, C.M., 1995. Planktonic sarcodines (Acantharia, Radiolaria, Foraminifera) in surface waters near Bermuda: abundance, biomass and vertical flux. *Journal of Plankton Research*, 17(1), pp.131-163.

Möller, K.O., John, M.S., Temming, A., Floeter, J., Sell, A.F., Herrmann, J.P. and Möllmann, C., 2012. Marine snow, zooplankton and thin layers: indications of a trophic link from small-scale sampling with the Video Plankton Recorder. *Marine Ecology Progress Series*, 468, pp.57-69.

Ohman, M.D., 2019. A sea of tentacles: optically discernible traits resolved from planktonic organisms *in situ*. *ICES Journal of Marine Science*. DOI 10.1093/icesjms/fsz184

Ohman, M.D., 1990. The demographic benefits of diel vertical migration by zooplankton. *Ecological Monographs*, 60(3), pp.257-281.

Ohman, M. D., 1988, Behavioral responses of zooplankton to predation. *Bulletin of Marine Science*, 43, pp. 530-550.

Ohman, M.D., Davis, R.E., Sherman, J.T., Grindley, K.R., Whitmore, B.M., Nickels, C.F. and Ellen, J.S., 2018. *Zooglider*: An autonomous vehicle for optical and acoustic sensing of zooplankton. *Limnology and Oceanography: Methods*, 17(1), pp.69-86.

Ohman, M.D. and Romagnan, J.B., 2016. Nonlinear effects of body size and optical attenuation on Diel Vertical Migration by zooplankton. *Limnology and Oceanography*, 61(2), pp.765-770.

Ohman, M.D., Frost, B.W. and Cohen, E.B., 1983. Reverse diel vertical migration: an escape from invertebrate predators. *Science*, 220(4604), pp.1404-1407.

Omand, M.M., Cetinić, I. and Lucas, A.J., 2017. Using bio-optics to reveal phytoplankton physiology from a Wirewalker autonomous platform. *Oceanography*, 30(2), pp.128-131.

Omori, M. and Hamner, W.M., 1982. Patchy distribution of zooplankton: behavior, population assessment and sampling problems. *Marine Biology*, 72(2), pp.193-200.

Picheral, M., Guidi, L., Stemmann, L., Karl, D.M., Iddaoud, G. and Gorsky, G., 2010. The Underwater Vision Profiler 5: An advanced instrument for high spatial resolution studies of particle size spectra and zooplankton. *Limnology and Oceanography: Methods*, 8(9), pp.462-473.

Pinel-Alloul, B. and Ghadouani, A., 2007. Spatial heterogeneity of planktonic microorganisms in aquatic systems. In *The Spatial Distribution of Microbes in the Environment* (pp. 203-310). Springer, Dordrecht.

Pitois, S.G., Bouch, P., Creach, V. and Van Der Kooij, J., 2016. Comparison of zooplankton data collected by a continuous semi-automatic sampler (CALPS) and a traditional vertical ring net. *Journal of Plankton Research*, 38(4), pp.931-943.

Powell, J.R. and Ohman, M.D., 2015. Covariability of zooplankton gradients with glider-detected density fronts in the Southern California Current System. *Deep Sea Research Part II: Topical Studies in Oceanography*, 112, pp.79-90.

Prairie, J.C., Ziervogel, K., Camassa, R., McLaughlin, R.M., White, B.L., Dewald, C. and Arnosti, C., 2015. Delayed settling of marine snow: Effects of density gradient and particle properties and implications for carbon cycling. *Marine Chemistry*, 175, pp.28-38.

Rines, J.E.B., Donaghay, P.L., Dekshenieks, M.M., Sullivan, J.M. and Twardowski, M.S., 2002. Thin layers and camouflage: hidden *Pseudo-nitzschia* spp.(Bacillariophyceae) populations in a fjord in the San Juan Islands, Washington, USA. *Marine Ecology Progress Series*, 225, pp.123-137.

Roberts, P.L., Jaffe, J.S., Orenstein, E.C., Laxton, B., Franks, P.J.S., Briseño, C., Carter, M.L. and Hilbern, M. (2014) Pier Recognition: An *In Situ* Plankton Web Camera. *Ocean Optics XXII*. Portland, ME, USA.

Rothschild, B.J. and Osborn, T.R., 1988. Small-scale turbulence and plankton contact rates. *Journal of Plankton Research*, *10*(3), pp.465-474.

Rovinsky, A.B., Adiwidjaja, H., Yakhnin, V.Z. and Menzinger, M., 1997. Patchiness and enhancement of productivity in plankton ecosystems due to the differential advection of predator and prey. *Oikos*, pp.101-106.

Ryan, J.P., McManus, M.A., Paduan, J.D. and Chavez, F.P., 2008. Phytoplankton thin layers caused by shear in frontal zones of a coastal upwelling system. *Marine Ecology Progress Series*, 354, pp.21-34.

Schulz, J., Barz, K., Mengedoht, D., Hanken, T., Lilienthal, H., Rieper, N., Hoops, J., Vogel, K. and Hirche, H.J., 2009, May. Lightframe on-sight key species investigation (LOKI). In *OCEANS 2009-Europe* (pp. 1-5). IEEE.

Sheng, J., Malkiel, E. and Katz, J., 2003. Single beam two-views holographic particle image velocimetry. *Applied optics*, *42*(2), pp.235-250.

Sherman, J., Davis, R.E., Owens, W.B. and Valdes, J., 2001. The autonomous underwater glider "Spray". *IEEE Journal of Oceanic Engineering*, 26(4), pp.437-446.

Shiota, T., Yamaguchi, A., Saito, R. and Imai, I., 2012. Geographical variations in abundance and body size of the hydromedusa *Aglantha digitale* in the northern North Pacific and its adjacent seas. 北海道大学水産科学研究彙報= *Bulletin of Fisheries Sciences*, Hokkaido University, 62(3), pp.63-69.

Silver, M.W., Shanks, A.L. and Trent, J.D., 1978. Marine snow: microplankton habitat and source of small-scale patchiness in pelagic populations. *Science*, 201(4353), pp.371-373.

Spinelli, M., Derisio, C., Martos, P., Pájaro, M., Esnal, G., Mianzán, H. and Capitanio, F., 2015. Diel vertical distribution of the larvacean *Oikopleura dioica* in a North Patagonian tidal frontal system (42°–45° S) of the SW Atlantic Ocean. *Marine Biology Research*, *11*(6), pp.633-643.

Spinelli, M., Guerrero, R., Pájaro, M. and Capitanio, F., 2013. Distribution of *Oikopleura dioica* (Tunicata, Appendicularia) associated with a coastal frontal system (39°-41° S) of the SW Atlantic Ocean in the spawning area of *Engraulis anchoita* anchovy. *Brazilian Journal of Oceanography*, *61*(2), pp.141-148.

Steinbuck, J.V., Stacey, M.T., McManus, M.A., Cheriton, O.M. and Ryan, J.P., 2009. Observations of turbulent mixing in a phytoplankton thin layer: Implications for formation, maintenance, and breakdown. *Limnology and Oceanography*, 54(4), pp.1353-1368.

Stemmann, L., Picheral, M., Guidi, L., Lombard, F., Prejger, F., Claustre, H. and Gorsky, G., 2012. Assessing the spatial and temporal distributions of zooplankton and marine particles using the Underwater Vision Profiler. *Sensors for Ecology*, p.119.

Stoecker, D.K., 1984. Particle production by planktonic ciliates. *Limnology and Oceanography*, 29(5), pp.930-940.

Stukel, M.R., Ohman, M.D., Kelly, T.B. and Biard, T., 2019. The roles of suspension-feeding and flux-feeding zooplankton as gatekeepers of particle flux into the mesopelagic ocean in the Northeast Pacific. *Frontiers in Marine Science*, *6*, pp.397.

Stukel, M.R., Biard, T., Krause, J. and Ohman, M.D., 2018. Large Phaeodaria in the twilight zone: Their role in the carbon cycle. *Limnology and Oceanography*, *63*(6), pp.2579-2594.

Sullivan, J.M., Donaghay, P.L. and Rines, J.E., 2010. Coastal thin layer dynamics: consequences to biology and optics. *Continental Shelf Research*, 30(1), pp.50-65.

Swanberg, N., 1974. The feeding behavior of *Beroe ovata*. *Marine Biology*, 24(1), pp.69-76.

Taylor, A.G., Landry, M.R., Selph, K.E. and Wokuluk, J.J., 2015. Temporal and spatial patterns of microbial community biomass and composition in the Southern California Current Ecosystem. *Deep Sea Research Part II: Topical Studies in Oceanography*, 112, pp.117-128.

Taylor, A.G., Landry, M.R., Selph, K.E. and Yang, E.J., 2011. Biomass, size structure and depth distributions of the microbial community in the eastern equatorial Pacific. *Deep Sea Research Part II: Topical Studies in Oceanography*, 58(3-4), pp.342-357.

Tomita, M., Shiga, N. and Ikeda, T., 2003. Seasonal occurrence and vertical distribution of appendicularians in Toyama Bay, southern Japan Sea. *Journal of Plankton Research*, *25*(6), pp.579-589.

Trevorrow, M.V., Mackas, D.L. and Benfield, M.C., 2005. Comparison of multifrequency acoustic and *in situ* measurements of zooplankton abundances in Knight Inlet, British Columbia. *The Journal of the Acoustical Society of America*, 117(6), pp.3574-3588.

Visser, A.W., 2007. Motility of zooplankton: fitness, foraging and predation. *Journal of Plankton Research*, 29(5), pp.447-461.

Waggett, R. and Costello, J.H., 1999. Capture mechanisms used by the lobate ctenophore, *Mnemiopsis leidyi*, preying on the copepod *Acartia tonsa*. *Journal of Plankton Research*, 21(11), pp.2037-2052.

Weikert, H. and John, H.C., 1981. Experiences with a modified Bé multiple opening-closing plankton net. *Journal of Plankton Research*, 3(2), pp.167-176.

Wiebe, P.H. and Benfield, M.C., 2003. From the Hensen net toward four-dimensional biological oceanography. *Progress in Oceanography*, 56(1), pp.7-136.

Wiebe, P.H., Boyd, S.H., Davis, B.M. and Cox, J.L., 1982. Avoidance of towed nets by the euphausiid *Nematoscelis megalops*. *Fisheries Bulletin*, 80(1), pp.75-91.

Wiebe, P.H., Morton, A.W., Bradley, A.M., Backus, R.H., Craddock, J.E., Barber, V., Cowles, T.J. and Flierl, G.D.1., 1985. New development in the MOCNESS, an apparatus for sampling zooplankton and micronekton. *Marine Biology*, 87(3), pp.313-323.

Williamson, C.E. and Stoeckel, M.E., 1990. Estimating predation risk in zooplankton communities: the importance of vertical overlap. *Hydrobiologia*, 198(1), pp.125-131.

Wilson, S.E. and Steinberg, D.K., 2010. Autotrophic picoplankton in mesozooplankton guts: evidence of aggregate feeding in the mesopelagic zone and export of small phytoplankton. *Marine Ecology Progress Series,* 412, pp.11-27.

CHAPTER 2: A comparison between *Zooglider* and shipboard net and acoustic mesozooplankton sensing systems

2.1 Abstract:

Some planktonic patches have markedly higher concentrations of organisms compared to ambient conditions and are less than five meters in thickness (i.e., thin layers). Conventional net sampling techniques are unable to resolve this vertical microstructure, while optical imaging systems can measure it for limited durations. *Zooglider*, an autonomous zooplankton-sensing glider, uses a low-power optical imaging system (Zoocam) to resolve mesozooplankton at a vertical scale of 5 cm, while making concurrent physical and acoustic measurements (Zonar). In March 2017, *Zooglider* was compared with traditional nets (MOCNESS) and ship-based acoustics (Simrad EK80). Zoocam recorded significantly higher vertically integrated abundances of smaller copepods and appendicularians, and larger gelatinous predators and mineralized protists, but similar abundances of chaetognaths, euphausiids, and nauplii. Differences in concentrations and size-frequency distributions are attributable to net extrusion and preservation artifacts, suggesting advantages of in situ imaging of organisms by *Zooglider*. Zoocam detected much higher local concentrations of copepods and appendicularians (53,000 and 29,000 animals m^{-3}, respectively), than were resolvable by nets. The EK80 and Zonar at 200 kHz agreed in relative magnitude and distribution of acoustic backscatter. The profiling capability of *Zooglider* allows for deeper high-frequency acoustic sampling than conventional ship-based acoustics.

2.2 Introduction:

When observed at fine (1-10 m) and micro (<1 m) scales, the vertical structure of planktonic ecosystems is highly patchy (Haury et al., 1978) and thin layers are common. Thin layers have been defined as recurrent and persistent fine-scale features (<5 m in vertical extent)

that have elevated concentrations (e.g., three times the ambient concentration) of organisms, chlorophyll, or particles (Dekshenieks et al., 2001). These layers and patches can have significant ecological consequences within the planktonic community, such as predatory behavioral changes (Benoit-Bird et al., 2009), increased encounter rates between predators and prey or between potential mates, differential grazing rates (Menden-Deuer and Grunbaum 2006), enhanced water column productivity (Brentnall et al., 2003; Rovinsky et al., 1997) and altered carbon cycling (Pinel-Alloul and Ghadouani, 2007; Prairie et al., 2015; Wilson and Steinberg 2010).

Zooplankton vertical structure is currently investigated with three basic approaches: acoustic backscatter, physical collection, and optical imaging. Each sampling method has unique benefits and limitations. Acoustic backscatter methods can approximate biomass, are less susceptible to organismal avoidance, and can sample great volumes of water quickly. However, the acoustic sensing of zooplankton is complicated by several factors (e.g., target taxonomic composition, target orientation, material properties of organisms, frequency-dependence of acoustic backscatter), and targets cannot be identified explicitly (McGehee et al., 1998; Griffithes et al., 2002), unless the acoustic system is complemented with a net or imaging system (Briseño-Avena et al., 2015).

Net tows and plankton pumps physically retain organisms, allow for species-level classification, and with proper preservation the physical specimens can be examined, DNA sequenced, or analyzed for stable isotopes or other properties long after their initial collection date. All types of physical sample collection have associated financial constraints (e.g., ship-time, sample preservation and archiving, and processing time), which severely limit the number of samples that can be obtained and processed. Advances in image processing, including

ZooImage (Grosjean and Denis, 2007), the ZooScan (Gorsky et al., 2010), and the Flowcam (Fluid Imaging Technologies), have helped to improve the post-processing time of net, pump, and bottle-collected samples. However, physical collection systems are still hindered by systematic limitations. Pump systems such as CALPS (Pitois et al., 2016) and CUFES (Checkley et al., 1997), are mounted to the hull of a ship and can sample continuously while the ship is underway, but only at a single depth. Like traditional open nets, opening-closing nets give a sample integrated over a horizontal distance and depth range when towed obliquely (MOCNESS; Wiebe et al., 1985) or strictly a depth range when towed vertically (Multi-net; Weikert and John, 1981). Opening-closing nets are superior to traditional nets as they can isolate the vertical component of the plankton community in smaller bins (vertical resolution is generally > ~10 m), however, that resolution is not sufficient to resolve the multiple scales of patchiness and predator-prey interactions in the planktonic environment (Möller et al., 2012). Nets can also damage delicate organisms (Hamner et al., 1975; Omori and Hamner 1982), while other organisms dissolve in the preservation solution if not properly treated (Beers and Stewart 1970). Some planktonic organisms, such as euphausiids, exhibit net avoidance behavior (Brinton, 1967; Wiebe et al., 1982), while other zooplankton are extruded through net mesh (Nichols and Thompson 1991; Remsen et al., 2004; Skjoldal et al., 2013) and are thus underrepresented in samples.

Optical imaging systems can discern the identity or shape profile of organisms, however the volume sampled is much smaller than acoustic, net, and pump-based systems. Imaging systems differ widely in image resolution, capture rate, sample volume, and deployment method. Particle counters (e.g., Laser Optical Particle Counter) are only able to discern the rough shape profile of objects within the water column (Herman et al., 2004). Three-dimensional imaging

systems utilize either multiple cameras or a single holographic camera to reveal the three-dimensional orientation and identity of an organism in sample volumes ranging from much less than 1 mL to 2 L (Sheng et al., 2003; Wiebe and Benfield, 2003). Several additional imaging systems are also in use for plankton recognition that sample larger volumes of water at slightly lower resolution, e.g., *IS*IIS (Cowen and Guigand, 2008); LOKI (Schultz et al., 2010); SCP (Roberts et al., 2014); UVP (Picheral et al., 2010); VPR (Davis et al., 2005); and ZOOVIS (Trevorrow et al., 2005).

The specific configuration of these instruments on profiling devices or towed bodies can markedly affect the avoidance responses of the targeted zooplankton. Any instrument moving through the water will generate a hydrodynamic disturbance to some degree. For planktonic organisms, this disturbance can induce escape responses if it exceeds an organism-specific shear threshold (Bradley et al., 2012; Buskey et al., 2002; Fields and Yen 1997; Haury et al. 1980). Optical imaging systems have the potential to further influence the behavior of plankton through the illumination needed for imaging. The introduction of light has been shown to lure (Singarajah 1975) and mitigate the escape behavior of zooplankton (Wiebe et al., 2004; Wiebe et al., 2013). Therefore, in situ instruments should be engineered to minimize the effects of light and hydrodynamic disturbances on the organisms they are observing.

Zooglider, a modified *Spray* glider (Sherman et al., 2001), is novel in that it uses a low-power and completely autonomous acoustic (Zonar) and optical imaging system (Zoocam) (Ohman et al., 2018). The Zoocam captures images at 2 Hz, while the Zonar concurrently records acoustic backscatter at two frequencies (200 and 1000 kHz). *Zooglider* resolves both biological (e.g., zooplankton, phytoplankton, marine snow, chlorophyll-*a* fluorescence) and physical properties (temperature, salinity, pressure) at a vertical resolution of ~5 cm. It is

important to note that the Zoocam utilizes a specially designed sampling tunnel that effectively traps organisms and particles, well ahead of the *Zooglider*. The geometry of the sampling tunnel, as well as the placement of the Zoocam on the glider hull, were arrived at after a series of numerical simulations using Solidworks Flow Simulation (Ohman et al., 2018). The design intent was to minimize the effects of shear in simulated flows up to 25 cm s^{-1} and to shield the organisms from the Zoocam illumination until they are well within the tunnel. Moreover, the wavelength of light was selected to be in the red part of the spectrum where crustacean eyes are relatively insensitive (see Ohman et al., 2018 for details). The efficacy of these design features in natural ocean conditions is evaluated in the present manuscript.

The goal of the present study is to compare *Zooglider* measurements of the plankton assemblage with conventional net-based sampling (MOCNESS) and shipboard acoustic (Simrad EK80) measurements. We sought to determine the comparability between methods and to identify the limitations of each system. We compare the taxon-specific abundances, concentrations, and size distributions of organisms detected by the Zoocam in comparison with MOCNESS-collected zooplankton, and separately the volume backscatter reported by the two acoustic systems.

2.3 Materials and Procedures:

For a full description of *Zooglider* engineering details please see Ohman et al., 2018.

Zooglider was deployed near La Jolla Canyon offshore of San Diego, California from 9-16 March 2017. The R/V *Sally Ride* was near *Zooglider's* last successive reported positions from 11-13 March 2017 (Fig. 2.1). Mean and maximum distances between the active Zonar

dives and EK80 track, active Zoocam dives and MOCNESS tows, and CTD Casts and *Zooglider* dives were approximately 2.42, 1.83, 1.40 km and 3.3, 2.2, and 1.45 km respectively. Distances were calculated using the ship and *Zooglider* GPS at each surfacing. As a safety precaution it was necessary to avoid lowering equipment in close proximity to *Zooglider*.

The *Sally Ride* was equipped with a five frequency (18, 38, 70, 120, 200) Simrad EK80, which was active for the duration of the cruise. The Zonar was active for 14 dives that corresponded in time and space with the *Sally Ride's* EK80. The Zonar was in listening mode for one dive off station for the purpose of background noise estimation. The Zoocam was active for nine dives from 11-13 March 2017. *Zooglider* dives were made at 3-hr intervals continuously while on station near La Jolla Canyon. Each dive was to a depth of 400 m, and data were collected solely during the ascent portion of the dive.

Two day and two night 1-m^2 Multiple Opening/Closing Net and Environmental Sensing System (MOCNESS) tows were conducted from 400 m to the surface. The MOCNESS had ten 202- µm nets and was equipped with a front mounted CTD, Chl-*a* fluorometer, transmissometer, and a calibrated flow meter. The 202-µm mesh size was chosen as *Zooglider* was initially designed to target mesozooplankton ranging in size from 0.45-20 mm. CTD casts were conducted ~0.5 km away from the *Zooglider's* last surfacing to collect water for extracted Chl-*a* vertical distributions. Each MOCNESS tow began ~2 km south of the *Zooglider's* last reported location and was towed with the same heading as the *Zooglider*. The goal of each tow was to maintain a speed over ground of 0.75-1.0 m s^{-1} and a MOCNESS net angle of 45°. Net 0 of the MOCNESS was open for the descent and beginning ascent of the tow and was closed at 400 m. The MOCNESS was towed obliquely from 400 m to the surface, and nets were tripped sequentially at predetermined depths that were consistent for all four tows. For all tows, nets 1-9

sampled consistent depth intervals (~400-350-250-200-150-100-60-40-20-0 m) from 400 m to the surface. The smaller depth intervals near the surface (nets 7-9) were used to better define the structure of the upper layers of the water column. MOCNESS samples from nets 1-9 were immediately rinsed then preserved in a 1.8% solution of formaldehyde buffered with sodium tetraborate for post-processing on land.

2.3.1 Data Analysis:

MOCNESS samples were processed using the ZooScan flatbed scanner and ZooProcess software (Gorsky et al., 2010). Each net sample was passed through three sieves (5 mm, 1 mm, and 0.202 mm) for size fractionation. Each size fraction was then subsampled, using a Folsom splitter or Stempel pipette, into smaller aliquots based on the amount of material present within the sample. The aliquots were then scanned, imaged, segmented, and cropped into individual regions of interest (ROI) using ZooProcess. A total of 68 geometric features (e.g., area, min/mean/max intensity, etc.) were calculated for each ROI. The pixel resolution of the ZooScan is 10.6 µm pixel^{-1}, and the minimum threshold for a ROI to be counted and cropped is 0.45 mm equivalent circular diameter (ECD). The measured ROIs were pre-sorted into 26 categories by a Random Forest algorithm, then classifications of 100% of the images were manually confirmed. Each confirmed ROI was scaled by appropriate aliquot factors and the volume of water filtered in situ to obtain organismal densities as number m^{-3}.

The *Zooglider* CTD and fluorescence measurements were collected at different frequencies than the Zoocam images: 8 s and 0.5 s respectively, so the CTD and fluorescence data were linearly interpolated using the Zoocam image timestamps. The Zoocam images were 1.2 MB (960 x 1280 pixels), with an image resolution of 40 µm pixel^{-1}, and a sample volume of 250 mL image^{-1}. The raw Zoocam images were flat-fielded to allow for consistent illumination

across the frame (Ohman et al., 2018). The flat-fielded images were passed through a dual pass image detection and segmentation algorithm based on Canny (1986) in order to identify ROIs within each image. Each ROI had 70 geometric features calculated and embedded in XMP format within the image, together with the interpolated physical data from *Zooglider* (Ellen, 2018). The threshold for a ROI to be cropped and saved was 0.45 mm ECD. The 0.45 mm threshold was found to be the smallest identifiable target size after several thousand frames of testing. The cropped ROIs were manually sorted into 57 categories.

To ascertain whether *Zooglider* and ship-based instruments were sampling the same water parcel, we compared ship-based and *Zooglider* mounted conductivity-temperature-depth (CTD) profiles, as potential density (σ_θ), and chlorophyll-*a* in vivo fluorescence among the *Zooglider*, MOCNESS, and CTD fluorometers, as well as the extracted chlorophyll-*a* from the CTD-rosette Niskin bottle samples. Water samples were filtered onto GFF filters, extracted in 90% acetone, and analyzed with acidification on a Turner 10AU fluorometer.

Eight taxa were compared between the MOCNESS samples and the *Zooglider* in situ images: Appendicularia, chaetognaths, *Oithona* (copepod), other Copepoda, euphausiids, gelatinous predators (Cnidaria and Ctenophora), mineralized protists (Acantharia, Collodaria, Foraminifera, and Phaeodarea), and nauplii. These taxa were chosen because they had the greatest numbers of organisms within both the MOCNESS and *Zooglider* data sets.

The MOCNESS tows and *Zooglider* dives were divided into day and night samples to minimize expected diel differences in organismal concentrations. The day samples included two MOCNESS tows and five *Zooglider* dives, while the night samples included two MOCNESS tows and four *Zooglider* dives. Total abundances (No. m^{-2}) for the eight classes of organisms

were vertically integrated from 400 m to the surface for both the *Zooglider* and MOCNESS data. These abundances were compared using a two-sample paired t-test (ttest2, MATLAB). No difference was observed when the total abundance data were dichotomized by time of day for both the MOCNESS and *Zooglider*, thus all day and night sampling was pooled for each sampling system, and reanalyzed for differences in the total abundances.

Vertical distributions of the concentration of organisms (No. m^{-3}) were generated for the day and night sampling of all eight taxa, for both sampling systems. The *Zooglider* vertical distributions were binned at two different levels: the same depth intervals as sampled by the MOCNESS nets, and 25 cm. The first binning was done for a side-by-side comparison between the two systems, while the 25 cm bin shows the finer vertical structure resolvable by the *Zooglider*. While *Zooglider* is capable of resolving 5 cm bins, the vertical structure of the less abundant taxa was hard to discern when viewed at full resolution but more apparent at the 25 cm bin size. To emphasize the fine vertical structure of each taxon in the upper part of the water column, the graphs at the 0.25 cm bin size were truncated to 0-200 dBar. For the MOCNESS net depth intervals, the vertical distributions were compared using a two-sample paired t-test (ttest2, MATLAB).

In addition to the computer-generated geometric measurements, the width of each ROI was manually measured in ImageJ in order to make direct comparisons between organism sizes from Zoocam and ZooScan. Care was taken to not measure the moveable parts of each organism such as grasping spines, setae, tentacles, and antennae. It was necessary to measure these widths manually, as the ROIs had several characteristics that hindered consistent computer-generated width measurements (e.g., pose, existence of appendicularian houses, relatively transparent features of the organism). The measured widths (w) were used to generate taxon-specific

normalized probability distributions for both the MOCNESS and *Zooglider* datasets. Each probability distribution used a bin width of 40 µm (the largest pixel resolution between the *ZooScan* and Zoocam images). The normalized frequency distributions were then compared using a Kolmogorov-Smirnov test (kstest2, MATLAB). The 40 µm bin width resulted in probabilities well below 0.01 at the upper size range of each taxa size distribution. When such small probabilities were found, the smallest probability values were summed into one size class as to avoid artificially increasing the number of size classes being compared.

The width distribution data were subdivided into three size categories: small ($w \leq 0.28$ mm, the diagonal of the net mesh), medium ($0.28 < w \leq 1$ mm), and large organisms ($w > 1$ mm). These size categories were combined with the vertical distribution data to view taxon-specific size differences by depth. These MOCNESS and *Zooglider* size-dependent concentrations by depth were compared using a two-sample paired t-test (ttest2, MATLAB).

Active acoustic analysis focused on 200 kHz as this was the only common frequency between the EK80 and Zonar. Both instruments were calibrated using a standard tungsten carbide reference sphere (Foote et al. 1987). The EK80 transmitted at a rate of 23 kHz with a 1.024 ms pulse length. EK80 acoustic backscatter was analyzed in Myriax Echoview 8 software. Background noise was removed following De Robertis and Higginbottom (2007), with a signal-to-noise threshold of 10 dB, which limited the depth of analysis to 200 m for comparison between instruments. Zonar data were processed following Ohman et al. (2018). The Zonar used a 5 kHz sampling rate with a 6 ms pulse length. Backscatter data were analyzed over a range of 3-8.1 m from the Zonar transducer face. For both instruments, average profiles of mean volume backscattering strength (S_v, dB re 1 m^{-1}; details in Ohman et al. (2018)) were calculated for the time period of the upcast of each dive in 10 m vertical bins and compared via regression

analysis (r^2 from polyfit and polyval, p value from fitlm and anova, MATLAB) for daylight and night dives separately.

A potential source of disagreement between the Zonar and EK80 is the difference in the volume each instrument insonifies (Guihen et al. 2014; Moline et al. 2015). For comparison, we calculated the volume insonified between 7-8 m from the Zonar transducer (the widest insonified radius used from that instrument) and in 1m deep bins from 7-200 m from the EK80 transducer using equation 2.1.

$$V = \left(\pi {r_2}^2 \frac{h_2}{3}\right) - \left(\pi {r_1}^2 \frac{h_1}{3}\right) \quad \text{Equation 2.1.}$$

Where V is the insonified volume in m^3, r is the insonified radius in m, h is the distance from the transducer in m, the subscript 1 denotes the values for the shallower bound of the bin and the subscript 2 denotes the deeper bound of the bin. We calculated r using equation 2.2, where Ψ is the equivalent beam angle of the transducer in radians (0.17 rad for the Zonar and 0.12 rad for the EK80).

$$r = \Psi * h \quad \text{Equation 2.2.}$$

For analysis of the difference in insonified volumes between the two systems, we considered the ratio of EK80 sampling volume to the Zonar sampling volume as a function of depth.

2.4 Results:

The potential density profiles (Fig. 2.2a) from the CTD casts, MOCNESS tows, and *Zooglider* dives correspond well, showing a relatively mixed layer from 10 to 30 m. The

extracted chlorophyll-*a* values from the CTD casts agree with the in-vivo fluorescence measured by the CTD, MOCNESS, and *Zooglider* fluorometers (Fig. 2.2b), with all sampling methods showing a sharply defined subsurface chlorophyll maximum between 30 and 40 m, thus suggesting that we sampled similar water parcels with each instrument.

The vertically integrated abundances for all eight taxa are shown in figure 2.3. Significantly higher vertically integrated abundances were found for *Zooglider* relative to MOCNESS samples for other copepods ($p < 0.001$), *Oithona* ($p < 0.001$), appendicularians ($p < 0.01$), mineralized protists ($p < 0.01$), and gelatinous predators ($p < 0.05$). No difference was found for chaetognaths, euphausiids, and nauplii ($p > 0.20$).

The vertical distributions for all taxa, when binned at MOCNESS net depth intervals (Fig. 2.4), show relatively consistent patterns of distribution by depth; however, the concentrations measured by *Zooglider* were typically much greater than the MOCNESS concentrations. Significant differences were observed between the MOCNESS and *Zooglider* concentration profiles for both the day and night profiles of other copepods ($p < 0.05$), *Oithona* ($p < 0.01$), appendicularians ($p < 0.05$), mineralized protists ($p < 0.001$), and gelatinous predators ($p < 0.05$ day, $p < 0.01$ night). No differences were detected for chaetognaths, euphausiids, and nauplii ($p > 0.05$).

When the dives are examined individually at 0.05 dBar (5 cm) vertical intervals, markedly higher maximum concentrations were observed for all taxa, e.g., 53,000 other copepods m^{-3} and 29,000 appendicularians m^{-3} (not shown). However, as stated in the methods, at that resolution the relative scarcity of the other taxa makes it difficult for their vertical structure to be resolved from so few dives because of abundant zero counts. When the vertical

distributions for the *Zooglider* are instead binned at 0.25 dBar, the vertical microstructure becomes more clearly apparent, and the maximum concentrations remain greatly elevated relative to the MOCNESS measurements for all taxa (S. Fig. 2.1). Chaetognaths appear to be relatively evenly distributed with respect to depth, while the other taxa typically show elevated concentrations between 0-75 dBar.

Normalized size distributions for the body widths of organisms for all eight taxa are shown in figure 2.5. Significant differences were found between the MOCNESS and *Zooglider* size distributions for mineralized protists ($p < 0.01$), gelatinous predators ($p < 0.01$), euphausiids ($p < 0.05$), and nauplii ($p < 0.05$). Other copepods, *Oithona*, appendicularians, and chaetognaths showed no difference ($p > 0.05$) in size distributions. The vertical dotted line in figure 2.5 represents 0.28 mm, the diagonal measurement of the MOCNESS net mesh size.

Supplementary figure 2.2 shows the vertical distributions from figure 2.4 subdivided into three size groups based on organismal body width: small (0-0.28 mm), medium (0.28-1.0 mm), and large (>1.0 mm) with respective p-values, p_S, p_M, and p_L. For the small size class, significant differences in concentrations between the MOCNESS and *Zooglider* ($p < 0.05$) were shown for other copepods (day only), *Oithona*, and mineralized protists. The medium size class was significantly different for *Oithona* ($p < 0.001$ day; $p < 0.05$ night), appendicularians ($p < 0.05$), and mineralized protists ($p < 0.01$). The large size classes showed significant differences ($p < 0.05$ day; $p < 0.01$ night) for gelatinous predators and euphausiids. The remaining size classes showed no differences in concentrations between the MOCNESS and *Zooglider*.

Average day and night vertical profiles for acoustic volume backscatter at 200 kHz from the EK80 and Zonar are shown in figures 2.6A and 2.6B, respectively. The two instruments

generally agree in pattern and magnitude of acoustic backscatter, although agreement was markedly better at night (r^2=0.58, $p < 0.001$) when depth variability of scatters was lower, than during the day (r^2=0.21, $p < 0.05$). When comparing the volume backscatter of the two instruments within the upper 200 m, the volumes insonified are substantially different, with the surface-mounted EK80 insonifying approximately 350 times the volume of the Zonar at a depth of 200 m (Fig. 2.6C).

2.5 Discussion:

As to be expected, there were subtle variations in both the physical and biological properties as sampled by the multiple *Zooglider* dives, MOCNESS tows, and CTD profiles. However, to properly address the potential influence of these variations in water column properties, as well as zooplankton patchiness on a broad spectrum of spatial scales (e.g., Haury et al. 1978), on the organisms sampled many additional profiles and transects would be necessary and is beyond the scope of the present study. The general correspondence in potential density suggests that water parcels sampled by the CTD, MOCNESS, and *Zooglider* had similar physical properties. The agreement in chlorophyll-*a* profiles suggests that the water parcels sampled by both the *Zooglider* and the instruments aboard the R/V *Sally Ride* bore similar biological characteristics. These similarities are supported by the proximity of the *Zooglider* to the R/V *Sally Ride* and minimal time difference between dives and MOCNESS tows (± 3 hrs).

Zooglider and MOCNESS agreed on the abundances of taxa relative to one another within the water column (i.e., other copepods, appendicularians, and *Oithona* as the most abundant). However, there were stark differences between the MOCNESS and *Zooglider*

measurements with regards to total abundance, concentrations, and size distributions for many of the taxa. *Zooglider* showed significantly higher vertically integrated abundances and local concentrations for five of the eight taxa compared to the MOCNESS. There were significant differences between the two systems in the size distributions for four of the eight taxa. It should be recalled that *Zooglider* images organisms alive, *in situ*, while the MOCNESS/ZooScanned samples reflect both net capture and preservation artifacts, which could account for some of the size differences.

Previous studies have yielded similar results to *Zooglider*, concerning taxon-specific discrepancies in abundance, when comparing optical imaging systems to nets. The Video Plankton Recorder (VPR) showed discrepancies in numerical concentrations for medusae, appendicularians, and copepods by factors of 360, 16.4, and 2.9 respectively (Benfield et al., 1996). The Shadowed Image Particle Profiling and Evaluation Recorder (SIPPER) revealed that a 162 µm mesh net significantly underestimated the abundance of appendicularians (300%), doliolids (379%), protists (522%), and ctenophores/cnidarians (1200%), but no significant differences in chaetognaths, copepods, or euphausiids were detected (Remsen et al., 2004). These differences in taxon abundance or lack thereof, are primarily attributable to differences in net extrusion or robustness of different organisms, and in particular whether they are fragile, soft-bodied or hard-bodied taxa. We believe that these results cannot be explained by light attraction of organisms because (1) red light was used to which the organisms are insensitive, (2) the light source is recessed well inside the sampling tunnel and is difficult to discern, and (3) *Zooglider's* ascent speed exceeds the sustained swimming capacity of small copepods (Wong 1988; Yen 1988) and most other zooplankton (De Robertis et al., 2003; Genin et al., 2005; Seuront et al., 2004).

The harder bodied copepods are less likely to experience significant shrinkage due to preservation, thus any size discrepancies are most likely attributable to the sampling process. The majority of the *Oithona* that were captured by both systems were small, below 0.28 mm in body width, which is the open dimension of the diagonal of the net mesh (vertical dotted line, Fig. 2.5). It is likely that although the size distributions did not differ significantly, many *Oithona* were extruded through the MOCNESS 202 µm mesh with the added force of the water flowing through the net. Presumably, the *Oithona* that were captured by the net were more likely to be oriented orthogonal to the mesh opening. Similar reasoning applies to the other copepods category. As the discrepancy in concentration continues to persist into the medium size category of other copepods (0.28 - 1 mm), it is likely that some copepods exceeding 0.28 mm in body width were also extruded, but to a lesser extent. This is not the first study to find such conclusions. Di Mauro et al. (2009) showed that a 220 µm mesh underestimated the copepod *Oithona nana* by 96.29%, harpacticoid copepods by 96.52%, and copepodites (stage I-III) of small calanoids by 99.7% when compared to a 67 µm mesh. Copepods with prosome lengths less than 550 µm were most efficiently sampled by a 64-µm mesh off the central coast of California (Hopcroft et al., 2001).

The higher abundances and concentrations of appendicularians and gelatinous predators detected by *Zooglider* are also attributable to net extrusion, however, due to the softer bodies of these particular taxa, it is likely that the size range for extrusion may be higher than that of the harder-bodied copepods. Di Mauro et al. (2009) found that the soft bodied appendicularian *Oikopleura dioica* was significantly underestimated for trunk lengths less than 500 µm with 220 µm mesh nets. Furthermore, appendicularians and gelatinous predators (here cnidarians and ctenophores) are more susceptible to degradation via net collection and formaldehyde-induced

shrinkage and distortion (Beaulieu et al. 1999; Nishikawa and Terazaki 1996), which in turn makes those degraded samples more difficult to identify and count for abundance estimates.

Soft-bodied zooplankton are not the only organisms that are distorted by net collection and preservation. The fragile pseudopodia and spines of mineralized protists are often destroyed or degraded by the processes of net collection, rinsing, and fixation at sea. In the case of acantharians, their strontium sulfate spines are well known to dissolve in preservatives if sufficient strontium chloride is not added (Beers and Stewart 1970). Evidence of such sample degradation was clearly observed in the MOCNESS samples, as no mineralized protists (also including phaeodarians, foraminifera, and collodarians) retained their spines or pseudopodia. This degradation can render mineralized protists too small to be saved by our 0.45 mm ECD threshold and hinder their accurate classification, which would account for the size, concentration, and abundance differences seen by *Zooglider*. In contrast to the degradation associated with net samples, *Zooglider* images organisms in their natural posture within the water column, with delicate structures intact (Gaskell et al., 2019; Ohman et al., 2018). Accordingly, mineralized protists along with soft-bodied appendicularians and gelatinous predators are generally larger than their shrunken and broken preserved counterparts, which accounts for differences in size between the MOCNESS and *Zooglider* samples.

The abundance of nauplii did not differ between the two sampling approaches, although smaller nauplii made up a larger proportion of the MOCNESS samples compared to *Zooglider* samples. We believe this size discrepancy is due to the difference in pixel resolution between the two systems. The smaller appendages of many nauplii were more readily identifiable within the MOCNESS samples at the ZooScan resolution 10.6 µm pixel^{-1}, while many possible nauplii

were labeled "unsure" due to the Zoocam resolution of 40 μm pixel^{-1}, and therefore not included in the nauplii data.

Chaetognaths were sampled with similar vertically integrated abundances, depth-specific concentrations, and size distributions by the two methods. We presume that chaetognaths are less likely than fragile cnidarians, ctenophores, and appendicularians to be damaged by net collection, or to be extruded through the net mesh.

The MOCNESS and *Zooglider* captured similar abundances of euphausiids, with slightly larger body widths recorded by *Zooglider*. However, the very largest specimens we found were detected in MOCNESS net samples, albeit at very low abundances (<0.0001 animals m^{-3}). This size difference may be attributed to a relatively low abundance of large euphausiids within the water column, coupled with the discrepancies in sample volume between *Zooglider* and MOCNESS, or perhaps to avoidance behavior (*cf.*, Brinton 1967). However, the euphausiids in Zoocam images are in natural postures and do not exhibit abdominal flexure typically associated with avoidance. Furthermore, the Zoocam utilizes a sampling tunnel that was designed specifically to minimize hydrodynamic disturbances that may trigger escape responses (Ohman et al., 2018).

Zooglider was able to discern much greater concentrations and abundances of several taxa. When viewed at small scales (<< 1 m) maximum concentrations for other copepods and appendicularians reached 53,000 and 29,000 animals m^{-3}, respectively. The persistence and extent of these high concentrations will ultimately determine their effect on the planktonic community, a topic we will address in future publications.

The dual frequency Zonar records acoustic backscatter from smaller (1000 kHz) and larger zooplankton (200 kHz) and other organisms. However, the only acoustic frequency held in common between the Zonar and EK80 was 200 kHz, hence comparisons could only be made for the larger component of the acoustic backscatter. At 200 kHz, the vessel-mounted EK80 and *Zooglider*-mounted Zonar generally agree in magnitude and overall distribution of backscatter when averaged over all day and all night dives. Agreement was better at night when scatterers migrated to the surface and their distributions were less variable. The differences may be attributable to the difference in volume insonified between instruments. The detection probability for rare, but strong scatterers would be higher for larger sampling volumes. An acoustic beam insonifies an approximately conical volume of water that widens with increasing distance from the instrument. The vessel-mounted EK80 only samples from the surface and therefore the sampling volume increases proportionally with depth, while the Zonar sampling volume remains constant. Thus, the larger, rare, strong scatterers will be better represented in the EK80 backscatter data. However, the EK80 200 kHz has an effective depth sampling limit of 200 m due to a decline in the signal to noise ratio (SNR) in deeper depths. Conversely, the profiling glider-mounted Zonar permits the effective sampling of much deeper water than vessel-mounted echosounders (Guihen et al. 2014; Moline et al. 2015; Powell and Ohman 2015). The acoustic systems were not compared with the imaging and net collections in this study as that would require information regarding taxon-specific acoustic scattering models, frequency-dependent acoustic target strength, and orientation of the organisms insonified (Briseño-Avena et al., 2015).

2.6 Conclusion:

Zooglider captures greater numbers of smaller-sized organisms (i.e., copepods and appendicularians) and larger-sized organisms (i.e., mineralized protists, medusa, siphonophores, and ctenophores) compared to the MOCNESS. Comparable abundances and similar size distributions are found for other taxa (chaetognaths, euphausiids, and nauplii). A combination of net extrusion, net-induced damage, and preservation effects all contribute to these abundance and size discrepancies. *Zooglider* was able to resolve elevated concentrations of copepods and appendicularians, to 53,000 and 29,000 animals m^{-3}, respectively. The Zonar agrees with the EK80 in magnitude and overall distribution of acoustic backscatter at 200 kHz. The profiling nature of the *Zooglider* allows it to sample much deeper than vessel-mounted echosounders without losing sample resolution due to a decline in SNR. *Zooglider's* acoustic and optical sensing systems, in combination with its autonomy and endurance, make it uniquely capable to sample zooplankton distributions with minimal disruption to the organisms.

2.7 Figures and Tables:

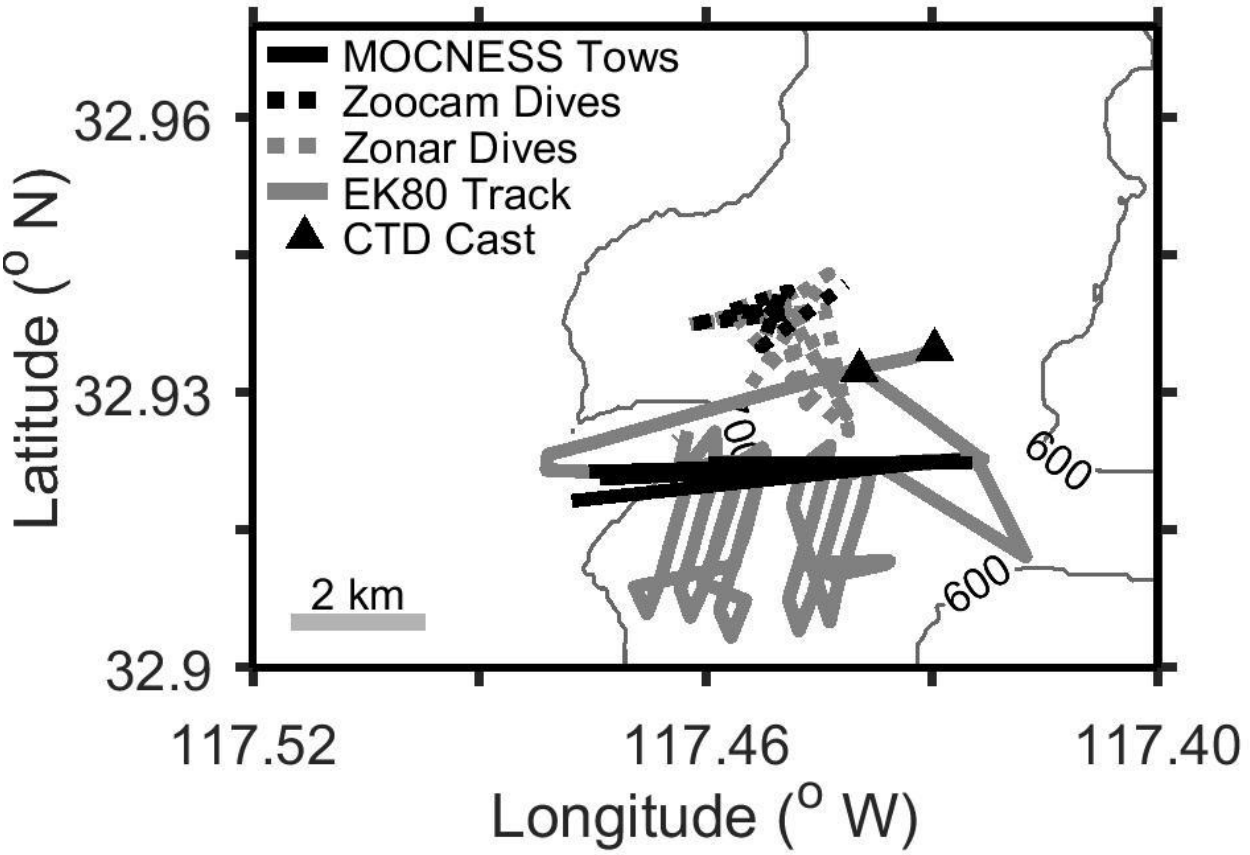

Figure 2.1. The locations of the CTD casts (triangles), EK80 survey (gray solid line), Zonar dives (gray dotted line), Zoocam dives (black dotted line), and MOCNESS tows (black solid line).

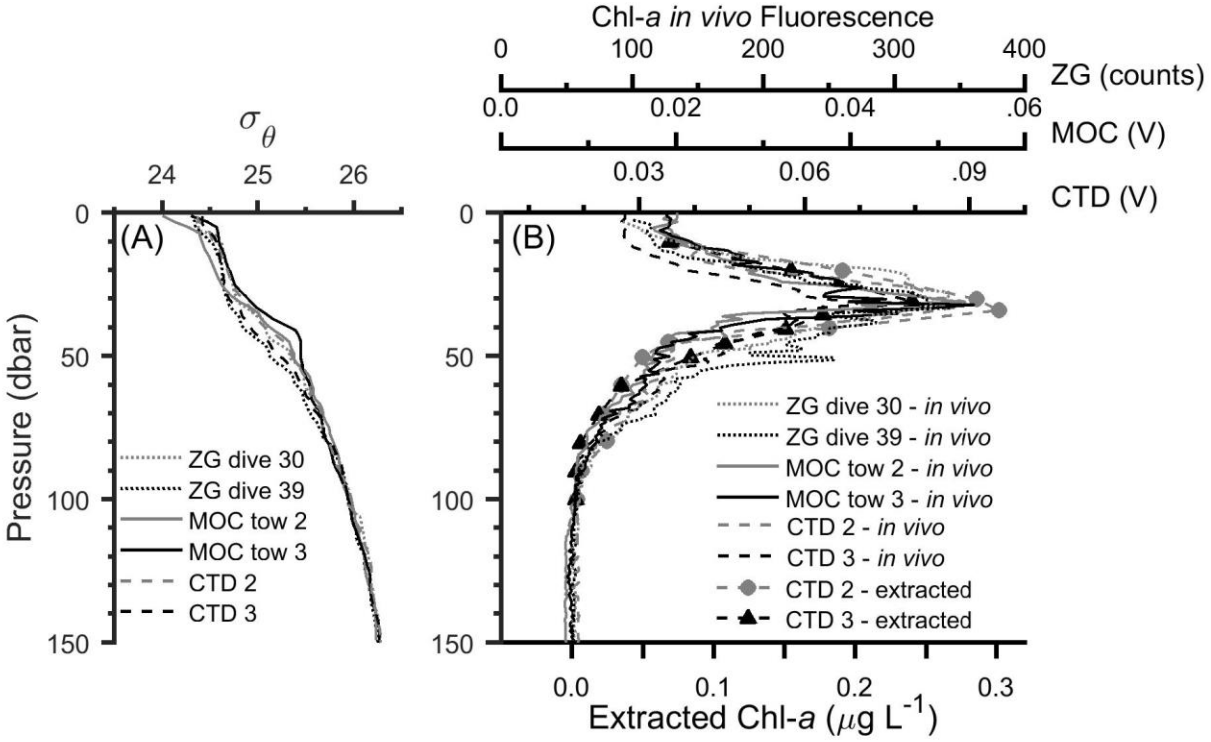

Figure 2.2. *Zooglider*, MOCNESS, and CTD-rosette measured (A) σ_θ and (B) Chl-*a* in vivo fluorescence (as digital counts, volts, and volts, respectively), together with extracted Chl-*a* (µg L^{-1}), plotted with respect to depth. The line color distinguishes the *Zooglider* dives, MOCNESS tows, and CTD casts that were closest in time to one another.

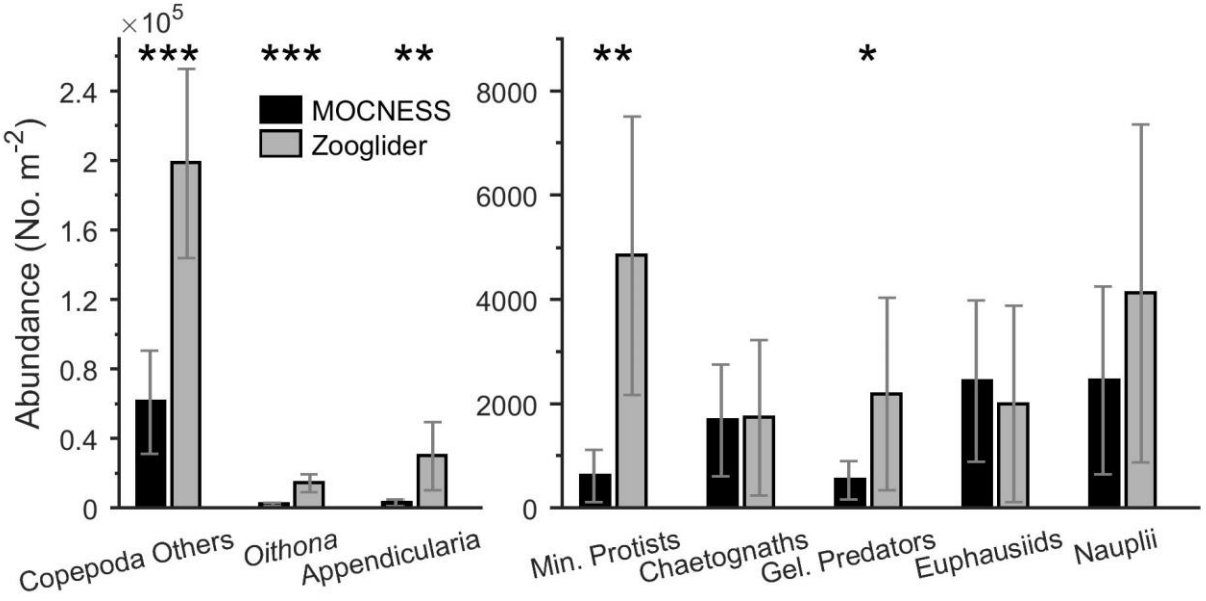

Figure 2.3. Total abundances (No. m^{-2}, $\bar{x}$ ± standard deviation) for all eight taxa as sampled by *Zooglider* (gray) and MOCNESS (black). Note the different y-label scales between the left and right columns. (* = $p < 0.05$; ** = $p < 0.01$; *** = $p < 0.001$).

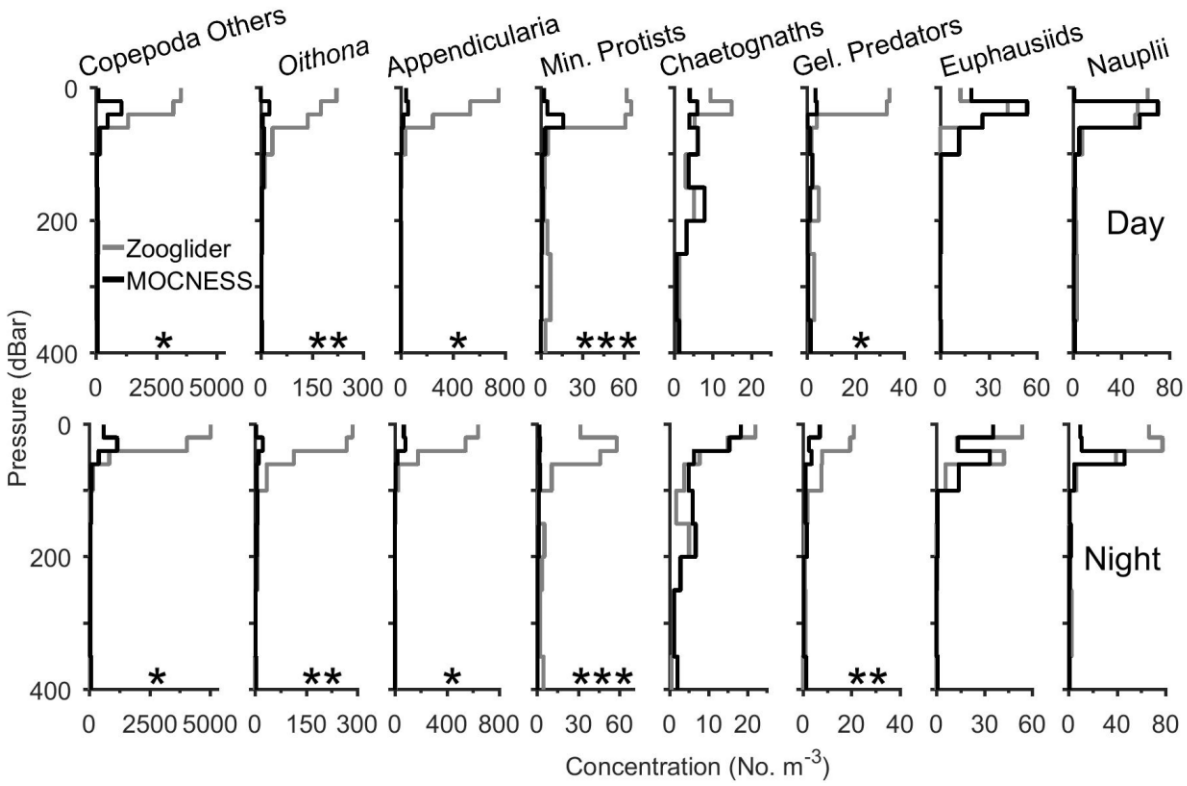

Figure 2.4. Vertical distributions of organismal concentrations for MOCNESS (black) and *Zooglider* (gray) samples. Data were binned at the MOCNESS depth intervals by day (upper row) and night (lower row). (* = $p < 0.05$; ** = $p < 0.01$; *** = $p < 0.001$).

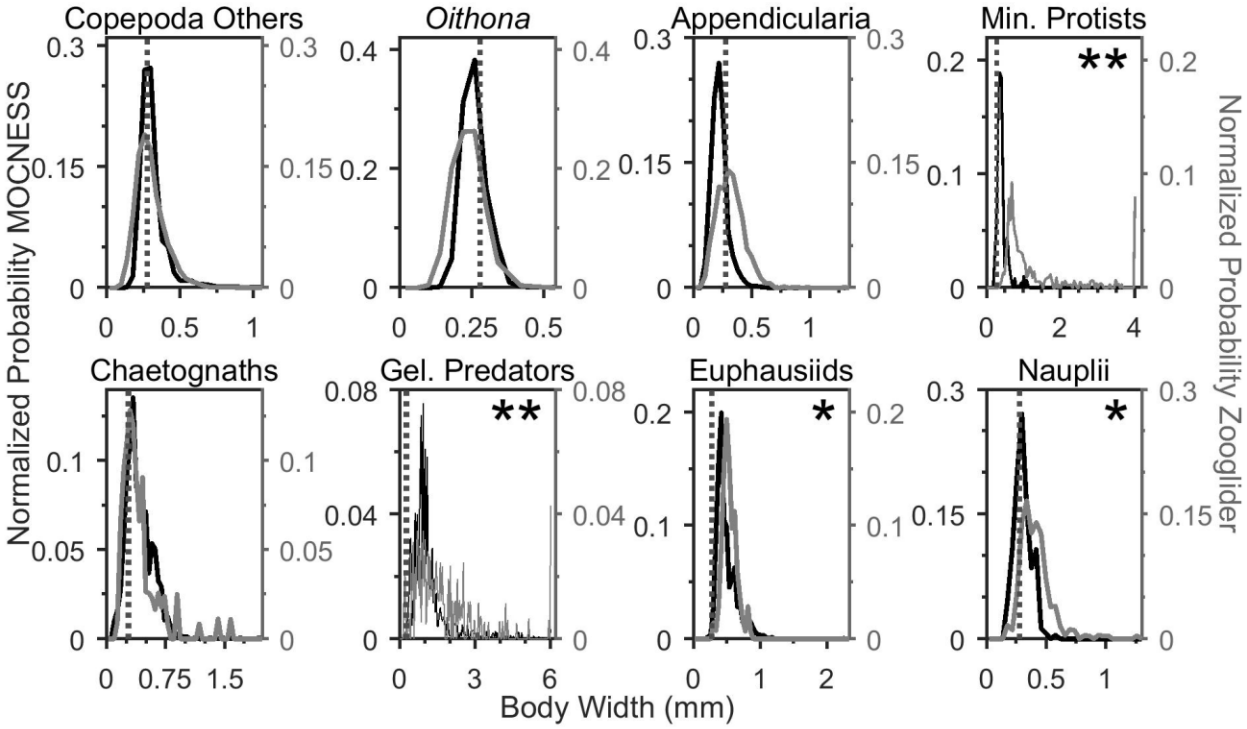

Figure 2.5. Comparison of normalized size distributions of body widths for *Zooglider* (gray) and MOCNESS (black) samples, by taxon. The vertical dotted line represents 0.28 mm (the diagonal of the MOCNESS mesh size). (* = $p < 0.05$; ** = $p < 0.01$). For ease of viewing mineralized protists and gelatinous predators, probabilities were pooled for body widths exceeding 4 and 6 mm, respectively.

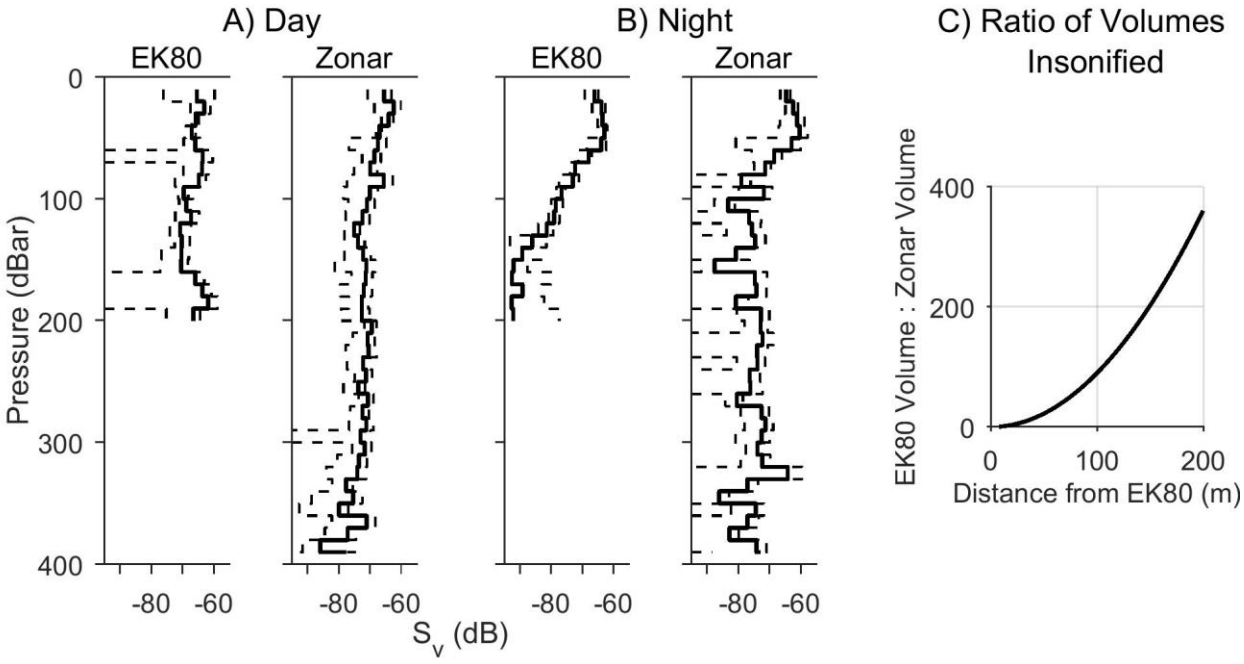

Figure 2.6. Vertical distributions of 200 kHz volume backscatter (S_v) from the EK80 and Zonar, binned at 10 dBar, in (A) day and (B) night profiles. The vertical distributions of S_v from the two instruments were correlated both by day ($p < 0.05$) and by night ($p < 0.001$). Gray dotted lines enclose 95% CI. Where the lower confidence bound goes out of the frame, the value was negative in linear space and has been set to an arbitrarily low number (-999) in log space. C) Ratio of volume insonified by the ship-mounted EK80 to *Zooglider*-mounted Zonar, as a function of increasing *Zooglider* depth. The Zonar volume remains constant with depth, while the EK80 volume increases.

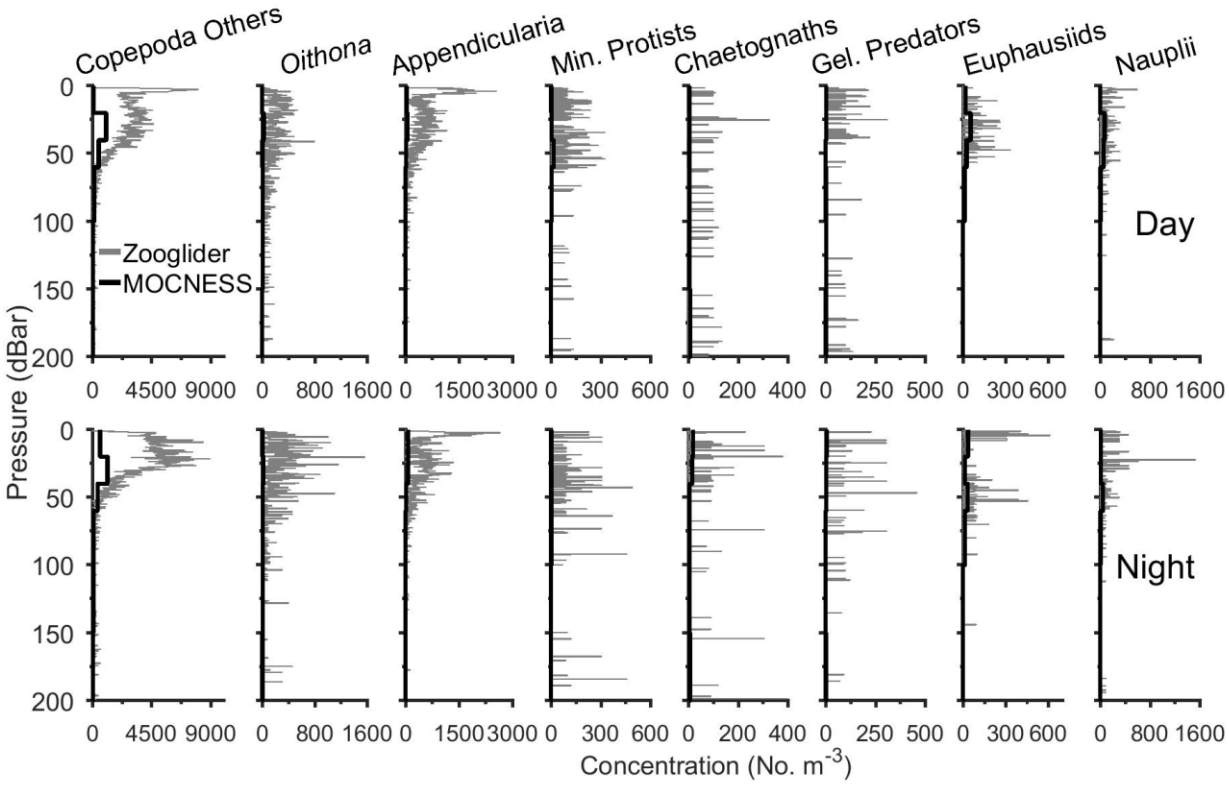

Supplementary Figure 2.1. Vertical distributions of concentration by taxa for MOCNESS and *Zooglider* samples. *Zooglider* data were binned to 0.25 dBar to show the vertical microstructure for each taxon.

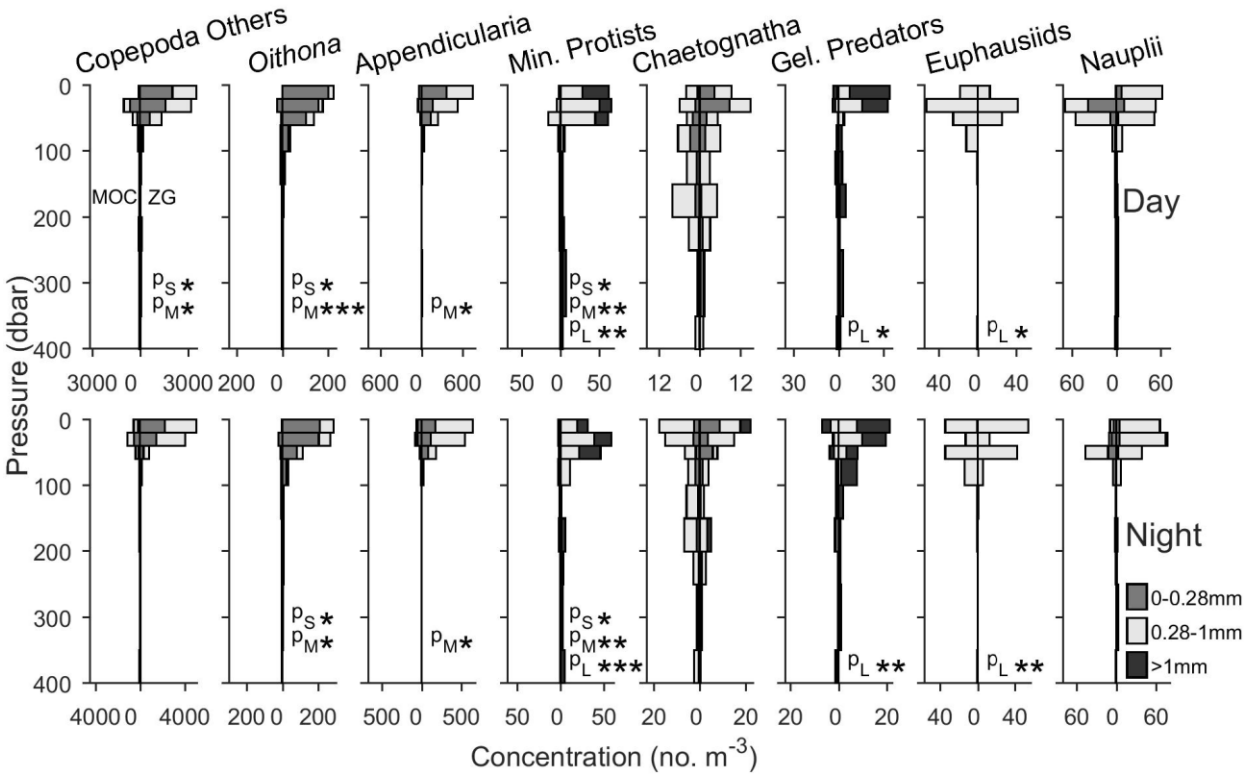

Supplementary Figure 2.2. Vertical distributions of the concentration of eight taxa, each divided into three different size classes. *Zooglider* data are on the right side of each plot, the MOCNESS data on the left. P values for the 0-0.28, 0.28-1.0, and greater than 1.0 mm size grouping are shown as p_S, p_M, and p_L respectively. (* = $p < 0.05$; ** = $p < 0.01$; *** = $p < 0.001$).

2.9 Acknowledgements:

The Instrument Development Group (R. Davis, J. Sherman, K. Grindley, B. Rieneman, E. Goodwin, D. Vana) is to be credited with the design and manufacture of *Zooglider*. We thank UC Ship Funds for research vessel time, and the crew of the R/V *Sally Ride*. E. Tovar ZooScanned the MOCNESS samples, J. Ellen assisted with post-processing of the Zoocam images, and J. Trickey assisted with EK80 processing. We thank the Gordon and Betty Moore foundation (Grants no. 3576 and 5479), CCE-LTER (NSF OCE-16-37632), and a DOD SMART fellowship for financial support, and UC Ship Funds for the award of ship-time.

Chapter 2, in full, is a reprint of the material as it appears in **Whitmore, B.M.,** Nickels, C.F. and Ohman, M.D., 2019. A comparison between *Zooglider* and shipboard net and acoustic mesozooplankton sensing systems. *Journal of Plankton Research*, 41(4), pp.521-533. The dissertation author was the primary author on this paper.

2.10 References:

Beaulieu, S.E., Mullin, M.M., Tang, V.T., Pyne, S.M., King, A.L. and Twining, B.S., 1999. Using an optical plankton counter to determine the size distributions of preserved zooplankton samples. *Journal of Plankton Research*, *21*(10).

Beers, J.R. and Stewart, G.L., 1970. The preservation of acantharians in fixed plankton samples. *Limnology and Oceanography*, 15, pp.825-827.

Benfield, M.C., Davis, C.S., Wiebe, P.H., Gallager, S.M., Lough, R.G. and Copley, N.J., 1996. Video Plankton Recorder estimates of copepod, pteropod and larvacean distributions from a stratified region of Georges Bank with comparative measurements from a MOCNESS sampler. *Deep Sea Research Part II: Topical Studies in Oceanography*, *43*(7-8), pp.1925-1945.

Benoit-Bird, K.J., 2009. Dynamic 3-dimensional structure of thin zooplankton layers is impacted by foraging fish. *Marine Ecology Progress Series*, *396*, pp.61-76.

Bradley, C.J., Strickler, J.R., Buskey, E.J. and Lenz, P.H., 2012. Swimming and escape behavior in two species of calanoid copepods from nauplius to adult. *Journal of Plankton Research*, *35*(1), pp.49-65.

Brentnall, S.J., Richards, K.J., Brindley, J. and Murphy, E., 2003. Plankton patchiness and its effect on larger-scale productivity. *Journal of Plankton Research*, *25*(2), pp.121-140.

Brinton, E., 1967. Vertical migration and avoidance capability of euphausiids in the California Current. *Limnology and Oceanography*, *12*(3), pp.451-483.

Briseño-Avena, C., Roberts, P.L., Franks, P.J. and Jaffe, J.S., 2015. ZOOPS-O2: A broadband echosounder with coordinated stereo optical imaging for observing plankton *in situ*. *Methods in Oceanography*, *12*, pp.36-54.

Buskey, E.J., Lenz, P.H. and Hartline, D.K., 2002. Escape behavior of planktonic copepods in response to hydrodynamic disturbances: high speed video analysis. *Marine Ecology Progress Series*, *235*, pp.135-146.

Canny, J., 1986. A computational approach to edge detection. *IEEE Transactions on pattern analysis and machine intelligence*, (6), pp.679-698.

Checkley Jr, D.M., Ortner, P.B., Settle, L.R. and Cummings, S.R., 1997. A continuous, underway fish egg sampler. *Fisheries Oceanography*, *6*(2), pp.58-73.

Cowen, R.K. and Guigand, C.M., 2008. *In situ* ichthyoplankton imaging system (*IS*IIS): system design and preliminary results. *Limnology and Oceanography: Methods*, *6*(2), pp.126-132.

Davis, C.S., Thwaites, F.T., Gallager, S.M. and Hu, Q., 2005. A three-axis fast-tow digital Video Plankton Recorder for rapid surveys of plankton taxa and hydrography. *Limnology and*

Oceanography: Methods, *3*(2), pp.59-74.

De Robertis, A. and Higginbottom, I., 2007. A post-processing technique to estimate the signal-to-noise ratio and remove echosounder background noise. *ICES Journal of Marine Science*, *64*(6), pp.1282-1291.

De Robertis, A., Schell, C. and Jaffe, J.S., 2003. Acoustic observations of the swimming behavior of the euphausiid *Euphausia pacifica* Hansen. *ICES Journal of Marine Science*, *60*(4), pp.885-898.

Dekshenieks, M.M., Donaghay, P.L., Sullivan, J.M., Rines, J.E., Osborn, T.R. and Twardowski, M.S., 2001. Temporal and spatial occurrence of thin phytoplankton layers in relation to physical processes. *Marine Ecology Progress Series*, *223*, pp.61-71.

Di Mauro, R., Capitanio, F. and Viñas, M.D., 2009. Capture efficiency for small dominant mesozooplankters (Copepoda, Appendicularia) off Buenos Aires Province (34ºS-41ºS), Argentine Sea, using two plankton mesh sizes. *Brazilian Journal of Oceanography*, *57*(3), pp.205-214.

Ellen, J., 2018. Improving Biological Object Classification in Plankton Images Using Convolutional Neural Networks, Geometric Features, and Context Metadata. PhD Thesis. University of California, San Diego.

Fields, D.M. and Yen, J., 1997. The escape behavior of marine copepods in response to a quantifiable fluid mechanical disturbance. *Journal of Plankton Research*, *19*(9), pp.1289-1304.

Foote, K.G., Knudsen, H.P. and Vestnes, G.,1983. Standard calibration of echo sounders and integrators with optimal copper spheres. *Fiskdir. Skr. Ser. Havunders*, 17, 335-346.

Foote, K. G., Knudsen, H.P., Vestnes, G., MacLennan, D.N., and Simmonds, E.J., 1987. Calibration of acoustic instruments for fish density estimation: a practical guide. *ICES Coop. Res. Rep.*, 144, pp. 1-69.

Gaskell, D.E., Ohman, M.D. and Hull, P.M., 2019. *Zooglider*-based measurements of planktonic foraminifera in the California Current System. *Journal of Foraminiferal Research*, *49*(4), pp.390-404.

Genin, A., Jaffe, J.S., Reef, R., Richter, C. and Franks, P.J., 2005. Swimming against the flow: a mechanism of zooplankton aggregation. *Science*, *308*(5723), pp.860-862.

Gorsky, G., Ohman, M.D., Picheral, M., Gasparini, S., Stemmann, L., Romagnan, J.B., Cawood, A., Pesant, S., García-Comas, C. and Prejger, F., 2010. Digital zooplankton image analysis using the ZooScan integrated system. *Journal of Plankton Research*, *32*(3), pp.285-303.

Griffiths, G., Fielding, S. and Roe, H.S., 2002. Biological–physical–acoustical interactions. *The Sea*, 12, pp. 441-474.

Grosjean P., and Denis K., 2007. *ZooImage user's manual.* http://www.sciviews.org/zooimage/index.html, last accessed on Mar. 6, 2019.

Guihen, D., Fielding, S., Murphy, E.J., Heywood, K.J. and Griffiths, G., 2014. An assessment of the use of ocean gliders to undertake acoustic measurements of zooplankton: the distribution and density of Antarctic krill (*Euphausia superba*) in the Weddell Sea. *Limnology and Oceanography: Methods*, *12*(6), pp.373-389.

Hamner, W.M., Madin, L.P., Alldredge, A.L., Gilmer, R.W. and Hamner, P.P., 1975. Underwater observations of gelatinous zooplankton: Sampling problems, feeding biology, and behavior. *Limnology and Oceanography*, *20*(6), pp.907-917.

Haury, L.R., McGowan, J.A. and Wiebe, P.H., 1978. Patterns and processes in the time-space scales of plankton distributions. In *Spatial Pattern in Plankton Communities* (pp. 277-327). Springer, Boston, MA.

Haury, L.R., Kenyon, D.E. and Brooks, J.R., 1980. Experimental evaluation of the avoidance reaction of *Calanus finmarchicus*. *Journal of Plankton Research*, *2*(3), pp.187-202.

Herman, A.W., Beanlands, B. and Phillips, E.F., 2004. The next generation of optical plankton counter: the laser-OPC. *Journal of Plankton Research*, *26*(10), pp.1135-1145.

Hopcroft, R.R., Roff, J.C. and Chavez, F.P., 2001. Size paradigms in copepod communities: a re-examination. *Hydrobiologia*, *453*(1), pp.133-141.

McGehee, D.E., O'Driscoll, R.L. and Traykovski, L.M., 1998. Effects of orientation on acoustic scattering from Antarctic krill at 120 kHz. *Deep Sea Research Part II: Topical Studies in Oceanography*, *45*(7), pp.1273-1294.

Menden-Deuer, S.M. and Grünbaum, D., 2006. Individual foraging behaviors and population distributions of a planktonic predator aggregating to phytoplankton thin layers. *Limnology and Oceanography*, *51*(1), pp.109-116.

Moline, M.A., Benoit-Bird, K., O'Gorman, D. and Robbins, I.C., 2015. Integration of scientific echo sounders with an adaptable autonomous vehicle to extend our understanding of animals from the surface to the bathypelagic. *Journal of Atmospheric and Oceanic Technology*, *32*(11), pp.2173-2186.

Möller, K.O., John, M.S., Temming, A., Floeter, J., Sell, A.F., Herrmann, J.P. and Möllmann, C., 2012. Marine snow, zooplankton and thin layers: indications of a trophic link from small-scale sampling with the Video Plankton Recorder. *Marine Ecology Progress Series*, *468*, pp.57-69.

Nichols, J.H. and Thompson, A.B., 1991. Mesh selection of copepodite and nauplius stages of four calanoid copepod species. *Journal of Plankton Research*, *13*(3), pp.661-671.

Nishikawa, J. and Terazaki, M.A.K.O.T.O., 1996. Tissue shrinkage of two gelatinous zooplankton, *Thalia democratica* and *Dolioletta gegenbauri* (Tunicata: Thaliacea) in

preservative. *Bulletin of Plankton Society of Japan*, *43*(1), pp.1-7.

Ohman, M.D., Davis, R.E., Sherman, J.T., Grindley, K.R., Whitmore, B.M., Nickels, C.F. and Ellen, J.S., 2019. *Zooglider*: An autonomous vehicle for optical and acoustic sensing of zooplankton. *Limnology and Oceanography: Methods*, *17*(1), pp.69-86. doi: 10.1002/lom3.10301.

Omori, M. and Hamner, W.M., 1982. Patchy distribution of zooplankton: behavior, population assessment and sampling problems. *Marine biology*, *72*(2), pp.193-200.

Picheral, M., Guidi, L., Stemmann, L., Karl, D.M., Iddaoud, G. and Gorsky, G., 2010. The Underwater Vision Profiler 5: An advanced instrument for high spatial resolution studies of particle size spectra and zooplankton. *Limnology and Oceanography: Methods*, *8*(9), pp.462-473.

Pinel-Alloul, B. and Ghadouani, A., 2007. Spatial heterogeneity of planktonic microorganisms in aquatic systems. In *The Spatial Distribution of Microbes in the Environment* (pp. 203-310). Springer, Dordrecht.

Prairie, J.C., Ziervogel, K., Camassa, R., McLaughlin, R.M., White, B.L., Dewald, C. and Arnosti, C., 2015. Delayed settling of marine snow: Effects of density gradient and particle properties and implications for carbon cycling. *Marine Chemistry*, *175*, pp.28-38.

Pitois, S.G., Bouch, P., Creach, V. and Van Der Kooij, J., 2016. Comparison of zooplankton data collected by a continuous semi-automatic sampler (CALPS) and a traditional vertical ring net. *Journal of Plankton Research*, *38*(4), pp.931-943.

Powell, J.R. and Ohman, M.D., 2015. Changes in zooplankton habitat, behavior, and acoustic scattering characteristics across glider-resolved fronts in the Southern California Current System. *Progress in Oceanography*, *134*, pp.77-92.

Roberts, P.L., Jaffe, J.S., Orenstein, E.C., Laxton, B., Franks, P.J.S., Briseño, C., Carter, M.L. and Hilbern, M., 2014. Pier Recognition: An *In Situ* Plankton Web Camera. *Ocean Optics XXII*. Portland, ME, USA.

Remsen, A., Hopkins, T.L. and Samson, S., 2004. What you see is not what you catch: a comparison of concurrently collected net, Optical Plankton Counter, and Shadowed Image Particle Profiling Evaluation Recorder data from the northeast Gulf of Mexico. *Deep Sea Research Part I: Oceanographic Research Papers*, *51*(1), pp.129-151.

Rovinsky, A.B., Adiwidjaja, H., Yakhnin, V.Z. and Menzinger, M., 1997. Patchiness and enhancement of productivity in plankton ecosystems due to the differential advection of predator and prey. *Oikos*, pp.101-106.

Schulz, J., Barz, K., Mengedoht, D., Hanken, T., Lilienthal, H., Rieper, N., Hoops, J., Vogel, K. and Hirche, H.J., 2009, May. Lightframe on-sight key species investigation (LOKI). In *Oceans 2009-Europe* (pp. 1-5). IEEE.

Seuront, L., Yamazaki, H. and Souissi, S., 2004. Hydrodynamic disturbance and zooplankton swimming behavior. *Zoological Studies*, *43*(2), pp.376-387.

Sheng, J., Malkiel, E. and Katz, J., 2003. Single beam two-views holographic particle image velocimetry. *Applied Optics*, *42*(2), pp.235-250.

Sherman, J., Davis, R.E., Owens, W.B. and Valdes, J., 2001. The autonomous underwater glider "Spray". *IEEE Journal of Oceanic Engineering*, *26*(4), pp.437-446.

Singarajah, K.V., 1975. Escape reactions of zooplankton: effects of light and turbulence. *Journal of the Marine Biological Association of the United Kingdom*, *55*(3), pp.627-639.

Skjoldal, H.R., Wiebe, P.H., Postel, L., Knutsen, T., Kaartvedt, S. and Sameoto, D.D., 2013. Intercomparison of zooplankton (net) sampling systems: Results from the ICES/GLOBEC sea-going workshop. *Progress in Oceanography*, *108*, pp.1-42.

Trevorrow, M.V., Mackas, D.L. and Benfield, M.C., 2005. Comparison of multifrequency acoustic and *in situ* measurements of zooplankton abundances in Knight Inlet, British Columbia. *The Journal of the Acoustical Society of America*, *117*(6), pp.3574-3588.

Weikert, H. and John, H.C., 1981. Experiences with a modified Bé multiple opening-closing plankton net. *Journal of Plankton Research*, *3*(2), pp.167-176.

Wiebe, P.H., Boyd, S.H., Davis, B.M. and Cox, J.L., 1982. Avoidance of towed nets by the euphausiid *Nematoscelis megalops*. *Fisheries Bulletin*, *80*(1), pp.75-91.

Wiebe, P.H., Morton, A.W., Bradley, A.M., Backus, R.H., Craddock, J.E., Barber, V., Cowles, T.J. and Flierl, G.D.1., 1985. New development in the MOCNESS, an apparatus for sampling zooplankton and micronekton. *Marine Biology*, *87*(3), pp.313-323.

Wiebe, P.H. and Benfield, M.C., 2003. From the Hensen net toward four-dimensional biological oceanography. *Progress in Oceanography*, *56*(1), pp.7-136.

Wiebe, P.H., Ashjian, C.J., Gallager, S.M., Davis, C.S., Lawson, G.L. and Copley, N.J., 2004. Using a high-powered strobe light to increase the catch of Antarctic krill. *Marine Biology*, *144*(3), pp.493-502.

Wiebe, P.H., Lawson, G.L., Lavery, A.C., Copley, N.J., Horgan, E. and Bradley, A., 2013. Improved agreement of net and acoustical methods for surveying euphausiids by mitigating avoidance using a net-based LED strobe light system. *ICES Journal of Marine Science*, *70*(3), pp.650-664.

Wilson, S.E. and Steinberg, D.K., 2010. Autotrophic picoplankton in mesozooplankton guts: evidence of aggregate feeding in the mesopelagic zone and export of small phytoplankton. *Marine Ecology Progress Series*, *412*, pp.11-27.

Wong, C.K., 1988. The swimming behavior of the copepod *Metridia pacfica*. *Journal of Plankton Research*, *10*(6), pp.1285-1290.

Yen, J., 1988. Directionality and swimming speeds in predator-prey and male-female interactions of Euchaeta rimana, a subtropical marine copepod. *Bulletin of Marine Science*, *43*(3), pp.395-403.

CHAPTER 3: The influences of the prey field and water column stability on the fine-scale vertical distributions of zooplankton

3.1 Abstract:

We use *Zooglider*, a novel low-power optical zooplankton-sensing glider, to test the covariability of the vertical distributions of six omnivorous zooplankton taxa with three different representations of their potential prey field: small suspended particles, marine snow, and Chl-*a*. We also assess the role water-column stability may play in determining the maximum abundances of zooplankton and their prey sources. We found that small particle and marine snow distributions do not correspond well with Chl-*a* values shallower than the depth of the chlorophyll maximum. Moreover, small particles or marine snow distributions were the primary explanatory variable for all zooplankton taxa tested. Chl-*a* distributions were a secondary explanatory variable for four of the six taxa tested (small copepods, appendicularia-*Fritillaria*, and both night and day large copepods), but an insignificant explanatory variable for the remaining two (appendicularia-others and large protists). An index of spatial overlap (Length of the Receiver Operating Characteristic [LROC]) showed improved overlap of zooplankton with marine snow or small particles than with Chl-*a* in most cases. No relationship was found between maximum water-column stability and the concentrations of zooplankton or their potential prey items. In sum, particle distributions appear to be more informative for explaining distributions of omnivorous zooplankton than Chl-*a* alone.

3.2 Introduction:

For decades, studies of planktonic trophic interactions have utilized vertical chlorophyll distributions as a proxy for the vertical structure of phytoplankton. These distributions are heterogeneous in nature and in most cases exhibit a subsurface chlorophyll maximum layer (SCML) (Cullen, 2015). The depth of the SCML is highly variable and is a function of nutrient and light availability, but also grazing pressure (Cowles et al., 1990; Mullin and Brooks, 1976) , physiological adaptation (Steele, 1964), sinking rate, buoyancy regulation, and swimming behavior (Cullen, 2015). Additional physical variables influencing the depth of the SCML are density, temperature, water-column stability (Lasker, 1981), turbulence, and internal waves (Franks, 1995). The depth of the chlorophyll maximum can sometimes correspond to the depth of the phytoplankton biomass maximum (Cullen, 1981). Thus, chlorophyll distributions can provide insight as to where potential food sources are located in relation to grazers, as long as they are measured at a scale at which the grazer interacts.

In addition to chlorophyll, vertical distributions of suspended detrital particles or organic aggregates (i.e., marine snow) are also measured in the water column. Marine snow ranges in size from sub-millimeters to centimeters, as measured by equivalent circular diameter (ECD). Typically, "large" marine snow is classified as having an ECD greater than 500 µm (Alldredge and Silver, 1988; Silver et al., 1978). These larger particles are primarily made up of biotic material, e.g., planktonic remains, fecal pellets (Stoecker, 1984; Turner and Ferrante, 1979), and molts (Fowler and Knauer, 1986), but can also contain inorganic components, e.g., clay aggregates, sediment particles, trace elements, and other compounds (see references in Fowler and Knauer, 1986). Due to varied sinking rates, it is possible for layers of higher

concentrations of marine snow to form at sharp density transitions (MacIntyre et al., 1995; Prairie et al., 2013).

Layers of marine snow are a potential food source for zooplankton grazers. Based on the evidence that many zooplankton taxa are often associated with marine snow, the broad size range of marine snow, and the presence of fecal pellets, Silver et al. (1978) argued that marine snow could be serving as a food source for zooplankton. Alldredge (1972) showed that planktonic copepods can use discarded appendicularian houses as a food source. Malkiel et al. (2006) revealed through holography that high densities of copepods were coincident with maximum concentrations of marine snow. Using a video plankton recorder in combination with a Multi-net, Möller et al. (2012) found that distributions of marine snow and copepods are positively correlated. Furthermore, Malkiel et al. (2006), Möller et al. (2012), and Ohman (2019) captured images of copepods appearing to be attached to marine snow. Shipboard incubations have confirmed that amphipods (*Themisto compressa),* copepods (*Calanus pacificus*), and euphausiids (*Euphausia pacifica*) all consume marine snow (Dilling et al.,1998; Lampitt et al., 1993). Euphausiid consumption of marine snow can influence carbon flux in two ways. Euphausiid-consumed marine snow is repackaged into fecal pellets that rapidly sink out of the euphotic zone, while the euphausiid feeding process fragments large aggregates of marine snow into smaller, slower-sinking particles that have longer residence times in surface waters (Dilling and Alldredge, 2000).

In contrast to direct feeding on suspended particles, some zooplankton taxa exhibit flux feeding behavior on sinking particles and marine snow. The concept of flux feeding was introduced by Jackson (1993) as an explanation for the existence of particle-consuming zooplankton (e.g., pteropods) in the subeuphotic zone, and has since been confirmed by several

studies. *In situ* observations from the particle sensing system SOLOPC (Checkley et al., 2008), a combined Sounding Oceanographic Lagrangian Observer (SOLO) and Laser Optical Particle Counter (LOPC), showed numerous zooplankton-like particles (i.e., flux feeders) at the base of a particle-rich (marine snow) zone (Jackson and Checkley, 2011). Aulosphaeridae, an abundant family of Phaeodaria in the California Current Ecosystem, are capable of intercepting > 20% of sinking particles produced in the euphotic zone before these particles reach 300 m (Stukel et al., 2018). *Limacina helicina* (pteropod) and Aulosphaeridae were found to be responsible for 10-20% and ~10%, respectively, of the total carbon flux attenuation directly below the euphotic zone (Stukel et al., 2019).

Advances in sampling technology have enabled the resolution of vertical distributions of chlorophyll, marine snow, and zooplankton to improve from meter to centimeter scales (Cowles et al., 1990; Doubell et al., 2014; Mitchell and Fuhrman, 1989). When viewed at the scale at which most planktonic organisms interact (<< 1 m), local peaks in chlorophyll concentration can exceed 55 times the ambient chlorophyll concentration (Ryan et al., 2008), and marine snow concentrations have been observed at 10 times above ambient concentrations (Alldredge et al., 2002). Typical maximum concentrations are still several times ambient conditions (McManus et al., 2003; Möller et al., 2012; Sullivan et al., 2010). These local peaks in concentration can range in thickness from a few centimeters to a few meters and are often referred to as "thin layers" (Dekshenieks et al., 2001). However, such fine-scale distributions are also susceptible to changes in water-column stability. Water-column stability is often measured by the strength of the vertical density gradient, (i.e., the buoyancy frequency squared, N^2). Higher N^2 means a more stratified, stable water column, and near-zero N^2 is associated with unstable water columns (Dekshenieks et al., 2001).

Dekshenieks et al. (2001) found that 71% of chlorophyll-*a* thin layers were spatially associated with the pycnocline and that no phytoplankton layers were observed when the Richardson number, a metric for the likelihood of shear-driven mixing (MacIntyre et al., 1995), was less than 0.23. Ríos et al. (2016) showed that stratified water columns had greater concentrations of integrated chlorophyll-*a* concentrations and SCML, and well-mixed conditions had more homogenous chlorophyll-*a* distributions. Greer (2013) showed in Monterey Bay, CA, that thin layers of phytoplankton were most common when the water column was thermally stratified, and that different zooplankton taxa exhibited different vertical patterns in relation to thin layers. The results of Haury et al. (1990) suggest broadened vertical distributions of zooplankton species in relation to strong wind.

The association of planktonic layering in stable ocean conditions was first described in 1975 when Lasker showed that a storm effectively diluted the previous chlorophyll maximum and specific prey dinoflagellates to levels that were unable to sustain first-feeding anchovy larvae. The association between thin layers, larval survival, and stable ocean environments lead to Lasker's Stable Ocean Hypothesis (SOH). Lasker (1975, 1981) hypothesized that the survival of larval fishes required suitable concentrations of prey organisms in coincidence with larval patches and that such conditions were only met in stable ocean conditions. Since then, several studies have been conducted to test the effect of water-column stability on zooplankton. Purcell et al. (2014) showed significant differences in ctenophore and copepod distributions between weakly and strongly stratified environments. McClatchie et al. (2007) found sardine larval densities to be higher in more stable water columns.

In contrast to the SOH, other researchers have proposed that turbulence enhances encounter rates of individuals and particles. Encounter is a necessary component of the

predation sequence, i.e., the sequential probabilities that a prey item is encountered, attacked, captured, and ingested (Ohman, 1988). Rothschild and Osborn (1988) argued that contact rates between predator-and-prey plankton do not rely solely on relative density of the organisms, but also on the relative velocities of the organisms. Mixing can be driven by winds, tides, breaking internal waves, shear instabilities, and convective cooling. Mixing events and the resulting overturns in the water column can occur anywhere within stratified water columns (MacIntyre et al., 1995). Therefore, according to the Rothschild and Osborn hypothesis (1988), higher encounter rates are expected during mixing events and more turbulent conditions.

However, an encounter does not always result in ingestion, as predation is the product of the probabilities of each component of the predation sequence (MacKenzie et al., 1994), and turbulence can make prey capture more difficult (Pécseli et al., 2012). Therefore, further analysis is needed to assess whether overall predation increases during mixing events. Sundby and Fossum (1990) tested this hypothesis and found that contact rate between first-feeding Arcto-Norwegian cod larvae and copepod nauplii increased by a factor of 2.8 with increases in wind speed. Franks (2001) proposed the turbulence avoidance hypothesis as an alternative explanation to turbulence directly enhancing ingestion rates. The turbulence avoidance hypothesis argues that organism behavior (i.e., swimming below the mixed layer when turbulent conditions are present) serves to concentrate organisms, thereby increasing encounter rates (Franks, 2001). Turbulence allowed larval cod (*Gadus morhua*) to sustain high ingestion rates of nauplii, despite low prey densities, < 5 animals L^{-1} (Kristiansen et al., 2014). The influence of turbulence on planktonic encounter rates can ultimately manifest in optimal foraging and predation strategies (Pécseli et al., 2014). For instance, found that suspension feeding has an

advantage over ambush feeding at high turbulence levels, whereas cruise feeding becomes more successful in low turbulence (Visser et al., 2008).

In summary, zooplankton can be associated with SCML and marine snow in several ways. SCMLs have been shown to be associated with stratified water columns and to be diluted during mixing events. There are conflicting hypotheses for how zooplankton are affected by disrupted SCMLs. Lasker's SOH argues that SCMLs are necessary for survival success. On the other hand, Rothschild and Osborne argue that mixing events enhance encounter rates and possibly increase ingestion rates of mesozooplankton. Observations confirming either mechanism in the ocean would have significant consequences for our understanding of trophic transfer rates, the fate of marine snow, and mesozooplankton survival.

For this reason, we address the following questions in this chapter: of potential food sources, are the vertical distributions of zooplankton better associated with chlorophyll-*a*, small particles, or marine snow? How does water column stability effect chlorophyll-*a*, marine snow, small particles, and grazing mesozooplankton distributions?

We address these questions using *Zooglider*, a fully autonomous mesozooplankton sensing glider, outfitted with a pumped conductivity-temperature-depth (CTD) probe, Chl-*a* fluorometer, and a low-power telecentric shadowgraph imaging camera (Zoocam) that is capable of resolving vertical distributions of mesozooplankton and marine snow at 5 cm vertical resolution (Gaskell et al., 2019; Ohman et al., 2018; Ohman, 2019; Whitmore et al., 2019).

3.3 Methods:

Zooglider was deployed in the San Diego Trough, approximately 30 km west of San Diego, CA. There were seven 1-2 week deployments from July 2017 to October 2018 (Table

3.1). Deployments were generally spaced about 2 to 3 months apart. Six of the seven deployments sampled approximately the same region with the mean dive locations < 1 km apart. The first deployment, July-August 2017, sampled ~10 km away from and had a much shorter duration than the other six deployments. Average water depth for the set of six deployments in proximity and the single offset deployment were > 900 m and >800 m, respectively.

Zooglider conducted 8 dives per day spaced by ~3-hour intervals to depths of at least 400 m. Each dive had an average vertical ascent speed of 10 cm s^{-1}, an average ascent angle of ~17°, and sampling was conducted solely during ascent. *Zooglider* was equipped with a Seabird CP41 pumped CTD and a Seapoint mini-SCR Chl-*a in vivo* fluorometer, both of which were recorded at 8 s intervals. *Zooglider* also has a 'Zoocam' that acquires ~1.2 MB images at 2 Hz. Each image sampled a 250 mL volume at a resolution of 40 µm $pixel^{-1}$. Due to the different sampling frequencies, each CTD measurement was assigned to the frame with the nearest timestamp, and linear interpolation was used to assign CTD measurements to frames that occurred between CTD measurements. For a complete description of *Zooglider* engineering details see Ohman et al., 2018.

3.3.1 Image Processing:

All images were flat-fielded, segmented, and cropped into specific regions of interest (ROI) following Ohman et al. (2018). If a ROI had an ECD between 0.25 and 0.45 mm, it was counted, but not extracted, because we found ROIs of that size consisted of too few pixels to assign a meaningful identity. If a ROI had an ECD ≥ 0.45 mm, it was extracted. Each extracted ROI had 70 geometric features calculated and was initially classified using a novel machine-learning algorithm (Ellen et al., 2019) into one of 27 categories. All of these categories were manually validated, with the exception of the "marine snow" category due to the number of

images. This machine-learning algorithm was shown to have a ~6.6% False Positive rate with respect to wrongly classifying one of the other 26 categories as marine snow (Ellen et al., 2019). Furthermore, this algorithm had a 1% False Positive rate with falsely classifying one of the six zooplankton taxa used in this study as marine snow (Ellen et al., 2019). Approximately half of the dives per deployment were manually validated and used for data analysis. Manual validation consisted of analyzing consecutive dives for ~5 consecutive days per deployment. Dives were labeled as either day or night depending on how the dive start and end times compared with nautical twilight. The total dives completed, dives processed, and number of day/night dives for each deployment are shown in Table 3.1.

Six categories of organisms were selected for this study consisting of zooplankton taxa that are primarily suspension-feeding or flux-feeding (Stukel et al., 2019) organisms: appendicularia (*Fritillaria*), appendicularia (others), large protists (including Acantharia, Collodaria, Foraminifera, and Phaeodarea, but dominated by Acantharia), small copepods (feret diameter $\leq$ 3 mm), large copepods day and night (feret diameter > 3 mm). The 3 mm feret diameter threshold for small and large copepods was chosen based on significant differences in respective day and night weighted mean depths (non-overlapping 95% confidence intervals). These six zooplankton categories consistently had the highest abundances among all deployments and have been shown to be associated with and/or feed upon either phytoplankton or marine snow (Möller et al., 2012; Sato et al., 2003; Stukel et al., 2019).

The potential prey spectrum for grazing/omnivorous zooplankton included small counted, but unidentified, ROIs between 0.25 and 0.45 mm (hereafter referred to as small particles), any ROIs identified as marine snow, and chlorophyll-*a* fluorescence digital counts (Chl-*a)*. Microzooplankton were most likely included in the counts of marine snow and small particles,

but could not be identified separately. For the marine snow and small particles, biovolume estimates were made using the volume of a sphere ($4/3\pi r^3$), assuming the third dimension (depth) was equivalent to particle width. The radius for snow biovolume was half the calculated ECD of each ROI labeled as snow, while the radius for the small particles was assumed to be a constant 0.175 mm (half the midpoint value for particles with ECD between 0.25 and 0.45 mm). This assumption, which does not allow for variation in the size of the small particles, was made because no size information was available for the small ROIs, which were not retained during the ROI detection process.

3.3.2 Physical and Biological Data Processing:

To compare physical and biological properties of the water column across deployments, the deployment means of potential density (σ_θ), buoyancy frequency squared (N^2), marine snow, small ROIs, and Chl-*a* were plotted against their corresponding depths (as pressure).

Vertical distributions of the concentrations (number L^{-1} or mm^3 of biovolume L^{-1}) for all categories were corrected for volume of water sampled per image and binned at 0.8 dBar intervals to correspond to the smallest vertical distance between CTD measurements. All categories were initially dichotomized by day and night to check for diel differences. Significant day-night differences in weighted mean depths ($p < 0.001$) were observed in both the large and small copepod categories. However, partitioning the small copepods by time of day did not significantly change results of their prey preference. Therefore, small copepods, *Fritillaria*, appendicularia-others, and large protists were analyzed as one pooled day+night group, whereas large copepods remained dichotomized by day and night samples.

For each deployment, all zooplankton taxa were also plotted as functions of each prey source to determine whether certain prey sources might better explain each respective vertical

profile. All profile data were binned at 2 dBar, and the means of all binned dives were plotted. To assess the effect of water-column stability on prey and grazer abundances, all prey sources and zooplankton taxa maximum abundances were analyzed as functions of the maximum $\log(N^2)$ value for each dive.

3.3.3 Calculation of Length of the Receiver Operating Characteristic:

To determine the degree of spatial overlap between vertical profiles, we used the Length of the Receiver Operating Characteristic (LROC), a statistic described by Maswadeh and Snyder (2012 and 2015). A Receiver Operating Characteristic (ROC) is created by plotting two sets of data on the same axis. These two sets of data will have four subdivisions, true positive (TP), true negative (TN), false positive (FP), and false negative (FN) associations. For example, if comparing two vertical distributions (e.g., copepods and Chl-*a* fluorescence), a TP is the probability of correctly identifying a copepod as a copepod, while a TN is the probability of correctly identifying a fluorescence count. Likewise, a FP is the probability of incorrectly classifying a fluorescence count as a copepod, and a FN is the probability of identifying a copepod as a fluorescence count. Plotting the TP rate for a given object as a function of the FP rate, throughout the extent of the profile, yields the ROC curve. After the ROC curve is generated, a summation of Euclidean distances between all points on the curve yields the LROC. LROC can vary between 1.41 (complete overlap of two variables) and 2.0 (complete separation of two variables). For a full description of the LROC method see Maswadeh and Snyder (2012 and 2015). LROCs were calculated for all predator taxa compared to each potential prey source at 2 dBar bins. Means and 95% confidence intervals were generated from all of the obtained LROC values. When the LROC values were analyzed per deployment, the rank order of zooplankton overlap with each prey source (i.e., small copepods overlapping best with small

particles) was consistent amongst deployments, with slight variations in the degree of overlap throughout the year. Therefore, values from all deployments were combined to form an across-mission overview of how particular zooplankton overlap with preferred prey sources.

3.3.4 Generalized Additive Models:

We created Generalized Additive Models (GAMs) to find the best explanatory variable for vertical abundance distributions of each zooplankton taxon, in R-studio (mgcv library, Wood 2017). The abundance of each taxon was estimated as a function of three predictor variables (Chl-*a*, marine snow, and small particles). Each predictor variable used a simple spline and 'k' was set to 5 for all variables to limit overfitting of the sparser data density near the maximum concentrations of each predictor variable. The best results (greatest deviance explained) were obtained for all taxa by combining all three predictor variables into one model. However, to simplify the model and identify the relative roles of the different prey types on each zooplankton taxa abundance, predictor variables were removed if they were deemed to have no significant effect on model performance. In this study, a significant effect on model performance was defined as a reduction of greater than 5% from the maximum deviance explained using all three predictor variables combined.

3.4 Results:

3.4.1 Variations in physical and biological variables across deployments:

Potential density (σ_θ) profiles depicted a range of mixed layer depths and pycnocline strengths (Fig. 3.1A). There was a progression of stratification from a shallower mixed layer in the summer (July-August 2017 and 2018), to a better defined, somewhat deeper mixed layer during the winter (January-February 2018) and spring (April 2018). N^2 profiles showed clear

differences in the degree of density stratification among the deployments (Fig. 3.1B). The July-August (2017 and 2018) deployments were the most stratified, while the January-February 2018 and April 2018 deployments were the least stratified. Chl-*a* profiles all had a single SCML and showed relatively low values of Chl-*a* in the near surface waters (Fig. 3.1C). Conversely, the maxima of the marine snow (Fig. 3.1D) and small particles (Fig. 3.1E) persisted over a much wider depth range and often had the highest concentrations in near-surface waters.

Fritillaria and appendicularia-others displayed markedly different distributions, with *Fritillaria* generally showing deeper abundance maxima than appendicularia-others (Fig. 3.2A and 2B). Large protists (dominated by acantharians) usually had the greatest densities from 0-50 dBar, and during summer months (July-August 2017 and 2018) had noticeably higher densities near the surface < 20 dBar (Fig. 3.2C). Small copepods (Fig. 3.2D) and appendicularian-others profiles did not have clearly defined maxima; however, both taxa generally showed their greatest densities in shallower waters. Large copepods exhibited classic diel vertical migration (DVM) behavior, with daytime distributions between 0 and 400 dBar and greater nighttime abundances concentrated shallower than 50 dBar (Fig. 3.2E and 3.2F).

3.4.2 Correlation with Potential Prey:

All of the prey variables had strong linear/curvilinear relationships with one another in deeper waters (R_{Dp}^2) between 100 dBar to the depth of the Chl-*a* maximum (DCM) (all R_{Dp}^2 values > 0.85), regardless of the degree of stratification (Fig. 3.3, black x's). However, from the DCM to the surface, the correlation coefficients (R_{Sh}^2) between prey sources were weaker and more variable (R_{Sh}^2: 0.049-0.794; Fig. 3.3, red circles). In near-surface waters, marine snow and small particles had the best correlation for each prey source combination, regardless of deployment. In Jan-Feb 2018, the shallow concentrations of marine snow and small particles

(red circles) remained consistently higher than their corresponding values deeper in the water column (black X's, at the same Chl-*a* count), (Fig. 3.3A and 3.3B). However, during the Jul-Aug 2018 deployment, the concentrations of marine snow and small particles had a more parabolic shape in the near-surface water (red circles, Fig. 3.3D and 3.3E).

3.4.3 Correlation of Zooplankton Taxa and Potential Prey:

Small copepod abundance showed a strong positive relationship with all prey variables in the depth zone from 100 dBar to the DCM, regardless of the stratification level of the deployment (R_{Dp}^2>0.90, black X's, Fig. 3.4A-C and Fig. 3.5A-C). However, in near-surface waters, (DCM to the surface), small copepod abundance had more variable correlation coefficients with each prey source in the less stratified deployment (Fig. 3.4, R_{Sh}^2: 0.036-0.972) and more intermediate correlation coefficients during the highly stratified deployment (Fig. 3.5, R_{Sh}^2: 0.362-0.520). In contrast, large copepod abundances generally showed poorer correlations with all potential prey variables. Daytime large copepod abundance (Fig. 3.4D-4F and 3.5D-5F) was not well explained by any potential prey variable regardless of deployment stratification or location in the water column (R_{Dp}^2: 0.125-0.422; R_{Sh}^2: 0.013-0.176). Nighttime large copepod abundance (Fig. 3.4G-4I and Fig. 3.5G-5I) had greater correlation with each prey variable (R_{Dp}^2: 0.569-0.924; R_{Sh}^2: 0.197-0.669) compared to the large copepod daytime population.

Fritillaria abundance had an intermediate positive relationship with prey at depth (R_{Dp}^2: 0.442-0.692) and weak to negligible relationship with prey near the surface, R_{Sh}^2: 0.034-0.287, (Fig. 3.6A-6C and Fig. 3.7A-7C). Compared to *Fritillaria*, appendicularia-others abundance had a much stronger positive relationship, R_{Dp}^2: 0.909-0.948, with prey at depth and a highly variable weak to intermediate relationship at the surface, R_{Sh}^2: 0.022-0.614, (Fig. 3.6D-6F and Fig. 3.7D-7F). Large protists also showed high correlations with all prey variables at depth R_{Dp}^2: 0.798-

0.920 and weaker correlations near the surface, R_{Sh}^2: 0.000-0.578, (Fig. 3.6G-6I and Fig. 3.7G-7I).

Overall, small copepods, appendicularia-others, large protists, and nighttime large copepods consistently had higher correlations with all prey sources than daytime large copepods and *Fritillaria*. From these associations alone, it was difficult to distinguish any preferred prey source.

3.4.4 Influence of N^2 on Prey and Zooplankton Abundance:

There was no significant relationship between the magnitude of any potential prey maximum abundance and the maximum log(N^2) in a profile (R^2<0.05; p>0.05; Fig. 3.8). Moreover, there was no significant relationship between the maximum log(N^2) and zooplankton taxon abundance (R^2<0.14; p>0.05; Fig. 3.9).

3.4.5 LROC Association of Zooplankton with Potential Prey:

Fritillaria (Fig. 3.10A) and large copepods (day) (Fig. 3.10E) showed no significant difference in overlap among the three prey sources. Appendicularia-others (Fig. 3.10B) and large protists (Fig. 3.10C) had significantly greater overlap with both marine snow and small particles than with Chl-*a*. Small copepods had the greatest spatial overlap with small particles and the worst spatial overlap with Chl-*a* (Fig. 3.10D). Large copepods (night) had significantly greater overlap with Chl-*a* and marine snow compared to small particles (Fig. 3.10F). Overall, small copepods showed the greatest overlap with each potential prey among all taxa considered. In contrast, large copepods, both day and night, show the least overlap with the potential prey. *Fritillaria* also showed limited overlap with these potential prey, while appendicularia-others and large protists showed similar overlaps with marine snow and small particles.

3.4.5 GAM Results:

GAM results showed that small copepods had the greatest deviance explained by potential prey sources (52.2%) of any taxon (Table 3.2). The abundance of small copepods was best explained by small particles, and secondarily by Chl-*a*. Chl-*a* appeared to have a linear positive effect on small copepod abundance, with a potential threshold effect at higher Chl-*a* counts (>800, Fig. 3.11A). Small particles had a positive linear effect on small copepods, similar to Chl-*a*, until concentrations of small ROIs exceed ~30 $mm^3 L^{-1}$. At such high concentrations the effect on small copepods increased to a greater extent, with increasing small particle concentration (Fig. 3.11B). Marine snow was deemed not to be a significant variable for small copepods.

In contrast to small copepods, the abundance of large copepods showed much less deviance explained for either the day (3.9%) or night (21.0%) categories. The significant prey variables, for large copepods (both day and night) were marine snow and Chl-*a*, (Fig. 3.11C-F, and Table 3.2). Marine snow had a positive linear association with large copepod nighttime abundance until concentrations of ~150 $mm^3 L^{-1}$ are reached (Fig. 3.11F). Marine snow concentrations exceeding 150-200 $mm^3 L^{-1}$ were relatively rare, but there was a suggestion of a weakening negative association at such high concentrations.

Compared to both the small and large copepods, both appendicularia-others and *Fritillaria* had intermediate and low levels of deviance explained (32.8% and 13.7%, respectively). Marine snow was the primary predictor variable for both appendicularia categories (F-values, Table 3.2), with both marine snow spline functions showing strong positive linear relationships up to ~50 $mm^3 L^{-1}$ (Figs. 12B and 12D). The remaining significant prey

variables were Chl-*a* for *Fritillaria* (Fig. 3.12A) and small particles for both appendicularia others and *Fritillaria* (Fig. 3.12C and 12E).

Large protists also showed only intermediate levels of deviance explained (24.9%). There was an increasing positive relationship between marine snow and large protists until concentrations exceeded 50 mm^3 L^{-1} (Fig. 3.12F). The small particles spline for large protists (Fig. 3.12G), showed a weaker positive relationship for concentrations up to 20 mm^3 L^{-1}, and then a negative relationship for concentrations exceeding 30 mm^3 L^{-1}.

3.5 Discussion:

Zooglider permitted resolution of fine-scale vertical distributions of Chl-*a*, marine snow, small suspended particles, in addition to several zooplankton including copepods, appendicularians and large protists. Analyses of these vertical profiles revealed that small particles, marine snow, and many zooplankton taxa had depth dependent relationships with Chl-*a* that changed throughout the year. For most zooplankton taxa, vertical overlap was generally strongest between most zooplankton taxa for either small particles or marine snow distributions compared to Chl-*a*. Moreover, small particles or marine snow biovolume were the primary explanatory variables for all zooplankton taxa abundances that we tested. Chl-*a* distribution was a secondary explanatory variable for four of the six taxa (small copepods, appendicularia-*Fritillaria*, and both night and day large copepods), and an insignificant explanatory variable for the remaining two taxa (appendicularia-others and large protists). Additionally, no relationships were found between maximum water column stability and the maximum concentrations of zooplankton or their potential prey items.

Pronounced differences above and below the DCM in the relationships between Chl-*a* fluorescence and other particles illustrate that a given Chl-*a* value can be associated with markedly different concentrations of marine snow or small particles, depending on the depth in the water column. Furthermore, these depth disparities in concentrations vary by time of year and degree of water-column stratification. This exposes a distinct limitation of using only Chl-*a* values as predictors of prey resources to omnivorous zooplankton.

This disagreement of Chl-*a* with particle distributions is likely due to three inherent sources of uncertainty associated with in vivo fluorescence measured in situ. The first is non-photochemical quenching (NPQ) of Chl-*a*, which is known to alter the fluorescence signal per unit Chl-a on a diel cycle, resulting in a diminution in recorded fluorescence in daylight hours (Cullen and Lewis 1995; Omand et al., 2017). However, our previous work with this type of glider-mounted Chl-*a* fluorometer has shown that NPQ was most significant in the upper 20-30 m of the water column in southern California waters (Davis et al. 2008). Moreover, extracted Chl-*a* and *in vivo* fluorescence are extremely well correlated with each other near our study site in the San Diego Trough (Whitmore et al., 2019). Furthermore, daytime and nighttime vertical distributions of most zooplankton categories showed no differences by time of day (see below). The second source of uncertainty is dark adaptation (Falkowski and Kiefer, 1985; Chekalyuk and Hafez, 2011) and depth-dependent Carbon:Chl-a ratios (Taylor et al., 2011). The depth-dependent Carbon:Chl-*a* effect will certainly influence our profiles. The third source of uncertainty is the species composition and community structure of the phytoplankton, some of which will be solitary picoplankton that are too small to be readily ingested by suspension-feeding crustaceans (Calbet et al., 2000) and others of which will be large (length > 14 mm)

and/or spiny chains that are essentially unavailable as prey to most crustacean zooplankton (Ohman, 2019).

The uncertainties associated with *in situ* measured *in vivo* fluorescence can explain some of the different relationships observed between Chl-*a* and particle distributions at different water column stabilities. For instance, in the less-stratified winter deployment (Jan-Feb 2018) the near surface small particles abundances were independent of Chl-*a*. As mixing can enhance nutrient flow to diatoms and other non-motile phytoplankton (Barton et al., 2014; Dell'Aquila et al., 2017), this lack of dependence on Chl-*a* was likely due to lower chlorophyll-*a* concentrations per unit C (Falkowski and LaRoche 1991). Lower surface Chl-*a* values with similar concentrations of small particles would be consistent with decreasing Carbon:Chl-*a* with greater depth (i.e., decreasing light levels (Taylor et al., 2011)). In contrast, the quadratic relationship of small particle concentrations to Chl-*a*, observed in Jul-Aug 2018, is likely attributable to nutrient limitation. Nutrient limitation ultimately results in the surface-dwelling phytoplankton becoming senescent and sinking rapidly out of the water column (Bienfang et al., 1982; Smayda and Boleyn, 1966).

The relationship between marine snow/small particles and Chl-*a* is further complicated by the fact that potential prey sources are not independent. The true identity of the small particles (e.g., microzooplankton, phytoplankton) could not be determined with the current Zoocam image resolution (40 μm $pixel^{-1}$), so we cannot determine the extent of overlap between Chl-*a* and small particle distributions, although we assume there is some coincidence. The marine snow category could also be contributing to Chl-*a* measurements caused by undigested phytoplankton, fecal pellets, discarded appendicularian houses, or other organic matter. Additionally, some recognizable diatoms could have been incorrectly classified as marine snow,

as this category was not manually validated. However, previous studies have shown this classifier to have a false positive rate, of falsely labeling recognizable diatoms as snow, of 5% (Ellen et al., 2019).

3.5.1 Copepods:

Bilinear and nonlinear relationships (i.e., marine snow/small particles and Chl-*a*) were also observed for both small copepods and large copepods at night as functions of Chl-*a*. Therefore, single Chl-*a* values could be associated with two different abundances of small copepods and large (night) copepods. Overall, the primary predictor variables for small copepods and large copepods (night) were small particles and marine snow, respectively. We interpret this result as indicating that surface-dwelling copepods were likely feeding on the small particles (small copepods) and marine snow (large copepods-night) that were associated with the lower Chl-*a* levels at the surface. The lower explanatory power for the large copepods suggests that they have a different preferred prey field compared to the small copepods. Alternatively, these larger copepods could be performing foraging sorties that would decrease the spatial overlap with their prey when they were not actively feeding (Karaköylü, 2010)

This difference in prey type could also be explained by the difference in diversity of copepod types within the large and small copepod taxa. The large copepods included predatory, omnivorous, and herbivorous copepods, while the smaller copepods were a mix of herbivores and omnivores. The difference in deviance explained between the day and night large copepods was likely attributed to DVM behavior, such that the day vertical distributions were constrained more by visual predation risk (e.g., Ohman and Romagnan, 2016) than by prey availability.

The copepod relationship with particle size and particle concentrations in the water column has been observed before. Approximately 5% of images of copepods (namely

Pseudocalanus acuspes) acquired by the Video Plankton Recorder showed copepods directly attached to marine snow particles and exhibiting feeding behavior (Möller et al., 2012). Kodoma et al., (2018) showed that copepods *Microsellela* spp. and *Oncaea* spp. consumed approximately 13% of discarded appendicularian houses. Wilson and Steinberg (2010) showed that copepods feeding on marine snow could enhance the flux of picoplankton to the benthos through fecal pellet production. Understanding the grazing preferences in copepods could improve our knowledge on the flux of carbon and other minerals to the seafloor.

3.5.2 Appendicularia

The lower deviance explained by both appendicularian taxa (Appendicularia-others and *Fritillaria*) compared to the small copepods means that the prey predictor variables may not be representative of the preferred prey of appendicularia. A portion of this difference, in deviance explained, may be attributed to the preferred prey size of appendicularia-others and *Fritillaria* being smaller than particles that were directly observable with the Zoocam's image resolution (40 µm pixel^{-1}). Appendicularia obtain ~80% of their diets generally from particles with diameters less than 15 µm (*Oikopleura* spp.) and 7 µm (*Fritillaria* spp.*)* (Fernández et al., 2004), although larger particles can be ingested, as it is the minimum particle size (and other attributes) that impacts how particles interact with the appendicularian feeding filters (Conley and Sutherland, 2017). Some of these smaller (appendicularian prey-sized) particles may be accounted for in the Chl-*a* and small particle measurements; however, the overall abundance contribution of these smaller sized particles may be diluted by the presence of larger or more fluorescent particles.

The appendicularian association with marine snow could be an indicator of great abundances of smaller (prey-sized) senescent phytoplankton cells, that are capable of

flocculating to form larger marine snow aggregates. Alternatively, it is likely that the positive association between marine snow and appendicularian abundance is a result of a high number of discarded appendicularian houses co-occurring with the appendicularians themselves. The discard of appendicularian houses might also help explain the great difference in deviance explained between appendicularia-others and *Fritillaria*. *Fritillaria* spp. renew their houses up to 40 times per day, while appendicularia-others (e.g., *Oikopleura* spp.) have house renewal rates ranging from 2-27 houses per day (Sato et al., 2003). The higher house-renewal rate of *Fritillaria* could be necessary to compensate for a feeding house that is more prone to clogging/lower feeding efficiency as a result of particles. Therefore, if *Fritillaria* spp. are more susceptible to house clogging, it would be more beneficial to them to inhabit a different sector of the water column with lower concentrations of particles. A particle concentration-driven vertical shift could also account for Chl-*a* as a significant variable for *Fritillaria*, but not for appendicularia-others.

Our observation that appendicularia-others were better explained by marine snow and small particles compared to Chl-*a* contrasts with previous work that found water column stability and Chl-*a* to be the main environmental factors affecting appendicularian distributions (Capitanio and Esnal, 1998; Kodama et al., 2018; Spinelli et al., 2013, 2015; Tomita et al., 2003). This difference is most likely due to systematic limitations of physical net collection. Net systems are unable to resolve the fine-scale vertical distributions of marine snow and small particles within the water column, while *Zooglider* can resolve these profiles.

3.5.3 Large Protists:

Large protists showed relatively low levels of deviance explained by marine snow and small particles, with marine snow the primary positive predictor variable. The increasing

positive relationship between marine snow and large protists may be indicative of how the large protists utilize marine snow as a food source. The negative effect and reduced positive effect of high concentrations of small particles and marine snow, respectively, on large protists might be attributable to a diminution in irradiance caused by increased particle concentration within the water column. Most of the large protists identified in this study (~90-95%) were acantharians. Michaels et al. (1995) also observed acantharians as the numerically dominant large protist in the upper 150 m of the water column. Many acantharia species have photosymbionts (Decelle and Not, 2015), and therefore need to reside in the surface waters with greater irradiance. If these photosymbionts provided the dominant component of nutrition for large protists, it could account for the lower deviance explained.

Our results contrast with recent evidence that Chl-*a*, the depth of the Chl-*a* maximum, and temperature were the best explanatory variables for acantharians (R^2=0.43, Biard and Ohman, in review). This difference is most likely attributable to the minimum detection size of the Underwater Vision Profiler (UVP) (> 600 µm); therefore, the small particles, marine snow, and acantharians (< 600 µm) that *Zooglider* was able to detect were likely missed by the UVP (Biard et al., 2016; Biard and Ohman, in review).

The grazing habits of mineralized protists have been difficult to judge in the past, as net collection often breaks the fragile spines and pseudopodia of many protists (Nakamura et al., 2017; Whitmore et al., 2019). Furthermore, acantharians still intact after net collection dissolve in fixed samples if not supersaturated with strontium sulfate (Beers and Stewart, 1970). With recent advances in imaging technology, we are starting to observe that mineralized protists account for a larger amount of biomass within the near-surface waters than previously thought

(Biard et al., 2016; Biard and Ohman in review; Nakamura et al., 2017; Whitmore et al., 2019) and are partitioned into taxon-specific vertical habitats (Biard and Ohman in review).

3.5.4 Water Column Stability:

Water column stability, as measured by the maximum of N^2, appeared to have no consistent effect on the concentrations of prey or omnivorous zooplankton considered here. This result was inconsistent with Lasker's (1981) SOH, that stability was necessary to maintain heightened levels of prey concentrations in the larvae's environment. I attribute this inconsistency to the prey organism (dinoflagellates) that Lasker studied when developing the SOH**.** Some phytoplankton groups (e.g., green algae, blue-green algae, diatoms, and dinoflagellates) have varying sensitives to turbulence, with dinoflagellates being the most sensitive (Thomas and Gibson, 1990). Three marine heterotrophic dinoflagellates showed reduced volume-based growth rates at realistic intensities of small-scale turbulence, $\varepsilon = 1.1 \times 10^{-2}$ cm^2 s^{-3} (Martinez et al., 2018). Some observed impacts of turbulence on dinoflagellates are reduced or cessation of feeding behavior (Martinez et al., 2018), loss of longitudinal flagella and the ability to swim forward (Thomas and Gibson, 1990). In contrast, diatoms and other non-motile phytoplankton respond more favorably to mixing and turbulent conditions, as dissolved nutrients are more readily accessible to their non-motile cells (Barton et al., 2014; Dell'Aquila, et al., 2017; Orefice et al., 2019). However, without adequate camera resolution to identify the phytoplankton assemblage composition, it is difficult to discern what phytoplankton species dominated during these *Zooglider* deployments.

3.6 Conclusions:

With the aid of *Zooglider*, we were able to resolve fine-scale vertical distributions of different suspension-feeding zooplankton, concurrently with different measurements of potential prey: Chl-*a* fluorescence, marine snow, and small particles. We found that 52.2% of the deviance in small copepod abundance was explained by the biovolume of small particles and secondarily by Chl-*a*. In contrast, only modest levels of deviance in abundance were explained for appendicularia-others (32.8%), large protists (24.9%), and large copepods at night (21%). Significant predictor variables for appendicularia-others and large protists were marine snow and small particles, while Chl-*a* was insignificant for these taxa. The significant predictor variables for large copepods at night were marine snow and Chl-*a*. Conversely, relatively low levels of deviance were explained for *Fritillaria* (13.7%) and large copepods by day (3.9%), therefore, their distributions were likely governed by other processes, or we have not measured their preferred prey. For all taxa, marine snow or small particles were the primary explanatory variables, rather than Chl-*a*. Finally, we detected no evidence that water column stability influenced the maximum abundances of prey and zooplankton.

3.7 Tables and Figures:

Table 3.1. Deployment summary of processed dives.

Deployment	Day Dives	Night Dives
Jul-Aug 2017	3	0
Sept 2017	23	16
Nov-Dec 2017	14	21
Jan-Feb 2018	14	25
Apr 2018	21	24
Jul-Aug 2018	26	18
Oct 2018	19	22

Table 3.2. Deviance explained by significant predictor prey variables and corresponding F-values. Percent difference in deviance explained is calculated as the difference between the deviance explained using all three prey predictor variables and the difference explained using only significant variables divided by the deviance explained using all three prey predictor variables. Insignificant variables resulted in less than a 5% difference in deviance explained when they are removed.

Insignificant variables were removed	Deviance Explained	F-value			% Dif in Deviance. Explained	Depth Range
		Chl-*a*	Marine Snow	Small Particles		
Small Copepods	52.22%	807.81		2402.91	-4.76%	0-100 m
App Others	32.84%		962.90	532.86	-1.02%	0-100 m
Fritillaria	13.70%	158.98	178.43	160.91		0-100 m
Large Protists	24.90%		514.61	370.25	-1.15%	0-100 m
Large Copepods Day	3.94%	77.75	168.08		-2.23%	0-400 m
Large Copepods Night	21.00%	292.45	1206.23		-0.52%	0-400 m

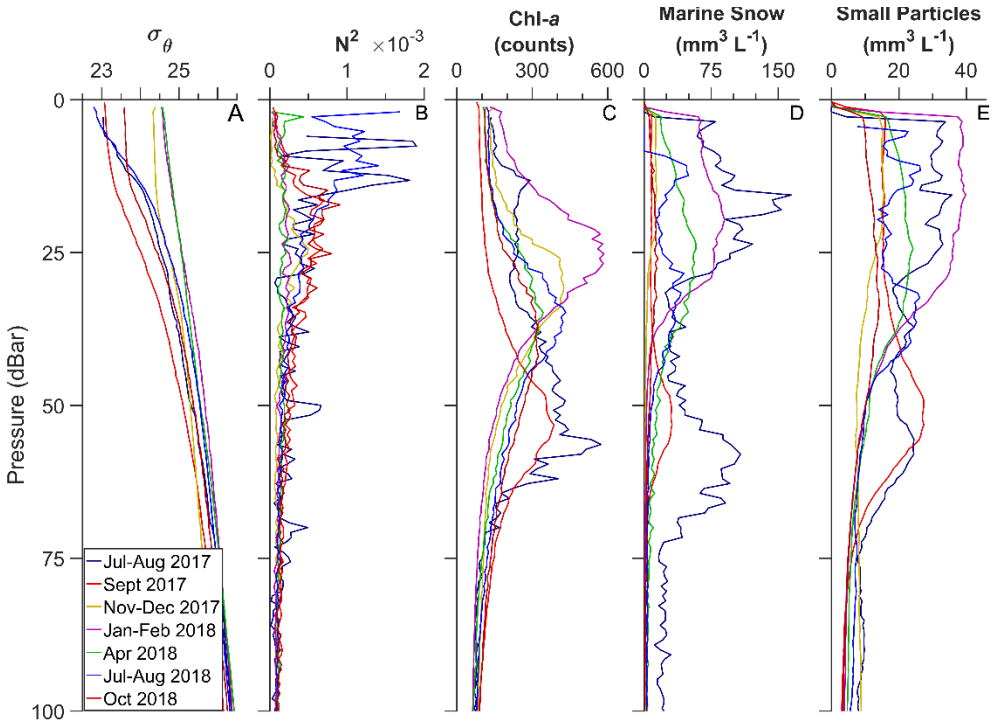

Figure 3.1. Potential density (σ_θ), buoyancy frequency (N^2), and prey source (Chl-*a* fluorescence, Marine Snow biovolume, and small particle biovolume) profiles from all seven *Zooglider* deployments. Each colored vertical profile represents the mean of all dives (both day and night) within a deployment.

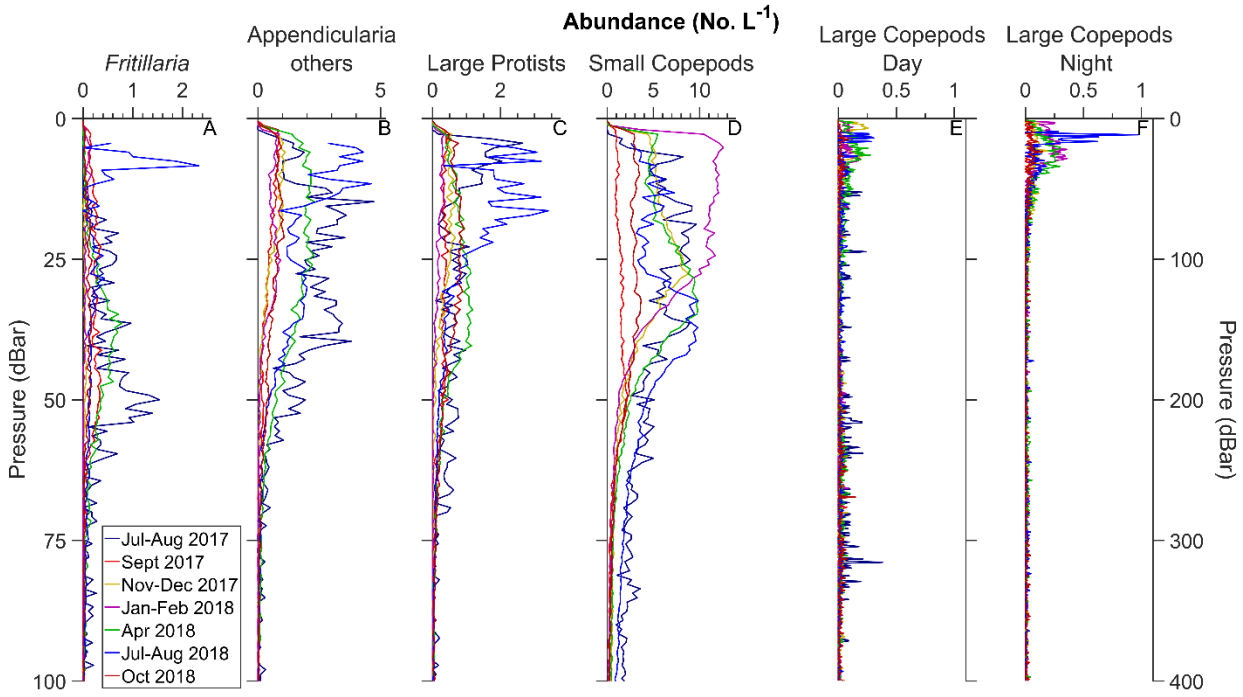

Figure 3.2. Vertical profiles of taxa abundance (No. L-1) as functions of depth. Panels A-D are to 100 dBar, while panels E and F are to 400 dBar. Small copepods have a feret diameter ≤3 mm, while large copepods have feret diameter > 3 mm. Each colored vertical profile represents the mean of all dives (both day and night) within a deployment.

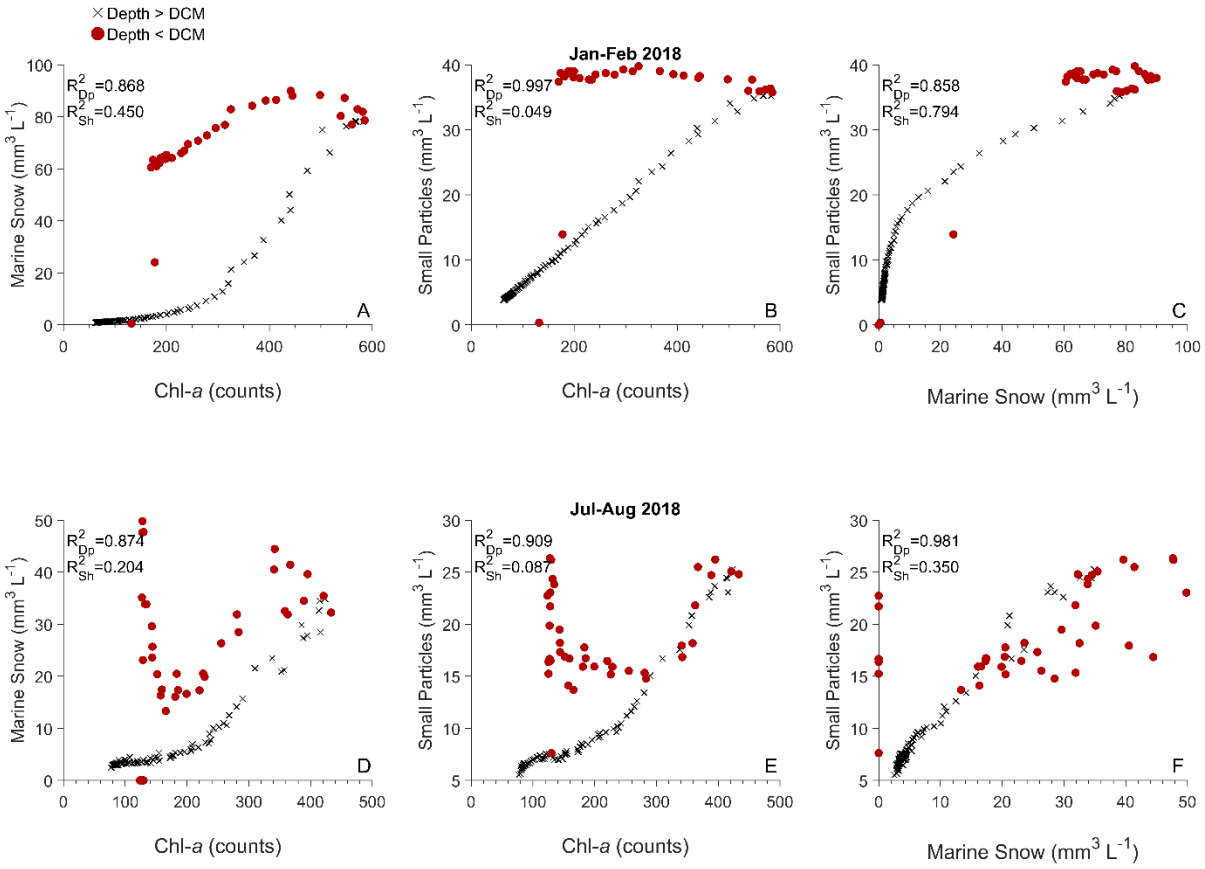

Figure 3.3. Associations of the three different prey types with one another during a low stratification deployment (Panels A-C; Jan-Feb 2018) and a highly stratified deployment (Panels D-F; Jul-Aug 2018). Red circles represent data from the depth of the Chl-*a* maximum (DCM) to the surface, while black X's denote data from the DCM to 100 dBar. R^2 values for the black X's and red circles are R_{Dp}^2 and R_{Sh}^2, respectively.

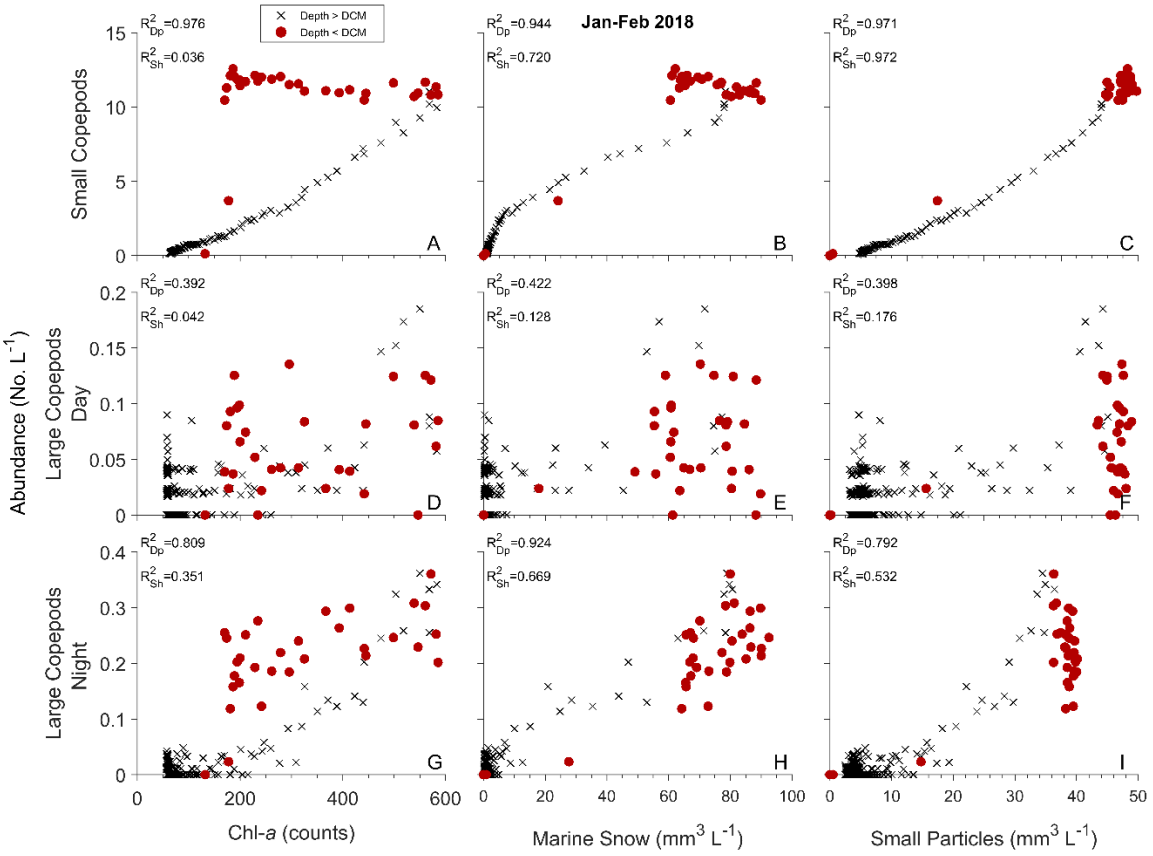

Figure 3.4. Associations of the three prey types with abundances of small copepods (Panels A-C), large copepods day (Panels D-F), and large copepods night (G-I) during a low stratification deployment (Jan-Feb 2018). Red circles represent data from the depth of the Chl-*a* maximum (DCM) to the surface, while black X's denote data from the DCM to 100 dBar (small copepods) and 400 dBar (large copepods day and night). R^2 values for the black X's and red circles are R_{Dp}^2 and R_{Sh}^2, respectively.

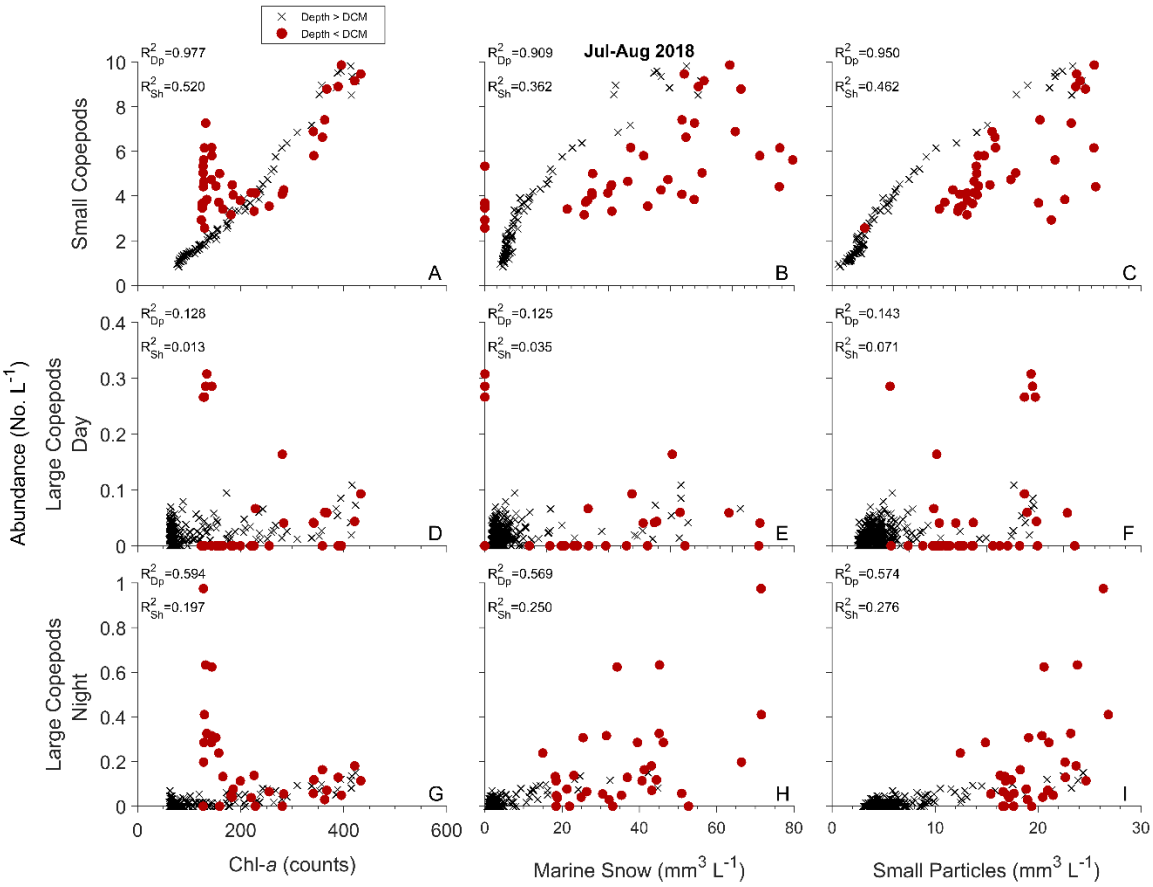

Figure 3.5. Associations of the three prey types with abundances of small copepods (Panels A-C), large copepods day (Panels D-F), and large copepods night (G-I) during a high stratification deployment (Jul-Aug 2018). Red circles represent data from the depth of the Chl-*a* maximum (DCM) to the surface, while black X's denote data from the DCM to 100 dBar (small copepods) and 400 dBar (large copepods day and night). R^2 values for the black X's and red circles are R_{Dp}^2 and R_{Sh}^2, respectively.

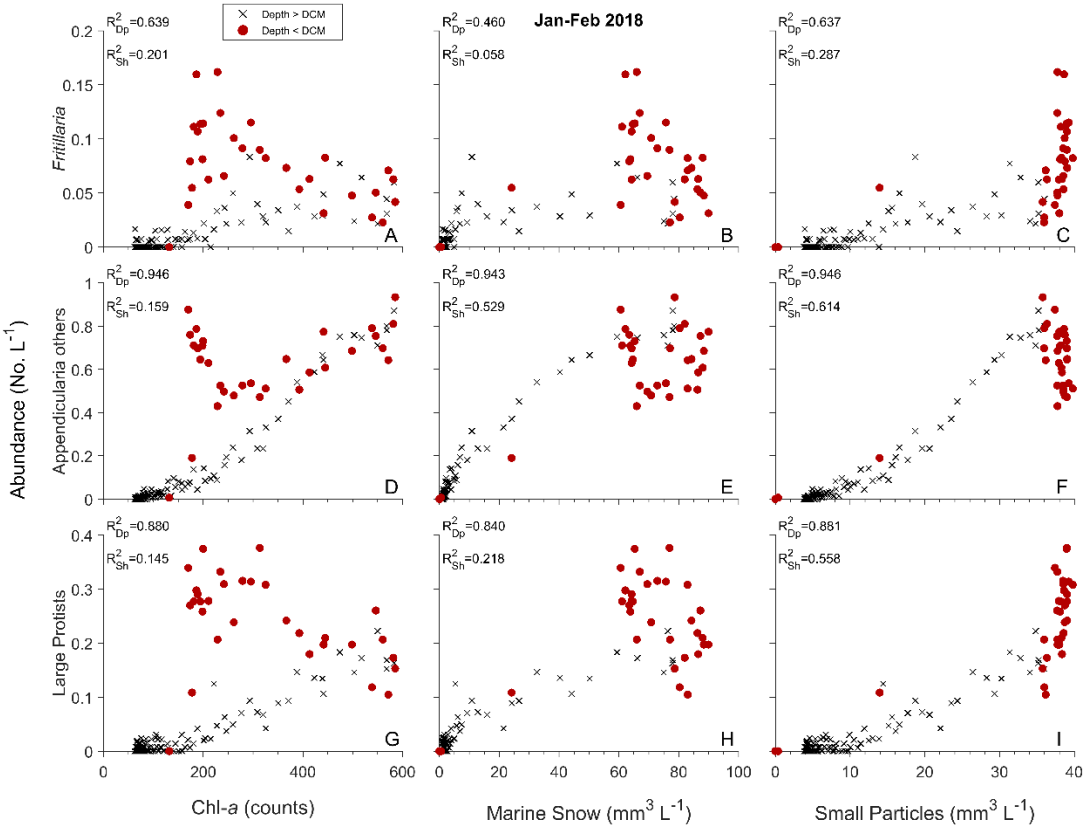

Figure 3.6. Associations of the three prey types with abundances of *Fritillaria* (Panels A-C), appendicularia-others (Panels D-F), and large protists (G-I) during a low stratification deployment (Jan-Feb 2018). Red circles represent data from the depth of the Chl-*a* maximum (DCM) to the surface, while black X's denote data from the DCM to 100 dBar. R^2 values for the black X's and red circles are R_{Dp}^2 and R_{Sh}^2, respectively.

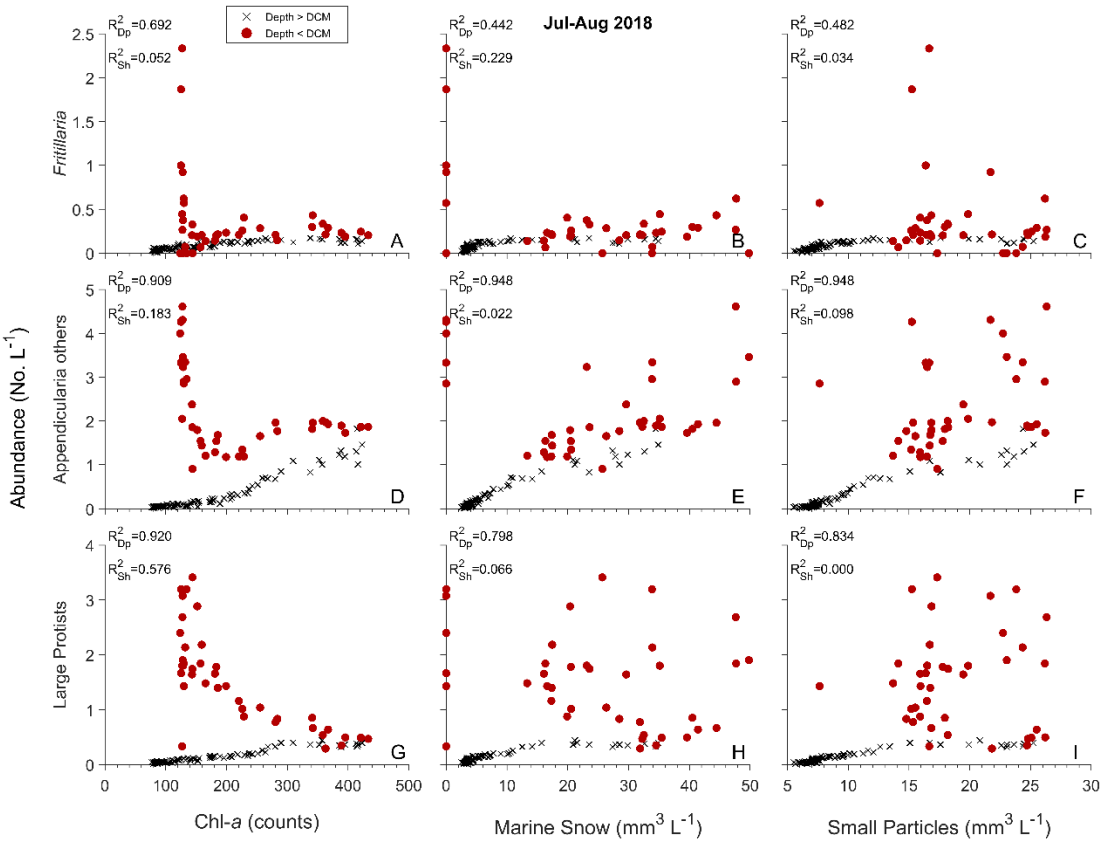

Figure 3.7. Associations of the three prey types with abundances of *Fritillaria* (Panels A-C), appendicularia-others (Panels D-F), and large protists (G-I) during a high stratification deployment (Jul-Aug 2018). Red circles represent data from the depth of the Chl-*a* maximum (DCM) to the surface, while black X's denote data from the DCM to 100 dBar. R^2 values for the black X's and red circles are R_{Dp}^2 and R_{Sh}^2, respectively.

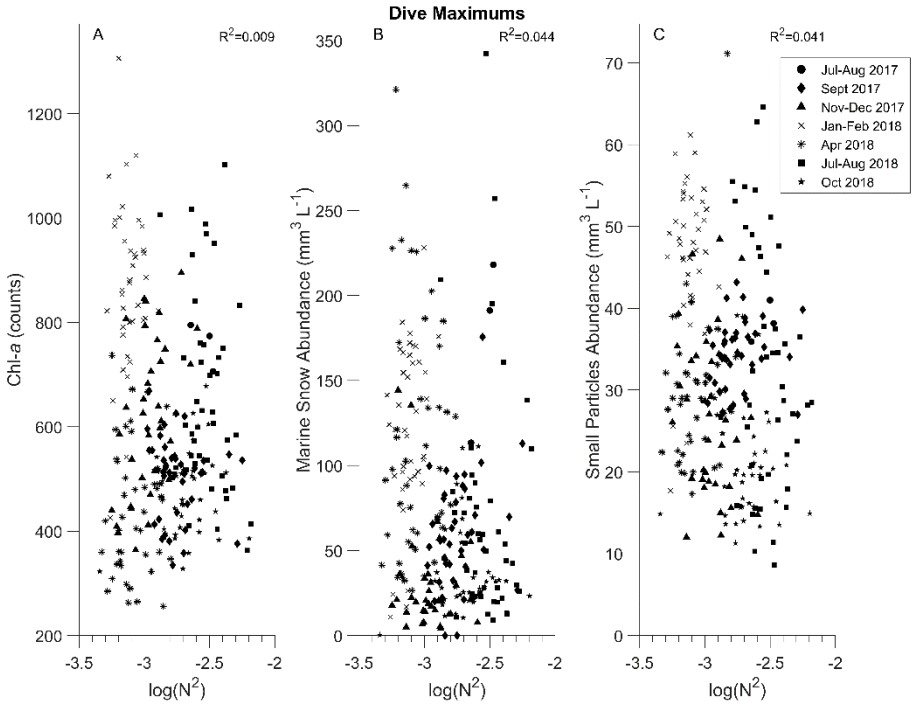

Figure 3.8. Maximum prey abundances as a function of the maximum log(N^2) value within a dive. Marker symbol denotes the deployment each dive was from.

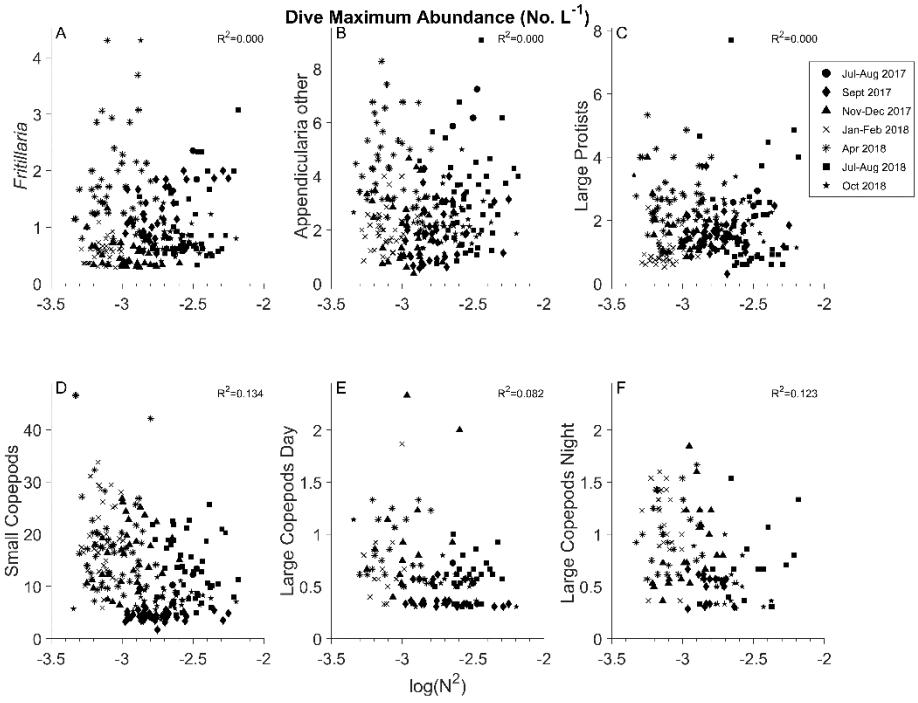

Figure 3.9. Maximum zooplankton taxa abundances as a function of the maximum log(N^2) value within a dive. Marker symbol denotes the deployment each dive was from.

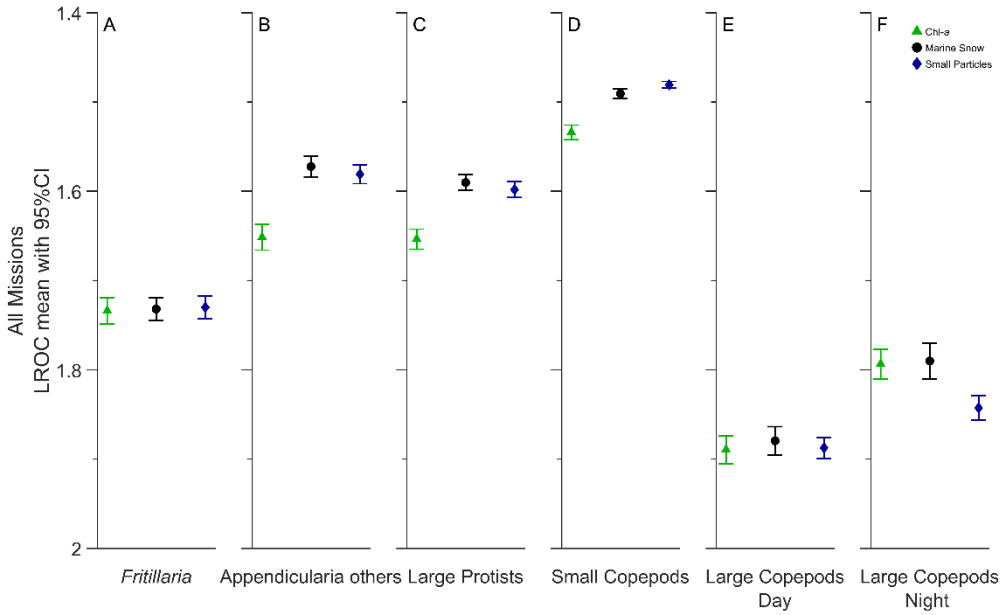

Figure 3.10. Length of the Receiver Operating Characteristic (LROC) for all zooplankton taxa and each potential prey. LROC's equal to 1.41 mean complete overlap, while LROC's equal to 2.0 mean complete separation. Symbols delineate the mean of all dives combined, while the error bars represent 95% confidence intervals. Panels A-D were from 0 to 100 dBar, while panels E and F were from 0 to 400 dBar.

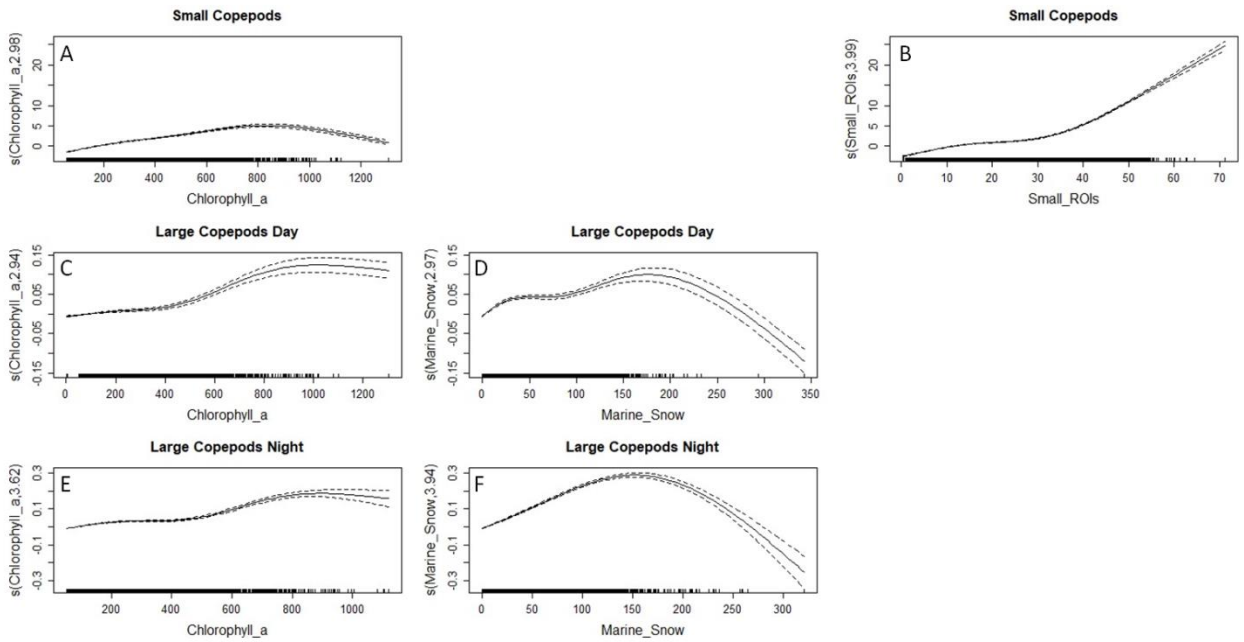

Figure 3.11. GAM spline curves of significant prey predictor variables for small copepods (panel A and B), large copepods day (panel C and D), and large copepods night (panel E and F). Solid lines represent the mean effect and dashed lines are 95% confidence intervals. The number in parenthesis on the y-axis is the effect degrees of freedom of the spline curve. Ticks on the x-axis delineate the density of the data used to generate each spline curve.

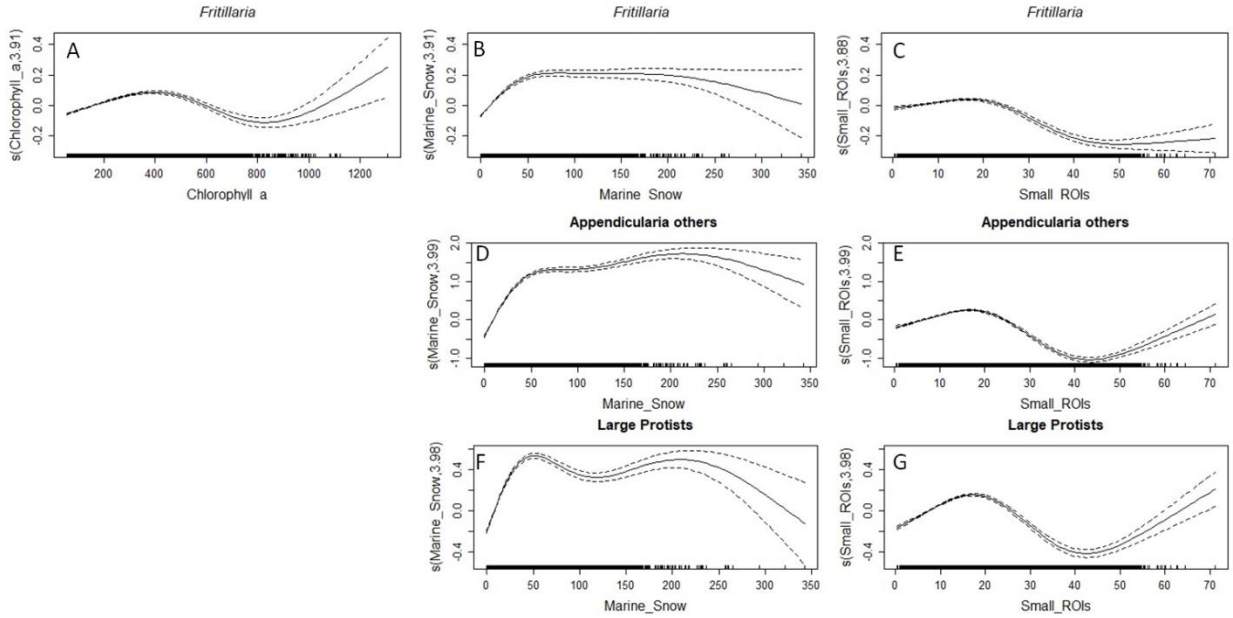

Figure 3.12. GAM spline curves of significant prey predictor variables for *Fritillaria* (panel A, B, and C), appendicularia-others (panel D and E), and large protists (panel F and G). Solid lines represent the mean effect and dashed lines are 95% confidence intervals. The number in parenthesis on the y-axis is the effect degrees of freedom of the spline curve. Ticks on the x-axis delineate the density of the data used to generate each spline curve.

3.8 Acknowledgements:

This work could not have been done without the help of the following individuals: E. Tovar and L. Sala for organism identification. S. Gastauer for implementation and help with the GAM modeling. J. Ellen for the machine learning sorting of the images, implementation of the LROC code, and paper edits. S. Somer for help with paper edits. M. D. Ohman for deployment design, paper edits, data analysis help, and organism identification. I would also like to thank the entirety of the Instrument Development Group at the Scripps Institution of Oceanography for the construction and operation of *Zooglider* as well as help on and during deployments of *Zooglider*. The Gordon and Betty Moore Foundation (grants to M.D. Ohman number) for funding the development of *Zooglider*. NSF for support of the CCE-LTER program, the NSF GRFP, and DoD SMART Scholarship program for funding me through the duration of my PhD work.

Chapter 3, in full, is currently being prepared for submission for publication of the material. **Whitmore, B.M.** and Ohman, M.D. The influences of the prey field and water column stability on the fine-scale vertical distributions of zooplankton. The dissertation author was the primary author on this paper.

3.9 References:

Alldredge, A.L., 1972. Abandoned larvacean houses: a unique food source in the pelagic environment. *Science*, *177*(4052), pp.885-887.

Alldredge, A.L., Cowles, T.J., MacIntyre, S., Rines, J.E., Donaghay, P.L., Greenlaw, C.F., Holliday, D.V., Dekshenieks, M.M., Sullivan, J.M. and Zaneveld, J.R.V., 2002. Occurrence and mechanisms of formation of a dramatic thin layer of marine snow in a shallow Pacific fjord. *Marine Ecology Progress Series*, *233*, pp.1-12.

Alldredge, A.L. and Silver, M.W., 1988. Characteristics, dynamics and significance of marine snow. *Progress in oceanography*, *20*(1), pp.41-82.

Alldredge, A.L. and Gotschalk, C.C., 1990. The relative contribution of marine snow of different origins to biological processes in coastal waters. *Continental Shelf Research*, 10(1), pp.41-58.

Barton, A.D., Ward, B.A., Williams, R.G. and Follows, M.J., 2014. The impact of fine-scale turbulence on phytoplankton community structure. *Limnology and Oceanography: Fluids and Environments*, 4(1), pp.34-49.

Beers, J.R. and Stewart, G.L., 1970. The preservation of acantharians in fixed plankton samples. *Limnology and Oceanography*, *15*(5), pp.825-827.

Bernstein, R.E., Betzer, P.R., Feely, R.A., Byrne, R.H., Lamb, M.F. and Michaels, A.F., 1987. Acantharian fluxes and strontium to chlorinity ratios in the North Pacific Ocean. *Science*, *237*(4821), pp.1490-1494.

Biard, T. and Ohman, M., Vertical niche definition of test-bearing protists (Rhizaria) into the twilight zone revealed by in situ imaging. *Limnology and Oceanography* (in review).

Biard, T., Stemmann, L., Picheral, M., Mayot, N., Vandromme, P., Hauss, H., Gorsky, G., Guidi, L., Kiko, R. and Not, F., 2016. *In situ* imaging reveals the biomass of giant protists in the global ocean. *Nature*, *532*(7600), p.504.

Bienfang, P.K., Harrison, P.J. and Quarmby, L.M., 1982. Sinking rate response to depletion of nitrate, phosphate and silicate in four marine diatoms. *Marine Biology*, 67(3), pp.295-302.

Calbet, A., Landry, M.R. and Scheinberg, R.D., 2000. Copepod grazing in a subtropical bay: species-specific responses to a midsummer increase in nanoplankton standing stock. *Marine Ecology Progress Series*, 193, pp.75-84.

Capitanio, F.L. and Esnal, G.B., 1998. Vertical distribution of maturity stages of *Oikopleura dioica* (Tunicata, Appendicularia) in the frontal system off Valdés Peninsula, Argentina. *Bulletin of Marine Science*, *63*(3), pp.531-539.

Checkley, D.M., Davis, R.E., Herman, A.W., Jackson, G.A., Beanlands, B. and Regier, L.A., 2008. Assessing plankton and other particles in situ with the SOLOPC. *Limnology and Oceanography*, 53(5, part 2), pp.2123-2136.

Chekalyuk, A. and Hafez, M., 2011. Photo-physiological variability in phytoplankton chlorophyll fluorescence and assessment of chlorophyll concentration. *Optics Express*, 19(23), pp.22643-22658.

Cowles, T.J., Desiderio, R.A., Moum, J.N., Myrick, M.L., Garvis, D.G. and Angel, S.M., 1990, September. Fluorescence microstructure using a laser/fiber optic profiler. In *Ocean Optics X* (Vol. 1302, pp. 336-345). International Society for Optics and Photonics.

Cullen, J.J., 2015. Subsurface chlorophyll maximum layers: enduring enigma or mystery solved? *Annual Review of Marine Science*, 7, pp. 207-239.

Cullen, J.J. and Lewis, M.R., 1995. Biological processes and optical measurements near the sea surface: Some issues relevant to remote sensing. *Journal of Geophysical Research*: Oceans, 100(C7), pp.13255-13266.

Cullen, J.J., 1981. Chlorophyll maximum layers of the Southern Californian Bight and possible mechanisms of their formation and maintenance. *Oceanologica Acta, 4*, pp.23-31.

Davis, R.E., Ohman, M.D., Rudnick, D.L. and Sherman, J.T., 2008. Glider surveillance of physics and biology in the southern California Current System. *Limnology and Oceanography*, 53(5 part 2), pp.2151-2168.

Decelle, J. and Not, F., 2015. Acantharia. In: *Encyclopedia of Life Sciences*. John Wiley & Sons, Ltd: Chichester. pp.1-10. DOI: 10.1002/9780470015902.a0002102.pub2

Dekshenieks, M.M., Donaghay, P.L., Sullivan, J.M., Rines, J.E., Osborn, T.R. and Twardowski, M.S., 2001. Temporal and spatial occurrence response thin phytoplankton layers in relation to physical processes. *Marine Ecology Progress Series*, *223*, pp.61-71.

Dell'Aquila, G., Ferrante, M.I., Gherardi, M., Lagomarsino, M.C., D'alcalà, M.R., Iudicone, D. and Amato, A., 2017. Nutrient consumption and chain tuning in diatoms exposed to storm-like turbulence. *Scientific Reports*, 7(1), pp.1828.

Dilling, L. and Alldredge, A.L., 2000. Fragmentation of marine snow by swimming macrozooplankton: A new process impacting carbon cycling in the sea. *Deep Sea Research Part I: Oceanographic Research Papers*, 47(7), pp.1227-1245.

Dilling, L., Wilson, J., Steinberg, D. and Alldredge, A., 1998. Feeding by the euphausiid *Euphausia pacifica* and the copepod *Calanus pacificus* on marine snow. *Marine Ecology Progress Series*, 170, pp.189-201.

Doubell, M.J., Prairie, J.C. and Yamazaki, H., 2014. Millimeter scale profiles of chlorophyll fluorescence: Deciphering the microscale spatial structure of phytoplankton. *Deep Sea Research Part II: Topical Studies in Oceanography*, *101*, pp.207-215.

Ellen, J.S., Graff, C.A. and Ohman, M.D., 2019. Improving plankton image classification using context metadata. *Limnology and Oceanography: Methods*, *17*(8), pp.439-461.

Falkowski, P.G. and LaRoche, J., 1991. Acclimation to spectral irradiance in algae. *Journal of Phycology*, 27(1), pp.8-14.

Falkowski, P. and Kiefer, D.A., 1985. Chlorophyll *a* fluorescence in phytoplankton: relationship to photosynthesis and biomass. *Journal of Plankton Research*, 7(5), pp.715-731.

Fowler, S.W. and Knauer, G.A., 1986. Role of large particles in the transport of elements and organic compounds through the oceanic water column. *Progress in Oceanography*, *16*(3), pp.147-194.

Franks, P.J., 2001. Turbulence avoidance: An alternate explanation of turbulence-enhanced ingestion rates in the field. *Limnology and Oceanography*, 46(4), pp.959-963.

Franks, P.J., 1995. Thin layers of phytoplankton: a model of formation by near-inertial wave shear. *Deep Sea Research Part I: Oceanographic Research Papers*, *42*(1), pp.75-91.

Gaskell, D. E., Ohman, M. D., and Hull, P. M. 2019. *Zooglider*-based measurements of planktonic foraminifera in the California Current System. *Journal of Foraminiferal Research*, 49, pp. 390-404.

Greer, A.T., 2013. Fine-scale Distributions of Plankton and Larval Fishes: Implications for Predator-prey Interactions near Coastal Oceanographic Features. Open Access Dissertations, University of Miami, Paper 1102.

Haury, L.R., Yamazaki, H. and Itsweire, E.C., 1990. Effects of turbulent shear flow on zooplankton distribution. *Deep Sea Research Part A. Oceanographic Research Papers*, *37*(3), pp.447-461.

Hopcroft, R.R. and Roff, J.C., 1995. Zooplankton growth rates: extraordinary production by the larvacean *Oikopleura dioica* in tropical waters. *Journal of Plankton Research*, *17*(2), pp.205-220.

Jackson, G.A. and Checkley Jr, D.M., 2011. Particle size distributions in the upper 100 m water column and their implications for animal feeding in the plankton. *Deep Sea Research Part I: Oceanographic Research Papers*, 58(3), pp.283-297.

Jackson, G.A., 1993. Flux feeding as a mechanism for zooplankton grazing and its implications for vertical particulate flux. *Limnology and Oceanography*, 38(6), pp.1328-1331.

Karaköylü, E.M., 2010. The foraging sorties hypothesis: evaluating the effect of gut dynamics on copepod foraging behavior (Doctoral dissertation, UC San Diego).

Kodama, T., Iguchi, N., Tomita, M., Morimoto, H., Ota, T. and Ohshimo, S., 2018. Appendicularians in the southwestern Sea of Japan during the summer: abundance and role as secondary producers. *Journal of Plankton Research*, *40*(3), pp.269-283.

Kristiansen, T., Vollset, K.W., Sundby, S. and Vikebø, F., 2014. Turbulence enhances feeding of larval cod at low prey densities. *ICES Journal of Marine Science*, 71(9), pp.2515-2529.

Lampitt, R.S., Wishner, K.F., Turley, C.M. and Angel, M.V., 1993. Marine snow studies in the Northeast Atlantic Ocean: distribution, composition and role as a food source for migrating plankton. *Marine Biology*, *116*(4), pp.689-702.

Lasker, R., 1975, Field criteria for survival of anchovy larvae-relation between inshore chlorophyll maximum layers and successful 1st feeding: *Fishery Bulletin*, 73(3), p. 453-462.

Lasker, R., 1981, The role of a stable ocean in larval fish survival and subsequent recruitment: *Marine fish larvae: morphology, ecology and relation to fisheries*, pp. 81-87.

MacIntyre, S., Alldredge, A.L. and Gotschalk, C.C., 1995. Accumulation of marine snow at density discontinuities in the water column. *Limnology and Oceanography*, *40*(3), pp.449-468.

MacKenzie, B.R., Miller, T.J., Cyr, S. and Leggett, W.C., 1994. Evidence for a dome-shaped relationship between turbulence and larval fish ingestion rates. *Limnology and Oceanography*, *39*(8), pp.1790-1799.

Malkiel, E., Abras, J.N., Widder, E.A. and Katz, J., 2006. On the spatial distribution and nearest neighbor distance between particles in the water column determined from *in situ* holographic measurements. *Journal of plankton research*, *28*(2), pp.149-170.

Maswadeh, W.M. and Snyder, A.P., 2015. Variable ranking based on the estimated degree of separation for two distributions of data by the length of the receiver operating characteristic curve. *Analytica chimica acta*, *876*, pp.39-48.

Maswadeh, W.M. and Snyder, A.P., 2012. Multivariable and multigroup Receiver Operating Characteristics curve analyses for qualitative and quantitative analysis (No. ECBC-TR-922). Army Edgewood Chemical Biological Center APG MD Research and Technology Dir.

McClatchie, S., Rogers, P.J. and McLeay, L., 2007. Importance of scale to the relationship between abundance of sardine larvae, stability, and food. *Limnology and Oceanography*, *52*(4), pp.1570-1579.

McManus, M.A., Kudela, R.M., Silver, M.W., Steward, G.F., Donaghay, P.L. and Sullivan, J.M., 2008. Cryptic blooms: are thin layers the missing connection?. *Estuaries and Coasts*, *31*(2), pp.396-401.

Michaels, A.F., Caron, D.A., Swanberg, N.R., Howse, F.A. and Michaels, C.M., 1995. Planktonic sarcodines (Acantharia, Radiolaria, Foraminifera) in surface waters near Bermuda: abundance, biomass and vertical flux. *Journal of Plankton Research*, *17*(1), pp.131-163.

Mitchell, J.G. and Fuhrman, J.A., 1989. Centimeter scale vertical heterogeneity in bacteria and chlorophyll-*a*. *Marine Ecology Progress Series. Oldendorf*, *54*(1), pp.141-148.

Möller, K.O., John, M.S., Temming, A., Floeter, J., Sell, A.F., Herrmann, J.P. and Möllmann, C., 2012. Marine snow, zooplankton and thin layers: indications of a trophic link from small-scale sampling with the Video Plankton Recorder. *Marine Ecology Progress Series*, *468*, pp.57-69.

Mullin, M.M. and Brooks, E.R., 1976. Some consequences of distributional heterogeneity of phytoplankton and zooplankton 1. *Limnology and Oceanography*, *21*(6), pp.784-796.

Nakamura, Y., Somiya, R., Suzuki, N., Hidaka-Umetsu, M., Yamaguchi, A. and Lindsay, D.J., 2017. Optics-based surveys of large unicellular zooplankton: a case study on radiolarians and phaeodarians. *Plankton and Benthos Research*, *12*(2), pp.95-103.

Ohman, M.D., 2019. A sea of tentacles: optically discernible traits resolved from planktonic organisms *in situ*. *ICES Journal of Marine Science*. DOI 10.1093/icesjms/fsz184

Ohman, M.D., 1988. Behavioral responses of zooplankton to predation. *Bulletin of Marine Science*, *43*(3), pp.530-550.

Ohman, M.D., Davis, R.E., Sherman, J.T., Grindley, K.R., Whitmore, B.M., Nickels, C.F. and Ellen, J.S., 2018. *Zooglider*: An autonomous vehicle for optical and acoustic sensing of zooplankton. *Limnology and Oceanography: Methods*, *17*(1), pp.69-86, doi 10.1002/lom3.10301

Omand, M.M., Cetinić, I. and Lucas, A.J., 2017. Using bio-optics to reveal phytoplankton physiology from a Wirewalker autonomous platform. *Oceanography*, 30(2), pp.128-131.

Orefice, I., Musella, M., Smerilli, A., Sansone, C., Chandrasekaran, R., Corato, F. and Brunet, C., 2019. Role of nutrient concentrations and water movement on diatom's productivity in culture. *Scientific Reports*, 9(1), p.1479.

Pécseli, H.L., Trulsen, J.K. and Fiksen, Ø., 2014. Predator–prey encounter and capture rates in turbulent environments. *Limnology and Oceanography: Fluids and Environments*, 4(1), pp.85-105.

Pécseli, H.L., Trulsen, J. and Fiksen, Ø., 2012. Predator–prey encounter and capture rates for plankton in turbulent environments. *Progress in Oceanography*, 101(1), pp.14-32.

Prairie, J.C., Ziervogel, K., Camassa, R., McLaughlin, R.M., White, B.L., Dewald, C. and Arnosti, C., 2015. Delayed settling of marine snow: Effects of density gradient and particle properties and implications for carbon cycling. *Marine Chemistry*, *175*, pp.28-38.

Purcell, J.E., Decker, M.B., Breitburg, D.L. and Broughton, K.J., 2014. Fine-scale vertical distributions of *Mnemiopsis leidyi* ctenophores: predation on copepods relative to stratification and hypoxia. *Marine Ecology Progress Series*, *500*, pp.103-120.

Ríos, F., Kilian, R. and Mutschke, E., 2016. Chlorophyll-*a* thin layers in the Magellan fjord system: the role of the water column stratification. *Continental Shelf Research*, *124*, pp.1-12.

Rothschild, B.J. and Osborn, T.R., 1988. Small-scale turbulence and plankton contact rates. *Journal of Plankton Research*, *10*(3), pp.465-474.

Ryan, J.P., McManus, M.A., Paduan, J.D. and Chavez, F.P., 2008. Phytoplankton thin layers caused by shear in frontal zones of a coastal upwelling system. *Marine Ecology Progress Series*, *354*, pp.21-34.

Sato, R., Tanaka, Y. and Ishimaru, T., 2001. House production by *Oikopleura dioica* (Tunicata, Appendicularia) under laboratory conditions. *Journal of Plankton Research*, *23*(4), pp.415-423.

Sato, R., Tanaka, Y. and Ishimaru, T., 2003. Species-specific house productivity of appendicularians. *Marine Ecology Progress Series*, *259*, pp.163-172.

Silver, M.W., Shanks, A.L. and Trent, J.D., 1978. Marine snow: microplankton habitat and source of small-scale patchiness in pelagic populations. *Science*, *201*(4353), pp.371-373.

Smayda, T.J. and Boleyn, B.J., 1966. Experimental observations on the flotation of marine diatoms. II. *Skeletonema costatum* and *Rhizosolenia setigera*. *Limnology and Oceanography*, 11(1), pp.18-34.

Spinelli, M., Derisio, C., Martos, P., Pájaro, M., Esnal, G., Mianzán, H. and Capitanio, F., 2015. Diel vertical distribution of the larvacean *Oikopleura dioica* in a North Patagonian tidal frontal system (42°–45° S) of the SW Atlantic Ocean. *Marine Biology Research*, *11*(6), pp.633-643.

Spinelli, M., Guerrero, R., Pájaro, M. and Capitanio, F., 2013. Distribution of *Oikopleura dioica* (Tunicata, Appendicularia) associated with a coastal frontal system (39°-41° S) of the SW Atlantic Ocean in the spawning area of *Engraulis anchoita* anchovy. *Brazilian Journal of Oceanography*, *61*(2), pp.141-148.

Steele, J., 1964, A study of production in the Gulf of Mexico: *Journal of Marine Research*, 22, pp. 211-222.

Stoecker, D.K., 1984. Particle production by planktonic ciliates. *Limnology and Oceanography*, *29*(5), pp.930-940.

Stukel, M. R., Ohman, M. D., Kelly, T. B., and Biard, T. 2019. The roles of suspension-feeding and flux-feeding zooplankton as gatekeepers of particle flux into the mesopelagic ocean in the Northeast Pacific. *Frontiers in Marine Science*, DOI 10.3389/fmars.2019.00397

Stukel, M.R., Biard, T., Krause, J. and Ohman, M.D., 2018. Large Phaeodaria in the twilight zone: Their role in the carbon cycle. *Limnology and Oceanography*, 63(6), pp.2579-2594.

Sullivan, J.M., Donaghay, P.L. and Rines, J.E., 2010. Coastal thin layer dynamics: consequences to biology and optics. *Continental Shelf Research*, *30*(1), pp.50-65.

Sundby, S. and Fossum, P., 1990. Feeding conditions of Arcto-Norwegian cod larvae compared with the Rothschild–Osborn theory on small-scale turbulence and plankton contact rates. *Journal of Plankton Research*, *12*(6), pp.1153-1162.

Taylor, A.G., Landry, M.R., Selph, K.E. and Wokuluk, J.J., 2015. Temporal and spatial patterns of microbial community biomass and composition in the Southern California Current Ecosystem. *Deep Sea Research Part II: Topical Studies in Oceanography*, 112, pp.117-128.

Taylor, A.G., Landry, M.R., Selph, K.E. and Yang, E.J., 2011. Biomass, size structure and depth distributions of the microbial community in the eastern equatorial Pacific. *Deep Sea Research Part II: Topical Studies in Oceanography*, 58(3-4), pp.342-357.

Thomas, W.H. and Gibson, C.H., 1990. Effects of small-scale turbulence on microalgae. *Journal of Applied Phycology*, 2(1), pp.71-77.

Tomita, M., Shiga, N. and Ikeda, T., 2003. Seasonal occurrence and vertical distribution of appendicularians in Toyama Bay, southern Japan Sea. *Journal of Plankton Research*, *25*(6), pp.579-589.

Turner, J.T. and Ferrante, J.G., 1979. Zooplankton fecal pellets in aquatic ecosystems. *BioScience*, *29*(11), pp.670-677.

Visser, A.W., Mariani, P. and Pigolotti, S., 2008. Swimming in turbulence: zooplankton fitness in terms of foraging efficiency and predation risk. *Journal of Plankton Research*, 31(2), pp.121-133.

Whitmore, B.M., Nickels, C.F. and Ohman, M.D., 2019. A comparison between *Zooglider* and shipboard net and acoustic mesozooplankton sensing systems. *Journal of Plankton Research.* DOI 10.1093/plankt/fbz033

Wilson, S.E. and Steinberg, D.K., 2010. Autotrophic picoplankton in mesozooplankton guts: evidence of aggregate feeding in the mesopelagic zone and export of small phytoplankton. *Marine Ecology Progress Series*, *412*, pp.11-27.

CHAPTER 4: Size-dependent predator-prey encounters in the zooplankton

4.1 Abstract:

Predation is a major force structuring planktonic assemblages. The probability of a predator-prey encounter is dependent upon the spatial overlap between predators and prey, specific organismal velocities, abundances, and detection radii. All of these variables can be influenced by the size of the prey or predatory organism; therefore, it is necessary to measure planktonic predator-prey encounter variables at scales << 1 m. Here I use the fully autonomous *Zooglider* to detect size-dependent diel vertical migration behavior in both copepods and chaetognaths, and size-dependent vertical distributions in three prey taxa and five predatory taxa. *Zooglider* was deployed on six missions in the San Diego Trough between September 2017 and October 2018. *Zooglider* sampled between 400-0 m for each 10-14 day mission. Spearman rank correlations showed that abundances of smaller sized predatory taxa (chaetognaths, ctenophores, siphonophores, and trachymedusae) had stronger positive relationships with the abundances of smaller prey taxa than larger prey taxa. Analysis of *in situ* potential predator-prey encounters, i.e., a carnivorous zooplankton and prey items co-occurring within a single optical frame (250 mL sample volume), revealed that smaller predators have greater probabilities of encountering smaller prey than larger prey.

4.2 Introduction:

Predation acts as a major force in controlling the structure of planktonic communities (Fields and Yen, 1997). During each component of the predation sequence, the probability that a prey organism is encountered, attacked, captured, and ingested (Holling, 1966; Ohman, 1988) can be mediated by a corresponding prey response. For example, Acantharia have spiny tests, which may reduce the probability of ingestion by a predator (Knoll and Kotrc, 2015). Copepod escape response behavior, a series of power strokes with their swimming legs that can propel the copepod away from predators at velocities ranging from ~200-600 mm s^{-1}, can reduce the probability of a copepod being captured (Kiørboe et al., 2010). The degree of spatial vertical overlap (i.e., separation or overlap of vertical distributions) between predatory and herbivorous zooplankton can greatly influence the probability of encounter.

Vertical distributions of zooplankton can vary widely depending on taxa, time of day (Hays, 2003), water column stability (Lagadeuc et al., 1997), the presence of visual or nonvisual predators (Ohman 1990), prey conditions, light conditions (Schuyler and Sullivan, 1997), body size (De Robertis et al., 2000; Ohman and Romagnan, 2016), and life stage of the organism (Huntley and Brooks 1982; Yamaguchi et al., 1999). One of the most common changes in zooplankton vertical distribution is diel vertical migration (DVM). Organisms that exhibit DVM behavior commonly remain at depth during the day and migrate to surface waters at night to feed. This behavior reduces predation risk by visual predators during the day, while still allowing for the consumption of prey located in surface waters at night, when the risk of predation by visual predators is reduced (Hays, 2003).

Many zooplankton taxa exhibit size-dependent DVM behavior. De Robertis et al. (2000) observed that smaller, less conspicuous euphausiids ascended earlier and descended later than

larger, more conspicuous euphausiids. Sullivan (1980) observed that juvenile chaetognaths, *Sagitta elegans*, (< 18 mm) did not perform DVM and were generally located shallower than 25 m, while mature *S. elegans* were located between 200 and 400 m during the day and migrated to depths shallower than 25 m during the night. Copepods have also been found to exhibit size-dependent DVM behavior, with the smallest (shallow-dwelling) and largest (deeper-dwelling) size classes of copepods refraining from DVM behavior, while intermediate-sized copepods exhibit large amplitude DVM (Ohman and Romagnan, 2016). In a mesocosm (deep tank) experiment, Huntley and Brooks (1982) showed that DVM behavior was not exhibited in *Calanus pacificus* until the first feeding stage (Nauplius III) and that as the life stages progressed and the organisms got larger, the amplitude of the migration became greater. Additionally, reverse DVM behavior (i.e., ascending during the day, and descending at night) can occur when prey are exposed to nonvisual predatory zooplankton (Ohman et al., 1983; Ohman, 1990).

Thus, zooplankton vertical distributions can vary greatly and there is much potential for the occurrence of vertical overlap between predatory and prey taxa. However, the probability of a predator encountering a prey is also a function of the concentrations and velocities of both predator and prey (Williamson and Stoeckel, 1990) and the detection radius of the predator (Gerritsen and Strickler, 1977). Biotic and abiotic factors can further influence the probability of encounter. Turbulence has been shown to enhance encounter rates between zooplankton (Kiørboe and MacKenzie, 1995; Sundby and Fossum, 1990). The swimming behavior of a predatory zooplankter can impact which velocity (i.e., predator or prey) has the greater impact on the probability of encounter. Gerritsen and Strickler (1977) mathematically found two optimal zooplankton predation strategies: ambush predators and cruising predators. The probability of encounter with ambush predators is primarily dependent upon the velocity of the prey, while the

velocity of the cruising predator has a greater influence on its probability of encountering a prey item.

Ambush predators, e.g., chaetognaths (Feigenbaum and Reeve, 1977), some lobate and cydippid ctenophores (Greene et al., 1986; Waggett and Costello, 1999), some cyclopoid copepods (Kiørboe, 2008; Kiørboe et al., 2009), colonial siphonophores, and trachymedusae (Costello et al., 2008), remain relatively stationary and rely upon fast-moving prey to encounter them. Benefits of the ambush-predation strategy are reduced metabolic rates (Paffenhöfer, 2006), reduced predation risk (Kiørboe, 2011), and overall reduced mortality rates (Eiane and Ohman, 2004). However, this strategy generally limits ambush predators' prey encounters to motile prey (Kiørboe, 2011; Visser, 2007). In contrast, cruising predators, e.g., some calanoid copepods (Kjellerup and Kiørboe, 2011), narcomedusae (Costello et al., 2008), and beroid ctenophores (Swanberg, 1974), expend substantial energy swimming, are more susceptible to predation risk, but have greater probabilities of encountering both motile and stationary prey (Kiørboe, 2011; Visser, 2007). Current feeding is an alternative feeding mode, in which a predator generates a feeding current to entrain non-motile and weakly swimming prey (Kiørboe et al.,1996). Current feeding has more predation risk and metabolic demand than ambush feeding, but less than cruise feeding (Kiørboe, 2011). Some taxa can exhibit multiple feeding behaviors depending on the prey field. For instance, *Acartia tonsa* can switch between current feeding when diatoms are abundant and ambush feeding when ciliates or more motile prey dominate the prey field (Kiørboe et al.,1996).

Calculating a realistic probability of a zooplankton predator-prey encounter is dependent upon several complex variables, many of which need to be measured at the scales of zooplankton interaction <<1 m (Haury et al., 1978). However, conventional opening-closing

nets are unsuitable for measuring micro-scale (<< 1 m) zooplankton vertical distributions (necessary for vertical overlap quantification) as their vertical resolution is approximately 10 m (Möller et al., 2012). Nets are also inadequate for quantifying delicate zooplankton predators (e.g., hydromedusae, ctenophores, foraminifera), as these animals can be deformed or damaged beyond recognition in the net collection and preservation process (Andersen et al., 1992, Gaskell et a., 2019; Whitmore et al., 2019).

An alternative solution to estimating planktonic predator-prey encounter rates is to measure predator and prey overlap directly in the field. Three-dimensional imaging systems (e.g., holography and Particle Image Velocimetry) can resolve small scale planktonic vertical distributions, observe co-occurrences of predators and prey, and measure *in situ* velocities of different planktonic organisms (Sheng et al., 2003; Wiebe and Benfield, 2003). However, due to high-power consumption, limitations of focal depth, and ship-time requirements, such measurements can only be conducted for short periods of time and for small sample volumes (~55 mL, Sheng et al., 2003). Two-dimensional imaging systems, e.g., *IS*IIS (Cowen and Guigand, 2008); LOKI (Schulz et al., 2009); SPC (Roberts et al., 2014); UVP (Picheral et al., 2010); VPR (Davis et al., 2005); *Zooglider* (Ohman et al., 2018); and ZOOVIS (Trevorrow et al., 2005), are unable to calculate specific planktonic velocities, but are able to resolve micro-scale planktonic vertical distributions and observe the co-occurence of predatory and prey zooplankton within relatively small sample volumes, 0.1-2 L (i.e., a likely encounter).

In this study, *Zooglider* was used to measure micro-scale vertical distributions of zooplankton in this study. *Zooglider* is a modified *Spray* glider (Sherman et al., 2001) that has been outfitted with a pumped CTD, chloropyll-*a in vivo* fluorometer, dual-frequency Zonar (200 and 1000 kHz), and low-power telecentric shadowgraph imaging system (Zoocam) (Ohman et

al., 2018). *Zooglider* is unique among other zooplankton imaging systems, as it is a low-power endurance vehicle, with a battery-limited endurance of ~50 days. The endurance of *Zooglider* allows for the relatively small sample image volume of 250 mL to be extended up to ~150 m^3 per deployment.

In this study, we use *Zooglider* to measure predator-prey distributions at scales <<1 m in vertical extent, and investigate how zooplankton size influences predator-prey potential interactions. We measure zooplankton size as a function of depth to test whether size-dependent differences exist in suspension-feeding and predatory zooplankton vertical distributions. We assess whether body size influences predator-prey abundance relationships. Zoocam also detected several potential encounters between carnivorous zooplankton and suspension-feeding zooplankton (i.e. prey). In this study, we define a potential encounter as a predatory zooplankton and 'x' number of prey items occuring within a single image (250 mL sample volume). We examine how organism body size may influence the probability of potential predator-prey encounter.

4.3 Methods:

4.3.1 Zooglider Deployments:

Zooglider was deployed six times in the San Diego Trough, ~30 km west of San Diego, California, between September 2017 and October 2018. All deployments were approximately 2 weeks in duration, had mean dive locations < 1 km apart, and sampled in water depths > 900 m. *Zooglider* sampling dives occurred eight times per day and were equally spaced approximately 3 hours apart. All dives had average vertical ascent speeds of 10 cm s^{-1} and sampled on the ascent portion of the dive from 400 m to the surface. Temperature, salinity, pressure, and chlorophyll-*a*

fluorescence (Chl-*a*) data were measured at eight second intervals, while *Zooglider*'s optical imaging system, Zoocam, captured images at 2 Hz. Zoocam images were 1280 x 960 pixels (~1.2 MB), with a pixel resolution of 40 µm pixel^{-1}, and sampled a 250 mL volume. Physical and Chl-*a* data are linearly interpolated using Zoocam image timestamps and assigned to their corresponding images. Ohman et al. (2018) detail complete engineering specifications and capabilities of *Zooglider*.

4.3.2 Image processing:

All Zoocam images are flat-fielded to create uniform background illumination. Flat-field corrected frames pass through a Canny detection and segmentation algorithm to identify regions of interest (ROIs), following Ohman et al. (2018). All ROIs with an equivalent circular diameter (ECD) exceeding 0.45 mm are extracted and have 70 geometric features calculated. Extracted ROIs are then classified into one of 27 categories using a novel machine-learning algorithm developed by Ellen et al. (2019). All but one of these 27 categories, "marine snow," are manually validated. Marine snow is not manually validated, as this machine-learning algorithm has a low false positive rate of 6.6% (i.e., wrongly classifying an identifiable ROI from one of the other 26 categories, as marine snow). Manual validation of dive images was conducted for ~5 consecutive days per deployment, and only manually validated dives are used in this analysis. Dives are assigned either a day or night label depending on nautical twilight.

4.3.3 Taxon Size Selection:

Prey taxa considered in this study were suspension-feeding appendicularia (*Fritillaria*), appendicularia that are not *Fritillaria* (appendicularia-others), and copepods. Predatory taxa were chaetognaths, ctenophores (lobate, cydippid, and *Beroe*), narcomedusae, siphonophores (colonial and solitary zooids), and trachymedusae. These taxa were the most abundant

organisms found across all *Zooglider* deployments. Due to a wide range of animal sizes, vertical distributions and weighted mean depths (WMD) are calculated for various size classes of each taxon. Feret diameter (FD, the maximum distance measurable across a ROI) was deemed to be the most appropriate measurement for copepods, chaetognaths, *Fritillaria*, and appendicularia-others. ECD was used for ctenophores, narcomedusae, siphonophores, and trachymedusae, as the tentacles of many of these taxa greatly impact feret diameter. Three size classes were initially chosen for each taxon, but size classes were then merged if no differences in WMD or vertical distributions were detected. The final chosen size classes and corresponding names associated with each size class are shown in Table 4.1. Copepods and siphonophores each had three size classes (small, medium, and large). Chaetognaths were split into small and medium sizes, as the large size class is currently too sparse to be informative. The remaining taxa were split into small and large size classes. Due to variable spatial orientations of each animal, both FD and ECD are likely underestimates of the true size of the animal and should be taken as minimum sizes (cf. Ohman et al. 2018).

4.3.4 Predator-Prey encounters:

Numerical densities for all size classes were grouped in depth bins of 2 dBar, but the maximum pressure used for comparisons is variable by size class (small = 200 dBar, medium = 300 dBar, and large = 400 dBar). Maximum pressure varied based on observed depth distributions of the organisms. All binned data were then averaged over all deployments by time of day to generate mean distributions of predators and prey. Predator densities were plotted as functions of prey abundances for all size classes. Day and night data were plotted separately, to examine potential diel differences. Spearman rank correlations were generated using Matlab's "Corr" function.

Potential predator-prey encounters were defined as a predator and 'x' number of prey organisms co-occurring within a single image (250 mL volume). Probabilities of a predator-prey potential encounter were calculated as the conditional probability of 'x' prey occurring within a frame, given the occurrence of a predator within a frame (Equation 4.1).

$$P_{enc}(Prey|Predator) = \frac{P(Predator\ and\ Prey)}{P(Predator)} \qquad \text{Equation 4.1}$$

Theoretical probabilities of predator-prey encounters were generated as the product of the percent of frames with 'x' number of prey and the percent of frames with a predator (Equation 4.2).

$$P_{Theoretical} = (\%\ frames\ with\ 'x'prey)(\%\ frames\ with\ predator) \qquad \text{Equation 4.2}$$

Probabilities of potential encounters, both theoretical and observed, were calculated using *Zooglider's* highest vertical resolution, ~0.05 dBar, and then subsequently binned into 2 dBar bins. Observed probabilities of encounter were plotted against theoretical probabilities of encounter, then Spearman rank correlations were conducted (Matlab, "corr" function) to determine whether the observed probabilities of encounter exceeded the theoretical probabilities of encounter, and were therefore likely not random.

Observed and theoretical probabilities were calculated for all size classes of predatory and prey taxa and for variable numbers of prey occurrence (prey number ≥1, equal to 1, equal to 2, and ≥3 per frame). If the total number of detected predator-prey encounter data points was < 6, after binning, the dataset was deemed to be too sparse to be informative and was not analyzed further. Many of the predatory organism large size classes (ctenophores, narcomedusae, and siphonophores) and the large *Fritillaria* (prey source) had too few encounters to be informative and were excluded. This resulted in the following prey group divisions being used for

comparison: 1, 2, and ≥ 3 small copepods, ≥ 1 medium copepods, ≥ 1 small *Fritillaria*, ≥ 1 small appendicularia-others, and ≥ 1 large appendicularia-others per image.

4.4 Results:

4.4.1 Vertical Distributions:

All prey taxa imaged by *Zooglider* were most abundant shallower than 50 dBar (Fig. 4.1). In general, copepods were the most abundant, followed by appendicularia-others, and *Fritillaria*. Copepods and *Fritillaria* both had distinct peaks in abundance at approximately 50 dBar regardless of size, while appendicularia-others had consistently high abundances from 50 dBar to the surface. The overall abundance of organisms was greatest in the smallest prey sizes (Fig. 41A-4.1C) and abundances continually decreased with increasing size of the prey organism (Fig. 4.1D-4.1F and 4.1G-4.1I). DVM behavior was exhibited (non-overlapping 95% confidence intervals) in the two smallest size classes of copepods, (FD ≤ 3mm and 3 < FD ≤ 9 mm; Fig. 4.1A and 4.1D, respectively), but not in the largest size class of copepods (FD > 9 mm; Fig. 4.1G).

Most smaller size classes of predators also showed their greatest abundances shallower than 50 dBar, and abundances decreased rapidly with increasing depth (Fig. 4.2). The largest predators showed more even dispersion from 400 dBar to the surface. The largest chaetognaths (FD > 16 mm) appeared to exhibit DVM behavior (non-overlapping 95% confidence intervals), although data in this size category were sparse. The smallest trachymedusae (ECD ≤ 3 mm; Fig. 4.2E) had a distinct abundance maximum at ~ 50 dBar, while the slightly larger trachymedusae (3 < ECD ≤ 6 mm) had abundances peaks near the surface. Additionally, a qualitative assessment of the sorted images revealed some morphological differences between size classes

of predators. Large trachymedusae, ECD > 3 mm, generally had much longer and more apparent tentacles than the smaller organisms. The smallest siphonophores, ECD ≤ 3 mm, were a heterogeneous mix of siphonophore parts, solitary zooids, and small colonial siphonophores. The larger siphonophores, FD > 3 mm, were almost exclusively large colonial siphonophores.

4.4.2 Weighted Mean Depth and Size Characterization:

All predatory and prey taxa showed increases in WMD between the smallest and largest size classes of organisms, while the intermediate size classes were more variable (Fig. 4.3). As all three copepod and siphonophore size classes had significantly different WMD (non-overlapping 95% confidence intervals), both of these taxa remained categorized by three size classes (i.e., small, medium, and large). Chaetognaths also had significantly different WMD for all size classes; however, due to the scarcity of data in the largest size class, only medium and small chaetognaths were retained for predator-prey encounter analysis. The WMD for the smallest size classes (FD ≤ 3 mm) of both *Fritillaria* and appendicularia-others were significantly different than their larger size classes (Fig. 4.3B and 4.3C). Thus, the larger two size classes, for *Fritillaria* and appendicularia-others, were combined into a single large class (FD > 3), while the small (FD ≤ 3 mm) class was retained. Similarly, the two largest size classes of trachymedusae appeared to be more closely associated with one another, and due to qualitative differences in observed vertical distributions and morphology, the two largest size classes of trachymedusae were combined, while the small category remained separate. For both ctenophores and narcomedusae the smaller and medium size-classes showed no significant difference in WMD, but both differed from the largest size classes (ECD > 9 mm; Fig. 4.3E and 4.3F). Therefore, the ctenophores and narcomedusae data were both subdivided into small organisms (ECD ≤ 9 mm) and large organisms (ECD > 9 mm).

The only taxa that showed significant differences in day-night distribution were copepods and chaetognaths, both of which showed size-dependent DVM behavior. Only the large chaetognaths (FD > 16 mm; Fig. 4.3D) exhibited DVM behavior, while smaller chaetognaths refrained from DVM. Conversely, the small and medium-sized copepods exhibited DVM behavior, while the large copepods did not migrate.

4.4.3 Co-occurrence Relationships:

Strong positive relationships ($\rho > 0.7$) were observed between abundances of small chaetognaths and each prey size class: small copepods (day and night), medium copepods (night), small *Fritillaria* (day and night), small and large appendicularia-others (day and night) (Fig. 4.4A, 4.4B black circles, 4.4D, 4.4F, and 4.4G). The relationships between small chaetognaths and both size classes of appendicularia-others appeared to be bilinear (Fig. 4.4F and 4.4G). Intermediate positive relationships ($0.4 < \rho < 0.7$) were found between small chaetognaths and medium copepods (day), large copepods (day and night), and large *Fritillaria* (day and night) (Fig. 4.4B red circles, 4.4C, and 4.4E). Medium chaetognaths had an intermediate positive relationship with medium copepods during the day ($\rho = 0.57$; Fig. 4.4I; red circles).

Small ctenophores had intermediate-strength relationships with both day and night abundances of large copepods and large *Fritillaria*; remaining abundance relationships were all strong (Fig. 4.5) and statistically significant. Abundances of large-sized ctenophores, narcomedusae, and siphonophores all showed no discernable relationship between any prey, regardless of size ($p>0.10$); thus, these figures were omitted for brevity.

Abundances of small narcomedusae had intermediate positive relationships with all potential prey taxa except large *Fritillaria* at night (Fig. 4.6). The relationship between small *Fritillaria* and small narcomedusae was not linear.

Small siphonophore abundances had strong positive relationships with day and night abundances of small and medium copepods, small *Fritillaria*, and small and large appendicularia-others (Fig. 4.7A, 4.7B, 4.7D, 4.7F, and 4.7G). Intermediate positive relationships were observed between small siphonophore and day and night abundances of large copepods and large *Fritillaria* (Fig. 4.7C and 4.7E). Small siphonophores had more variable relationships with both size classes of *Fritillaria*. Medium siphonophores had intermediate positive relationships with day and night abundance of small and medium copepods, small *Fritillaria*, and both size classes of appenidicularia-others (Fig. 4.7H, 4.7I, 4.7K, 4.7M, and 4.7N).

Small trachymedusae had relationships with prey items similar to small siphonophores, with strong positive relationships observed with day and night abundances of small and medium copepods, small *Fritillaria*, and all size classes of appendicularia-others (Fig. 4.8A, 4.8B, 4.8D, 4.8F and 4.8G). Small trachymedusae had intermediate positive relationships with large copepods and large *Fritillaria*, regardless of time of day (Fig. 4.8C and 4.8E). The relationship between small *Fritillaria* and small trachymedusae was nonlinear. Conversely, large trachymedusae had intermediate positive relationships with day and night small copepods, medium copepods, and small *Fritillaria* (Fig. 4.8A, 4.8B, and 4.8D, respectively). Relationships between large trachymedusae and both sizes of appendicularia-others abundance (Fig. 4.8M and 4.8N) were slightly variable between day ($\rho = 0.38$ and 0.32) and night ($\rho = 0.50$ and 0.57).

Furthermore, the highest abundances of large trachymedusae appeared to be offset from the abundance maxima of *Fritillaria* of either size class.

4.4.4 Vertical Distributions of Observed Encounter Rates:

Vertical distributions of the observed probability of potential encounters between small chaetognaths and each prey type revealed that small chaetognaths residing in the upper 50 dBar of the water column generally had the highest probability of encountering any prey (Fig. 4.9). Shallower than 50 dBar, the probability of a small chaetognath potentially encountering either a single small appendicularia-other, small copepod, or multiple small copepods within a 250 mL sample volume were quite similar (Fig. 4.9A-C and 4.9G). Deeper than 50 dBar, small chaetognaths had the highest probability of co-occurring with a single small copepod compared to other prey taxa. Overall, small chaetognaths were more likely to have a potential encounter with small prey compared to larger prey. Specifically, small chaetognaths had a greater probability of potentially encountering multiple small copepods compared to medium copepods. Small chaetognath potential encounters with large *Fritillaria* were extremely rare (Fig. 4.9F). Moreover, all predators were rarely observed encountering large *Fritillaria*, therefore, large *Fritillaria* were excluded from further predator-prey analyses.

Similar results to small chaetognaths were observed for large chaetognaths. Large chaetognaths predominately encountered their prey shallower than 50 dBar, and it appeared that smaller prey were encountered with greater likelihood than larger prey. However, as there were smaller numbers of observed large chaetognath encounters, the results showed more variability.

4.4.5 Observed vs. Theoretical Probabilities of Encounter:

Small chaetognaths showed strong positive relationships between the observed probability of potential encounters and the theoretical probability of potentially encountering 1,

2, and ≥ 3 small copepods (day and night; Fig. 4.11A-11C), ≥ 1 medium copepods (night; Fig. 4.11D; black circles), and ≥ 1 small and large appendicularia-others (day and night; Fig. 4.11F-11G). Intermediate positive relationships were found between small chaetognaths and ≥ 1 small *Fritillaria* (day and night; Fig. 4.11E) and ≥ 1 medium copepods (day; Fig. 4.11D; red circles). Large chaetognaths showed strong positive relationships for potentially encountering 2 small copepods (night; Fig. 4.12B; black circles), ≥ 3 small copepods (day and night; Fig. 4.12C), and ≥ 1 small appendicularia-others (day and night; Fig. 4.12F). Intermediate positive relationships were found for medium chaetognaths encountering single small copepods (day and night; Fig. 4.12A), 2 small copepods (day; Fig. 4.12B; red), ≥ 1 medium copepods (day and night; Fig. 4.12D), ≥ 1 small *Fritillaria* (day and night; Fig. 4.12E), and ≥ 1 large appendicularia-others (day and night; Fig. 4.12G).

Table 4.2 shows the Spearman rank ρ-values for all combinations of observed probabilities of predator-prey potential encounters and how those probabilities relate to theoretical probabilities of potential encounters. Predator-prey combinations that resulted in less than six observed encounter data points, when data were binned at 2 dBar, were omitted. Overall, the relationship between the probability of observed encounter with prey and the theoretical probability of encountering prey was stronger for small prey organisms compared to larger prey organisms. Moreover, a predator had stronger relationships with encountering multiple small copepods compared to single medium copepods.

4.5 Discussion:

4.5.1 Size-dependent Vertical Distributions:

In general, the weighted mean depth (WMD) of each taxon increased with increasing body size. However, differences in appendicularia-others and trachymedusae WMD were more subtle. The deeper habitat depth of larger animals was most likely attributable to their being more conspicuous to visual predators in shallower, better-illuminated waters (Brooks and Dodson, 1965; De Robertis, 2002; Ohman and Romagnan, 2016). Conversely, smaller zooplankton were less conspicuous and apparently experienced insufficient visual predation risk to lead them to sacrifice foraging time in higher prey concentrations near the surface. The relatively shallower depths of appendicularia-others could be explained by the requirement of vertical overlap with their preferred food source, i.e., small particles (Chapter 3), whereas trachymedusae may have temperature (Arai, 1992), salinity (Toda et al., 2010), or dissolved oxygen restrictions (FuadSaneen and Padmavati, 2017).

Nonlinear and bilinear relationships were observed between predators and both appendicularian groups: *Fritillaria* and appendicularia-others. These differences in relationship were likely caused by differences in vertical habitat. Appendicularia-others were most abundant from 50 dBar to the surface, whereas *Fritillaria* had peaks in abundance around 50 dBar, and surface concentrations were markedly reduced. The risk of visual predation to the larger predatory taxa likely reduces the degree of overlap between themselves and these prey taxa. Or perhaps copepods were the preferred prey source and relationships with appendicularia-others and *Fritillaria* are coincident.

Significant day-night differences in weighted mean depth were evident for large chaetognaths and both small and medium copepods. Conversely, both small and medium

chaetognaths and large copepods refrained from DVM. The copepod DVM results were similar to those of Ohman and Romagnan (2016), who found DVM behavior was exhibited solely in copepods with body size (as feret diameter) ranging from 2.5 and 7 mm, while smaller and large copepods did not perform DVM. However, here we found that even the smallest size class of copepods showed a small-amplitude DVM. The difference between the current study and that of Ohman and Romagnan (2016) probably occurred because of the vertical resolution of net sampling, with samples taken every ~50 m. At this coarse resolution, the subtle day-night difference of ~15 m in vertical distribution observed here in the small copepods would not have been resolvable. Due to the greater resolution capabilities of *Zooglider*, it was possible to measure this subtle DVM behavior of the smaller copepods. Ohman and Romagnan (2016) attributed these nonlinear effects of body size on copepod DVM behavior to visual predation risk, further modulated by the optical attenuation properties of the water column (Ohman and Romagnan, 2016). The present results showing that copepods with FD ≤ 3 mm exhibited DVM behavior indicate that these small copepods were conspicuous enough to have substantial visual-predation risk, thereby requiring energetically costly DVM.

Size-dependent DVM in chaetognaths was previously observed in *Sagitta elegans*, where juvenile chaetognaths less than 17 mm long remained consistently in shallow water (0-25 m) during both the day and night, while the larger chaetognaths migrated from deeper water (200-400 m) to shallower water during the night (Sullivan, 1980). In contrast, the other chaetognath species in the Sullivan (1980) study, *Eukrohnia hamata*, had a much broader and deeper vertical range in its juvenile size class (25-100 m), and no DVM behavior was observed in both the adult and juvenile *E. hamata*. These interspecific differences in DVM and vertical ranges were

attributed to juvenile *S. elegans* requiring higher prey densities, and *E. hamata* having temperature restrictions limiting their access to warmer surface waters.

This difference in how size influences DVM behavior in chaetognaths and copepods is likely attributable to differences in opacity and predation strategy between the two taxa. Chaetognaths have largely transparent bodies, while copepods are predominately opaque. Furthermore, chaetognaths are ambush feeders (Feigenbaum and Reeve, 1977), and are thus subjected to less predation risk than copepods that exhibit a broad range of predation strategies, i.e., ambush, cruise, current-feeding (Kiørboe et al., 1996; Kiørboe and Visser 1999; Kiørboe, 2011; Kjellerup and Kiørboe, 2011)

No DVM behavior was observed in any other predator or prey taxa; however, some hydromedusae (Andersen et al., 1992) and ctenophores (Haraldsson et al., 2014) have been observed to exhibit DVM. This lack of observed DVM behavior could be due to a combination of the relative transparency of many of the gelatinous predators combined with the fact that many of these taxa are primarily ambush predators (low motility while hunting) resulting in diminished visual predatory risk on these size ranges of gelatinous predators.

4.5.2 Size-dependent Predator-Prey Encounters:

In general, the abundances of small copepods, small *Fritillaria*, and both small and large appendicularia-others had the strongest relationships with the abundance of smaller predators, namely small chaetognaths, ctenophores, siphonophores, and trachymedusae. Small narcomedusae, and larger chaetognaths, siphonophores, and trachymedusae had more consistently intermediate relationships with prey, regardless of organismal size. Observations of *in situ* probabilities of potential encounters bolstered the evidence for size-dependent predator-prey encounters and provide evidence that small appendicularia-others were encountered with

greater likelihood than large appendicularia-others. Furthermore, multiple small copepods were encountered by predators more often than single medium copepods. The strong positive relationships between observed probabilities of potential encounter and theoretical probabilities of potential encounter likely mean that predator and prey were not encountering one another at random. Observations of i*n situ* probabilities of predator-prey potential encounters would not have been possible with any current zooplankton sensing system except *Zooglider*. Therefore, the encounters with multiple copepods and size-dependent appendicularia-other encounters may have been missed previously.

Chaetognaths have previously been observed to have size-dependent interactions with their prey organisms. For instance, Saito and Kiørboe (2001) found that chaetognaths had maximum clearance rates occurring for copepod prey that were 6-10% of the total chaetognath length. This prey size selectivity makes sense as chaetognaths are gape limited with the size of prey that they can consume, since they swallow their prey whole (Pearre, 1980). Therefore, larger chaetognaths would be able to ingest larger prey, but also be able to ingest the smaller prey (Saito and Kiørboe, 2001). Similarly, hydromedusae and ctenophores are limited in the size of prey that they can capture, handle and ingest (Wirtz, 2012). Hansson and Kiørboe (2006) found that *Sarsia tubulosa* was 10 times more efficient at handling smaller copepodite *Acartia tonsa* than larger cirripede larvae.

Small narcomedusae had different relationships with prey size compared to the other gelatinous predators. Specifically, small narcomedusae had more intermediate relationships with prey regardless of prey size. This may be explained by the fact that narcomedusae are primarily cruising predators. Cruise predators hunt while swimming, which increases their chances of encountering motile and non-motile prey compared to those available to an ambush predator

(Costello et al., 2008). Furthermore, narcomedusae have previously been shown to consume hydromedusae and other gelatinous predators (Purcell, 1997). However, net collection of gelatinous organisms can make feeding estimates suspect due to damage of the organism, gut evacuation, and net feeding (Purcell, 1989).

These size-dependent potential encounter rates could be viewed as contrasting to predator-prey encounter theory, i.e., larger sized organisms should have higher encounter rates (Gerritsen and Strickler, 1977). For instance, larger prey generate more hydrodynamic disturbances while swimming, which should make them more apparent (i.e., greater detection radius) to non-visual predators (Kiørboe and Visser, 1999; Visser, 2007). Additionally, larger prey swim faster than smaller prey (Dodson and Ramcharan, 1991) and should theoretically encounter predators more often (Gerritsen and Strickler, 1977; Kiørboe and Visser, 1999). Increased theoretical encounter rates (i.e., heightened predation risk) for large prey may cause them to select deeper habitats despite ample food availability in shallower waters. Alternatively, larger prey may be able to detect predators and escape before an encounter occurs or was observable by *Zooglider* (Suchman and Sullivan, 2000; Suchman, 2000).

Larger predators had drastically decreased observed probabilities of encountering prey. Thus, it is difficult to evaluate the relationships between larger predator and prey abundances. Due to low measured encounters with prey organisms, it makes sense that many gelatinous predators and chaetognaths have adapted to increase their chances of finding prey. Larger chaetognaths have adapted by performing DVM behaviors into higher predation risk waters with high concentrations of prey.

Gelatinous organisms have adapted by utilizing tentacles to increase their volume of water searched (Purcell, 1997; Ohman, 2019). Some siphonophores have adapted hunting

strategies to capture specific types of prey. Siphonophores can perform brief helical swimming bouts to cast their tentacles into a feeding net (Purcell, 1997). If larger prey are the preferred prey type, siphonophores swim slowly so the tentacles are closer together and likely to coalesce on a single prey item and reduce the probability of escape. Siphonophores that hunt smaller prey swim faster, and increase the distance between tentacles to increase the available contact volume for prey to encounter (Purcell, 1980). Other deeper dwelling siphonophores have developed red bioluminescent lures to attract prey to their tentacles (Haddock et al., 2005). Cruise feeding ctenophores utilize stealth swimming via their comb rows and auricles to allow them to approach prey with a minimized bow wave (Matsumoto and Harbison, 1993).

4.6 Conclusions:

Larger-sized zooplankton had deeper distributions than their smaller counterparts, both day and night, which was most likely attributable to increased predation risk to larger-bodied zooplankton in shallower waters. Copepods and chaetognaths exhibited different size-dependent DVM behaviors due to differing opacity and predation strategies. Smaller predatory chaetognaths, siphonophores, trachymedusae, and ctenophores showed stronger correlations with abundances of smaller prey copepods, *Fritillaria,* and appendicularia-others compared to larger organisms of these prey taxa. Small narcomedusae and medium chaetognaths, siphonophores, and large trachymedusae had more consistent positive relationships with all prey items regardless of size. These stronger co-occurrences with smaller prey items were likely due to gape and handling limitations of smaller predators. Conversely, larger predators were not hindered by morphological constraints, but instead were limited by increased predation risk and thus have different hunting strategies that increase their probabilities of encountering prey. These size-

dependent vertical distributions, predator-prey encounters, and observed probabilities of *in situ* encounters would not have been observable before the development of *Zooglider*.

4.7 Tables and Figures:

Table 4.1. Taxa size classifications and definitions. ECD stands for equivalent circular diameter and FD is an abbreviation for feret diameter.

Taxa	Size Class	Measurement (mm)
Copepods	Small	FD ≤ 3
	Medium	3 < FD ≤ 9
	Large	FD > 9
Fritillaria	Small	FD ≤ 3
	Large	FD > 3
Appendicularia-others	Small	FD ≤ 3
	Large	FD > 3
Chaetognaths	Small	FD ≤ 8
	Medium	16 ≥ FD > 8
Ctenophores	Small	ECD ≤ 9
	Large	ECD > 9
Narcomedusae	Small	ECD ≤ 9
	Large	ECD > 9
Siphonophores	Small	ECD ≤ 3
	Medium	3 < ECD ≤ 6
	Large	ECD > 6
Trachymedusae	Small	ECD ≤ 3
	Large	ECD > 3

Table 4.2. Spearman rank correlation ρ-values for the relationship between the observed probability of predator taxa encountering 'x' number of prey organisms within a 250 mL sample volume and the theoretical probability of the same encounter occurring. If <6 data points were observed for an encounter, the data are not displayed. Bold ρ-values represent strong positive relationships ($\rho \geq 0.70$).

			Spearman rank ρ-value						
			Copepods				*Fritillaria*	App-others	
			Small			Medium	Small	Small	Large
		No of Prey Frame-1	1	2	≥3	≥1	≥1	≥1	≥1
Chaetognath	Small	Day	**0.75**	**0.82**	**0.83**	0.60	0.61	**0.81**	**0.76**
		Night	**0.77**	**0.86**	**0.92**	**0.74**	0.62	**0.81**	**0.73**
	Medium	Day	0.54	0.57	**0.82**	0.51	0.57	**0.76**	0.47
		Night	0.56	0.69	**0.78**	0.58	0.53	**0.74**	0.44
Ctenophores	Small	Day	**0.74**	**0.77**	**0.83**	0.49	0.63	**0.80**	0.53
		Night	**0.73**	**0.82**	**0.89**	0.58	0.38	**0.80**	0.49
Narcomedusae	Small	Day	0.64	**0.75**	**0.76**		0.51	**0.76**	0.55
		Night	0.62	**0.82**	**0.79**	0.62	0.57	**0.83**	0.55
Siphonophores	Small	Day	0.59	**0.81**	**0.84**	0.61	0.66	**0.83**	**0.72**
		Night	**0.72**	**0.82**	**0.88**	**0.80**	0.55	**0.83**	**0.78**
	Medium	Day	0.51	0.58	**0.74**	0.37		**0.78**	
		Night	**0.7**	0.58	**0.78**			0.65	
Trachymedusae	Small	Day	0.56	**0.75**	**0.88**	0.65	0.68	**0.83**	**0.71**
		Night	0.68	**0.80**	**0.88**	**0.78**	**0.75**	**0.80**	0.69
	Large	Day	0.41	0.62	**0.76**		0.39	**0.70**	
		Night	0.61	0.61	0.46		0.41	**0.70**	

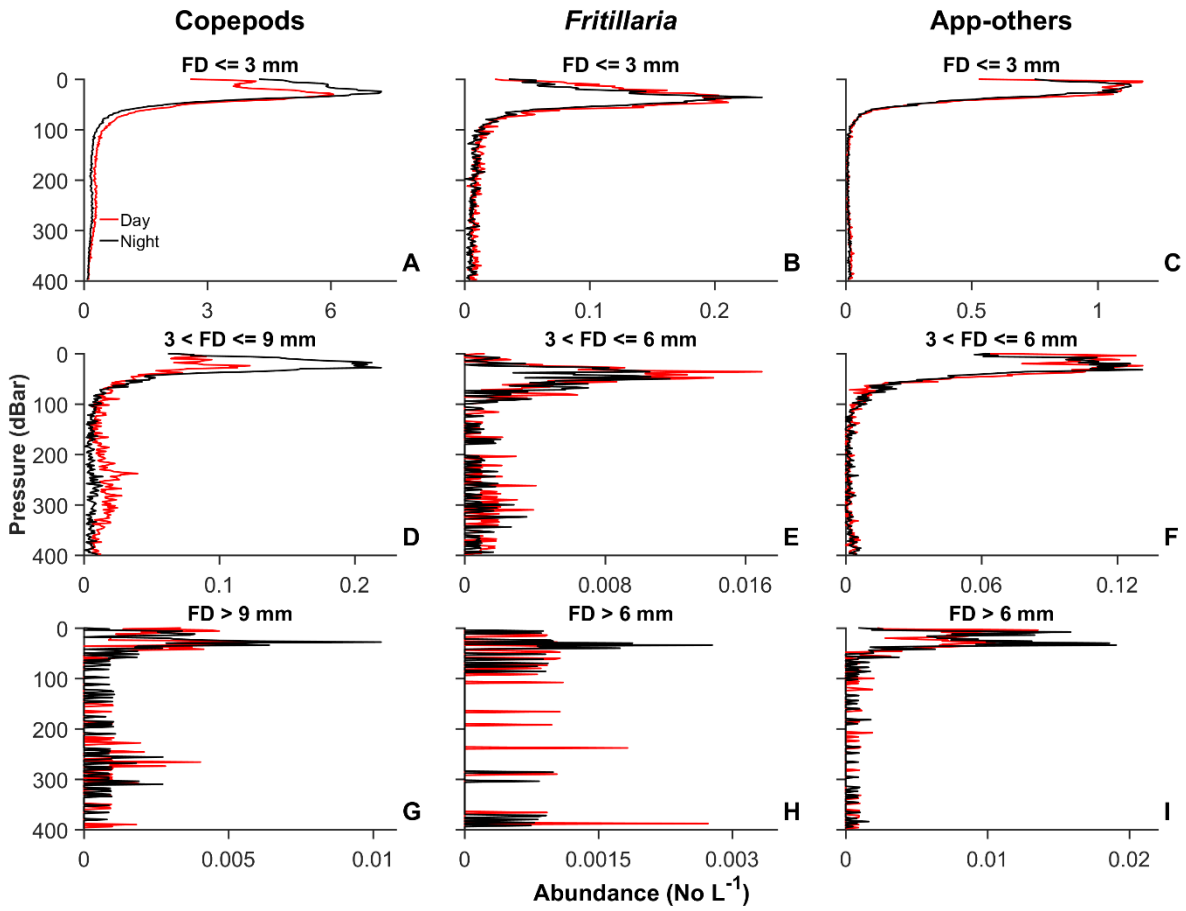

Figure 4.1. Vertical distributions (No. L^{-1}) for different size classes of suspension-feeding zooplankton. Vertical abundances are plotted by day (red lines) and night (black lines). Data are binned at 2 dBar intervals. Size classes are characterized by feret diameter (FD).

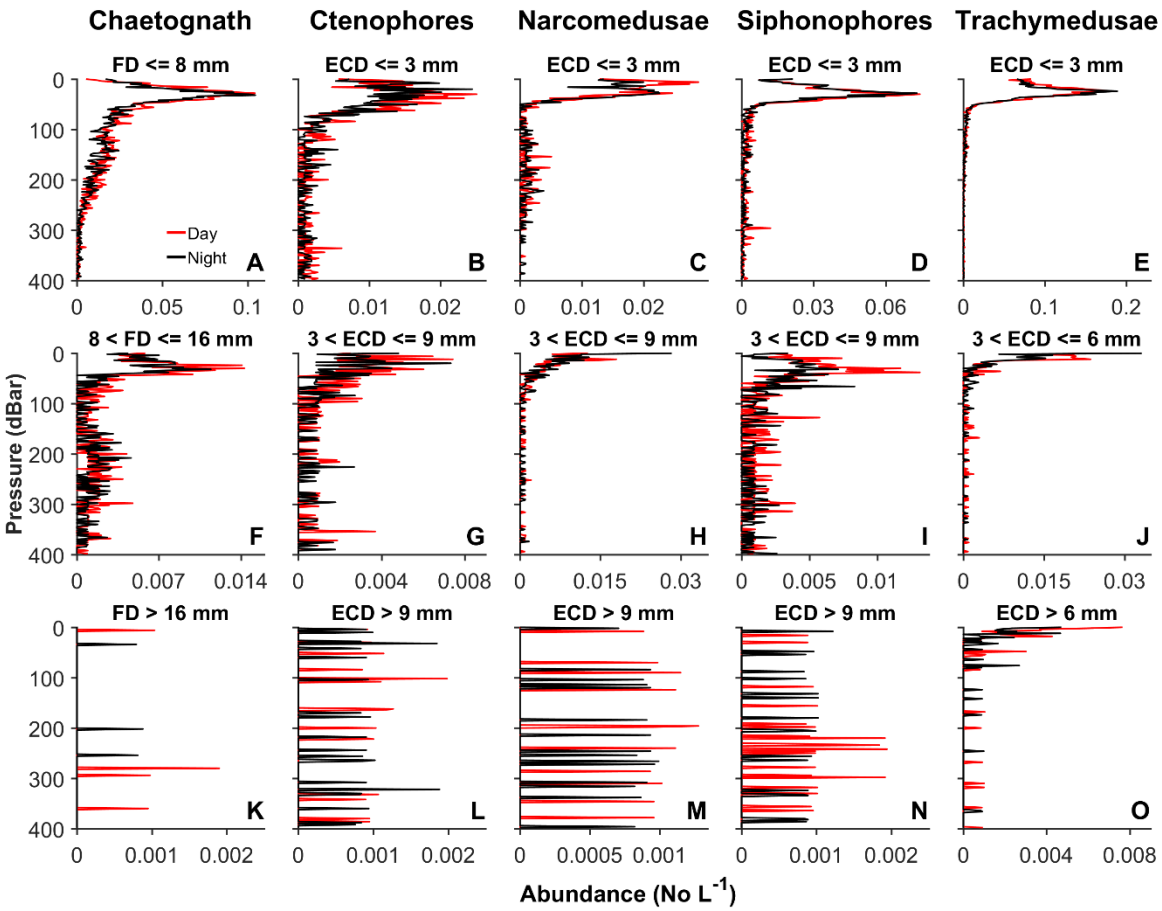

Figure 4.2. Vertical distributions (No. L^{-1}) for different size classes of predatory zooplankton. Vertical abundances are plotted by day (red lines) and night (black lines) dives. Data are binned at 2 dBar intervals. Size classes are characterized by feret diameter (FD) or equivalent circular diameter (ECD).

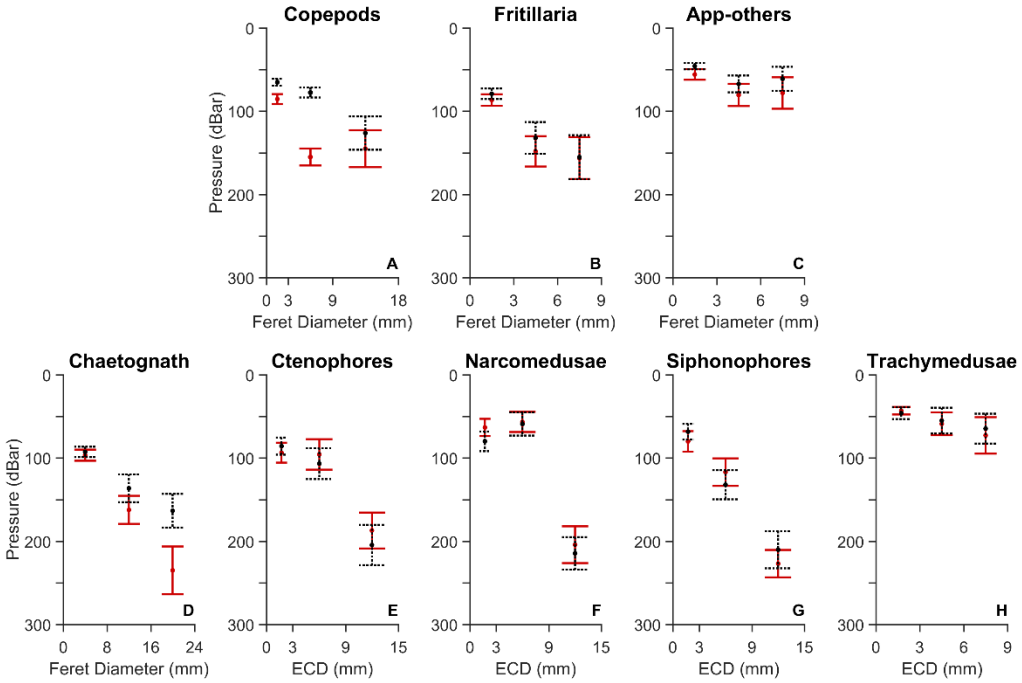

Figure 4.3. Weighted mean depths (WMD) of different size classes of suspension-feeding (A-C) and predatory (D-H) taxa. Day (red) and night (black) WMD are displayed with 95% confidence intervals. Size classes are characterized by either feret diameter or equivalent circular diameter (ECD). Values are plotted at the mid-point of each size interval.

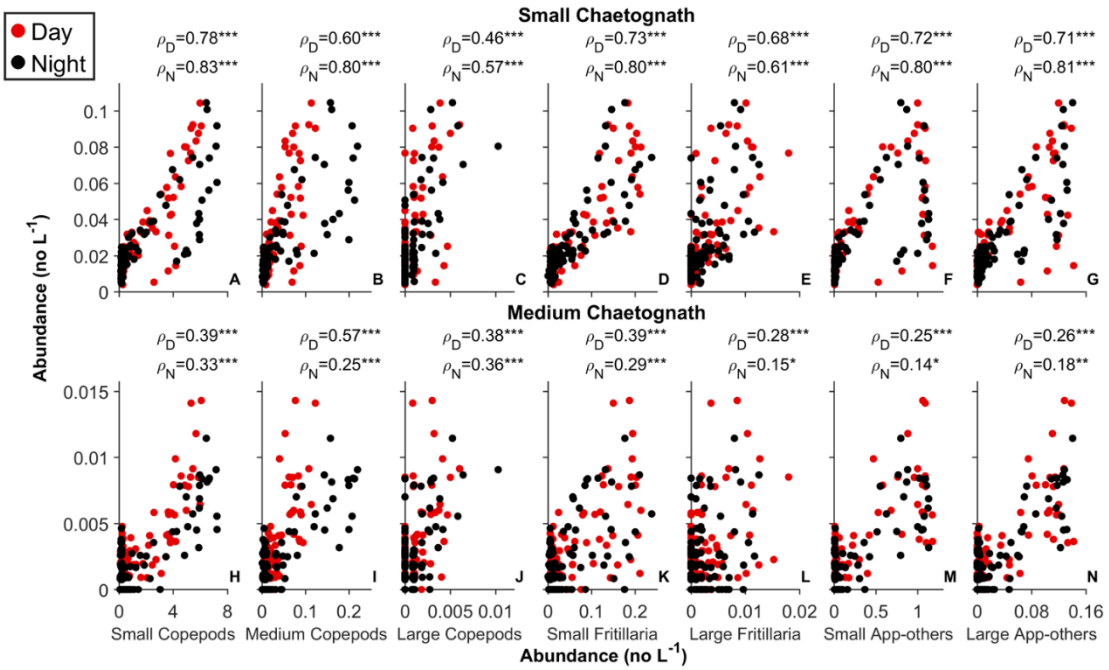

Figure 4.4. Abundance relationships between small and medium chaetognaths and varying prey organismal abundances by day (red) and night (black). Spearman rank correlation ρ-values are displayed. $p<0.05$ = *, $p<0.01$ = **, $p<0.001$ = ***.

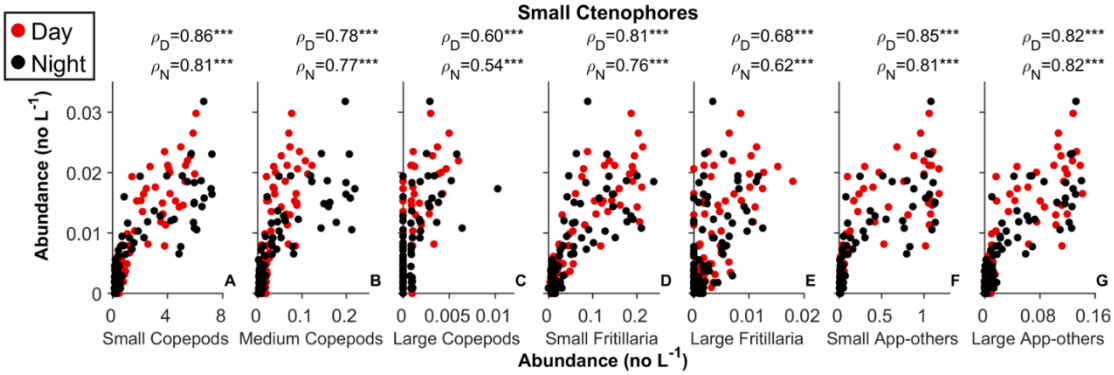

Figure 4.5. Abundance relationships between small ctenophores and varying prey organismal abundances by day (red) and night (black). Spearman rank correlation ρ-values are displayed. $p<0.05$ = *, $p<0.01$ = **, $p<0.001$ = ***.

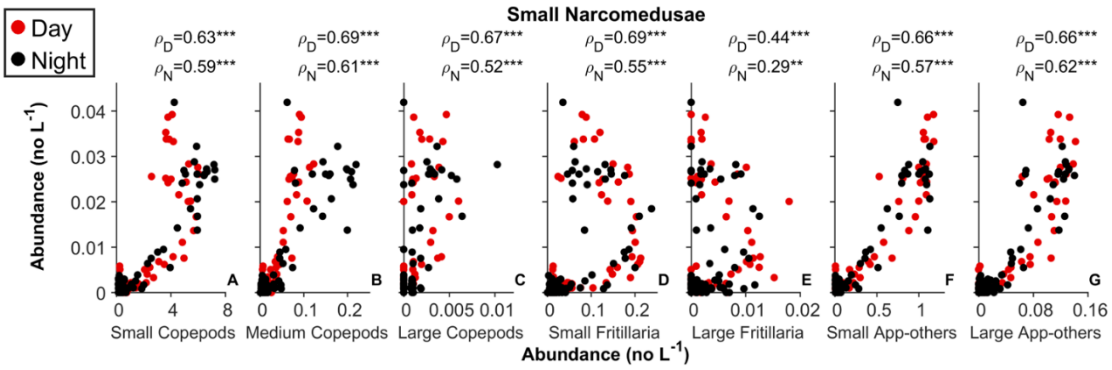

Figure 4.6. Abundance relationships between small narcomedusae and varying prey organismal abundances by day (red) and night (black). Spearman rank correlation ρ-values are displayed. p<0.05 = *, p<0.01 = **, p<0.001 = ***.

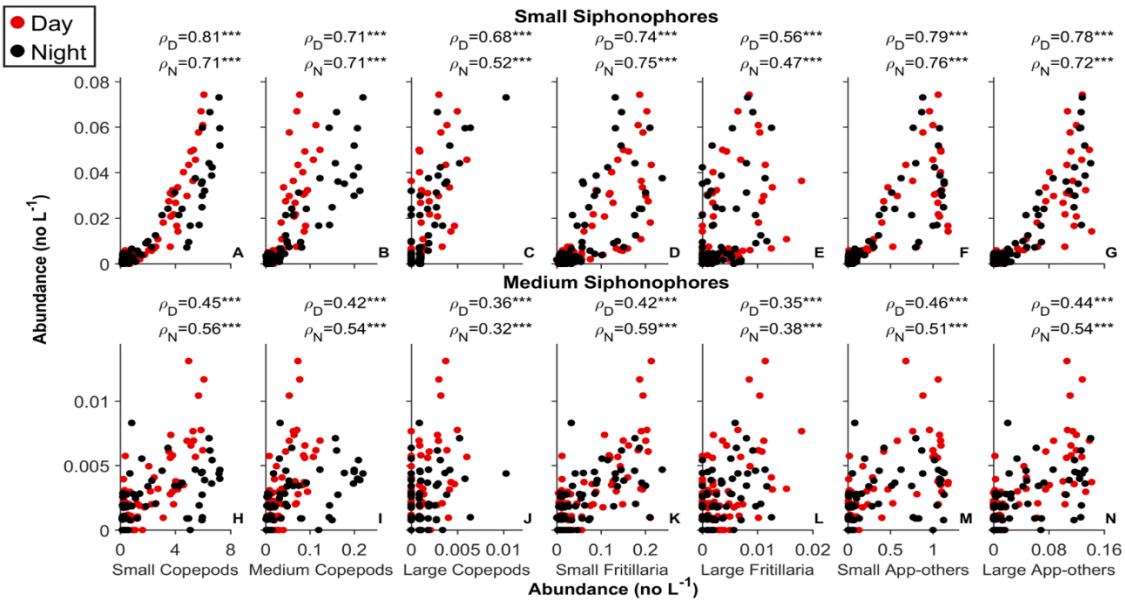

Figure 4.7. Abundance relationships between small and medium siphonophores and varying prey organismal abundances by day (red) and night (black). Spearman rank correlation ρ-values are displayed. p<0.05 = *, p<0.01 = **, p<0.001 = ***.

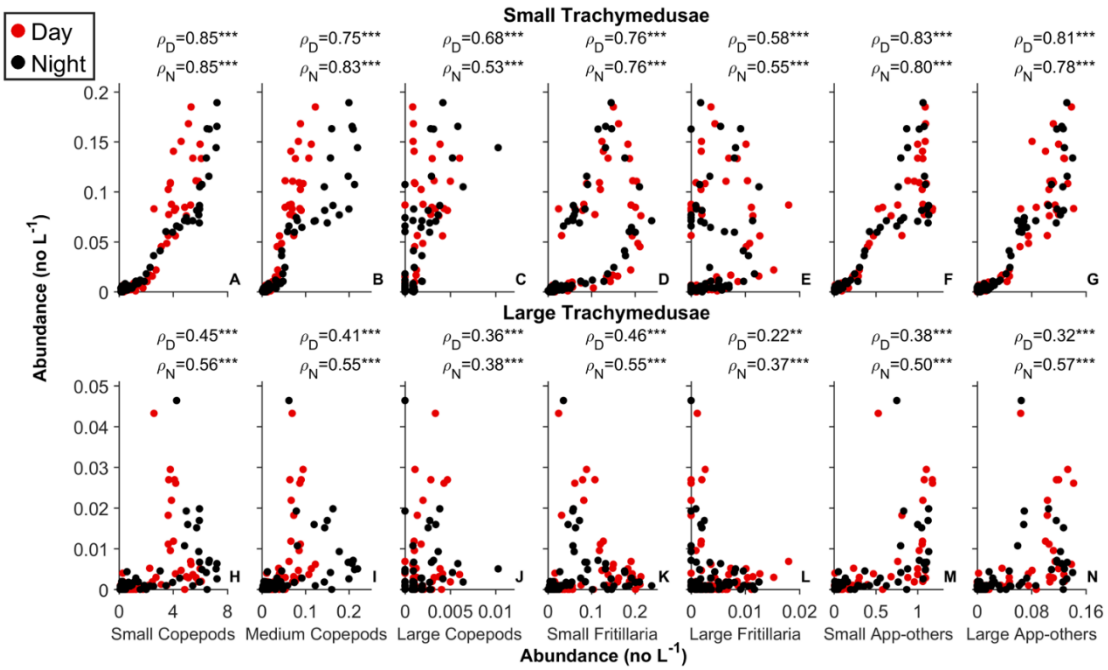

Figure 4.8. Abundance relationships between small and large trachymedusae and varying prey organismal abundances by day (red) and night (black). Spearman rank correlation ρ-values are displayed. $p<0.05$ = *, $p<0.01$ = **, $p<0.001$ = ***.

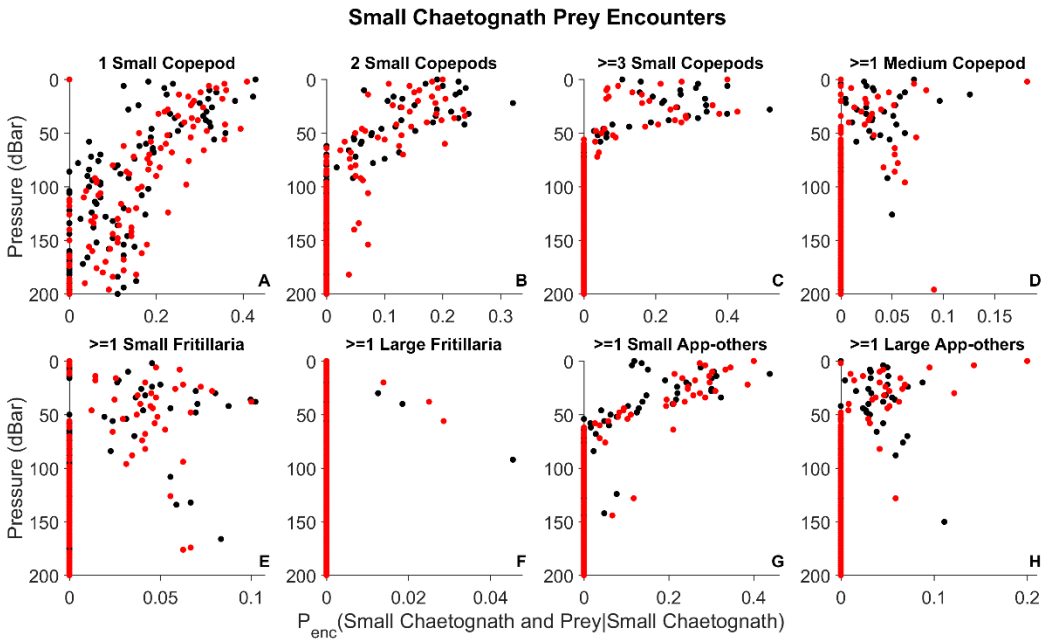

Figure 4.9. Vertical distributions of observed probabilities (P_{enc}) of a small chaetognath encountering 'x' number of prey organisms within a 250 mL sample. Data are dichotomized by day (red) and night (black) and binned at 2 dBar.

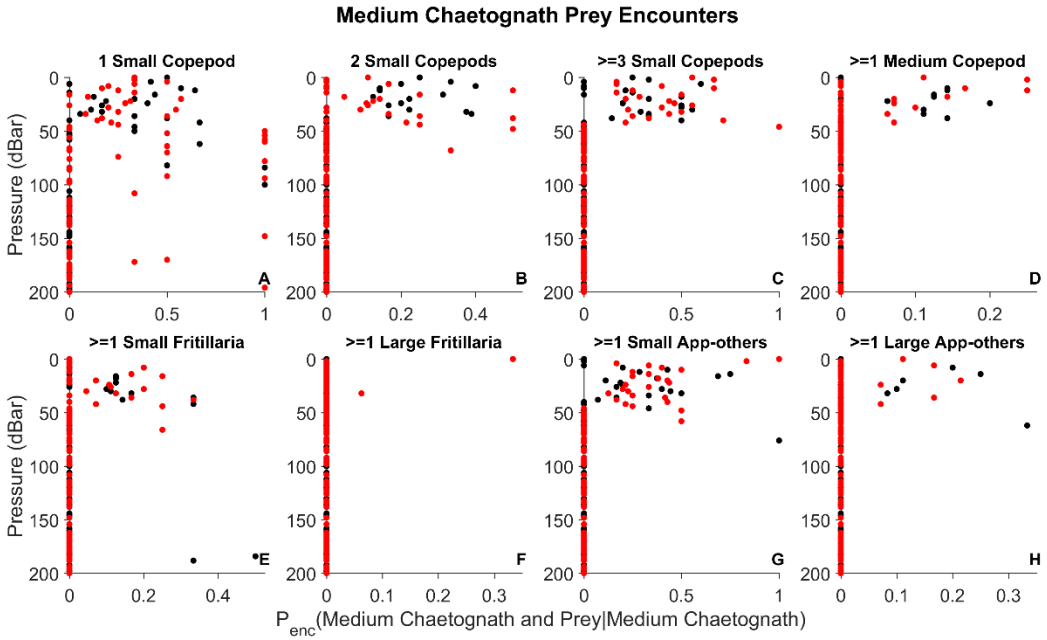

Figure 4.10. Vertical distributions of observed probabilities (P_{enc}) of a medium chaetognath encountering 'x' number of prey organisms within a 250 mL sample. Data are dichotomized by day (red) and night (black) and binned at 2 dBar.

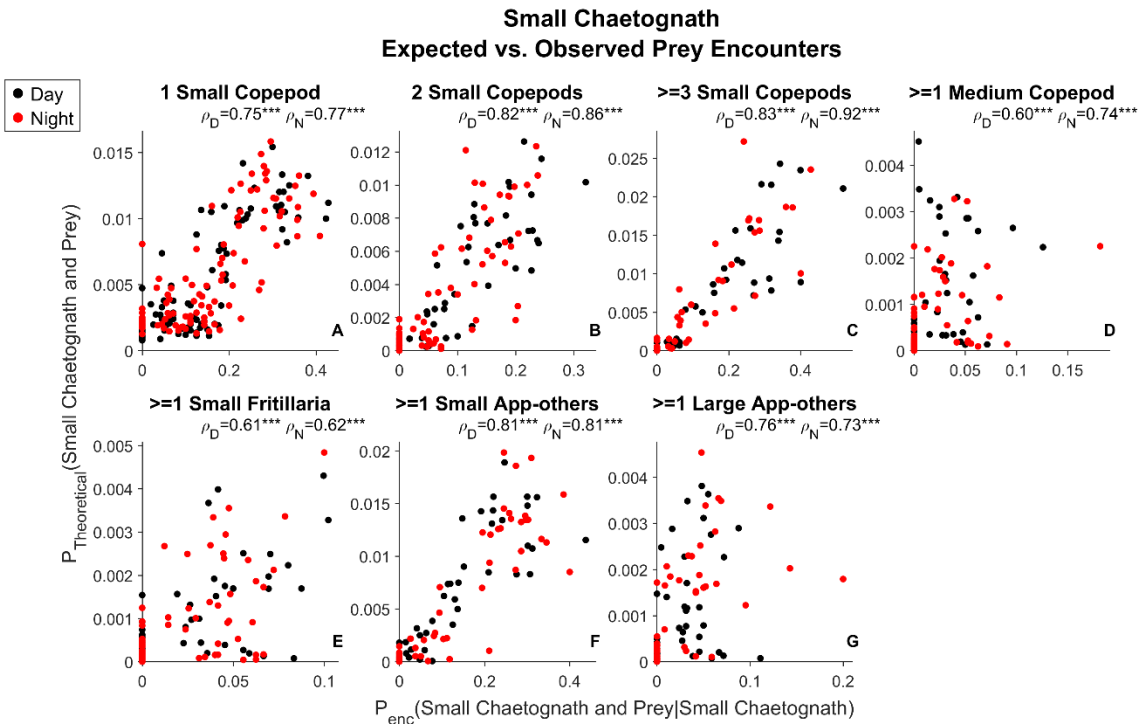

Figure 4.11. Relationships between the observed probability of a small chaetognath encountering 'x' number of prey organisms within a 250 mL sample volume and the theoretical probability of the same encounter occurring. Data are dichotomized by day (red) or night (black). Spearman rank correlation ρ-values are displayed. $p<0.05$ = *, $p<0.01$ = **, $p<0.001$ = ***.

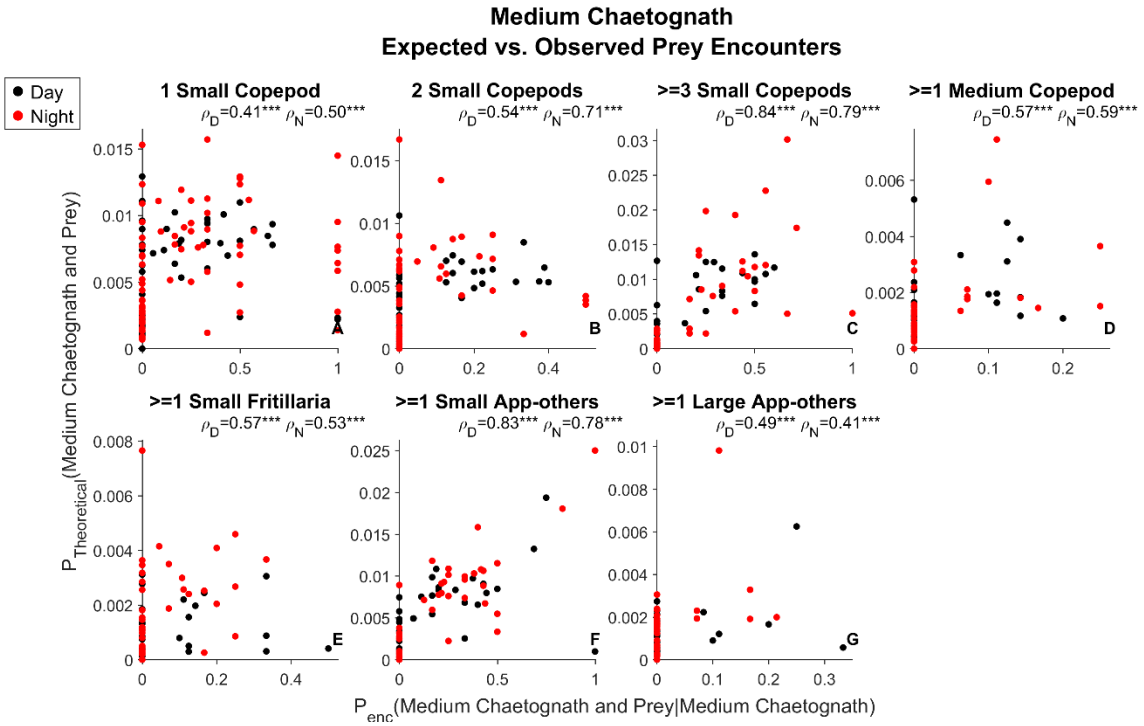

Figure 4.12. Relationships between the observed probability of a medium chaetognath encountering 'x' number of prey organisms within a 250 mL sample volume and the theoretical probability of the same encounter occurring. Data are dichotomized by day (red) or night (black). Spearman rank correlation ρ-values are displayed. P-values are displayed as either $p<0.05$ = *, $p<0.01$ = **, $p<0.001$ = ***.

4.8 Acknowledgements:

This work could not have been done without the help of the following individuals: E. Tovar and L. Sala for organism identification. J. Ellen for the machine learning sorting of the images and paper edits. P.J.S. Franks for help with probabilities of encounter calculations. M.D. Ohman for deployment design, paper edits, data analysis help, and organism identification. I would also like to thank the entirety of the Instrument Development Group (IDG) at the Scripps Institution of Oceanography for the construction and development of *Zooglider.* As well as IDG's continued help in maintaining, deploying, managing deployments, and recovering *Zooglider*. The Gordon and Betty Moore Foundation (grants to M.D. Ohman) for funding the development of *Zooglider*. NSF for support of the CCE-LTER program, the NSF GRFP, and DoD SMART Scholarship program for funding me through the duration of my PhD work.

Chapter 4, in part, is currently being prepared for submission for publication of the material. **Whitmore, B.M.** and Ohman, M.D. Size-dependent predator-prey encounters in the zooplankton. The dissertation author was the primary author on this paper.

4.9 References:

Arai, M.N., 1992. Active and passive factors affecting aggregations of hydromedusae: A review. *Scientia Marina*, 56(2), pp.99-108.

Brooks, J.L. and Dodson, S.I., 1965. Predation, body size, and composition of plankton. *Science*, 150(3692), pp.28-35.

Costello, J.H., Colin, S.P. and Dabiri, J.O., 2008. Medusan morphospace: phylogenetic constraints, biomechanical solutions, and ecological consequences. *Invertebrate Biology*, *127*(3), pp.265-290.

De Robertis, A., Jaffe, J.S. and Ohman, M.D., 2000. Size-dependent visual predation risk and the timing of vertical migration in zooplankton. *Limnology and Oceanography*, *45*(8), pp.1838-1844.

Dodson, S. and Ramcharan, C., 1991. Size-specific swimming behavior of *Daphnia pulex*. *Journal of Plankton Research*, 13(6), pp.1367-1379.

Eiane, K. and Ohman, M.D., 2004. Stage-specific mortality of *Calanus finmarchicus*, *Pseudocalanus elongatus* and *Oithona similis* on Fladen Ground, North Sea, during a spring bloom. *Marine Ecology Progress Series*, 268, pp.183-193.

Ellen, J.S., Graff C.A., and Ohman, M.D. 2019. Improving plankton image classification using context metadata. *Limnology and Oceanography-Methods*. 17, pp. 439-461. DOI 10.1002/lom3.10324

Feigenbaum D., and Reeve M.R., 1977. Prey detection in Chaetognatha: Response to a vibrating probe and experimental determination of attack distance in large aquaria. *Limnology and Oceanography*, 22, pp. 1052–1058.

Fields, D. M., and J. Yen, 1997, The escape behavior of marine copepods in response to a quantifiable fluid mechanical disturbance. *Journal of Plankton Research*, 19, pp. 1289-1304.

Fitzgeorge-Balfour, T., Hirst, A.G., Lucas, C.H. and Craggs, J., 2013. Influence of copepod size and behaviour on vulnerability to predation by the scyphomedusa *Aurelia aurita*. *Journal of Plankton Research*, 36(1), pp.77-90.

FuadSaneen C.V. and Padmavati, G., 2017. Distribution and Abundance of Gelatinous Zooplankton in Coastal Waters of Port Blair, South Andaman. *Journal of Aquaculture and Marine Biology*, 5(6), p.00139.

Gaskell, D.E., Ohman, M.D. and Hull, P.M., 2019. *Zooglider*-based measurements of planktonic foraminifera in the California Current System. *Journal of Foraminiferal Research*, 49(4), pp.390-404.

Gerritsen, J. and Strickler, J.R., 1977. Encounter probabilities and community structure in zooplankton: a mathematical model. *Journal of the Fisheries Board of Canada*, 34(1), pp.73-82.

Greene, C.H., Landry, M.R. and Monger, B.C., 1986. Foraging behavior and prey selection by the ambush entangling predator *Pleurobrachia bachei*. *Ecology*, 67(6), pp.1493-1501.

Haddock, S.H., Dunn, C.W., Pugh, P.R. and Schnitzler, C.E., 2005. Bioluminescent and red-fluorescent lures in a deep-sea siphonophore. *Science*, 309(5732), pp.263-263.

Hamner, W.M., Hamner, P.P., Strand, S.W. and Gilmer, R.W., 1983. Behavior of Antarctic krill, *Euphausia superba*: chemoreception, feeding, schooling, and molting. *Science*, 220(4595), pp.433-435.

Hansson, L.J. and Kiørboe, T., 2006. Prey-specific encounter rates and handling efficiencies as causes of prey selectivity in ambush-feeding hydromedusae. *Limnology and oceanography*, 51(4), pp.1849-1858.

Haraldsson, M., Båmstedt, U., Tiselius, P., Titelman, J. and Aksnes, D.L., 2014. Evidence of diel vertical migration in *Mnemiopsis leidyi*. *PloS one*, 9(1), p.e86595.

Hays, G.C., 2003. A review of the adaptive significance and ecosystem consequences of zooplankton diel vertical migrations. In *Migrations and Dispersal of Marine Organisms*, pp. 163-170. Springer, Dordrecht.

Holling, C.S., 1966, The functional Response of Invertebrate Predators to Prey Density. *Memoirs of the Entomological Society of Canada*, 98, pp. 5-86.

Huntley, M., and E. Brooks, 1982, Effects of age and food availability on diel vertical migration of *Calanus pacificus*. *Marine Biology*, 71, pp. 23-31.

Kiørboe, T., 2011. How zooplankton feed: mechanisms, traits and trade-offs. *Biological Reviews*, 86(2), pp.311-339.

Kiørboe, T., 2008. Optimal swimming strategies in mate-searching pelagic copepods. *Oecologia*, 155(1), pp.179-192.

Kiørboe, T., Andersen, A., Langlois, V.J. and Jakobsen, H.H., 2010. Unsteady motion: escape jumps in planktonic copepods, their kinematics and energetics. *Journal of the Royal Society Interface*, *7*(52), pp.1591-1602.

Kiørboe, T., Andersen, A., Langlois, V.J., Jakobsen, H.H. and Bohr, T., 2009. Mechanisms and feasibility of prey capture in ambush-feeding zooplankton. *Proceedings of the National Academy of Sciences*, *106*(30), pp.12394-12399.

Kiørboe, T. and Visser, A.W., 1999. Predator and prey perception in copepods due to hydromechanical signals. *Marine Ecology Progress Series*, 179, pp.81-95.

Kiørboe, T., Saiz, E. and Viitasalo, M., 1996. Prey switching behaviour in the planktonic copepod *Acartia tonsa*. *Marine Ecology Progress Series*, 143, pp.65-75.

Kiørboe, T. and MacKenzie, B., 1995. Turbulence-enhanced prey encounter rates in larval fish: effects of spatial scale, larval behaviour and size. *Journal of Plankton Research*, 17(12), pp.2319-2331.

Kjellerup, S. and Kiørboe, T., 2011. Prey detection in a cruising copepod. *Biology Letters*, 8(3), pp.438-441.

Knoll, A.H. and Kotrc, B., 2015. Protistan skeletons: a geologic history of evolution and constraint. In *Evolution of Lightweight Structures* (pp. 1-16). Springer, Dordrecht.

Lagadeuc, Y., Bouté, M. and Dodson, J.J., 1997. Effect of vertical mixing on the vertical distribution of copepods in coastal waters. *Journal of Plankton Research*, *19*(9), pp.1183-1204.

Matsumoto, G.I. and Harbison, G.R., 1993. *In situ* observations of foraging, feeding, and escape behavior in three orders of oceanic ctenophores: Lobata, Cestida, and Beroida. *Marine Biology*, 117(2), pp.279-287.

Ohman, M.D., 2019. A sea of tentacles: optically discernible traits resolved from planktonic organisms *in situ*. *ICES Journal of Marine Science*. DOI 10.1093/icesjms/fsz184

Ohman, M.D., 1990. The demographic benefits of diel vertical migration by zooplankton. *Ecological Monographs*, 60(3), pp.257-281.

Ohman, M.D., 1988. Behavioral responses of zooplankton to predation. *Bulletin of Marine Science*, *43*(3), pp.530-550.

Ohman, M.D., Davis, R.E., Sherman, J.T., Grindley, K.R., Whitmore, B.M., Nickels, C.F. and Ellen, J.S., 2018. *Zooglider*: An autonomous vehicle for optical and acoustic sensing of zooplankton. *Limnology and Oceanography: Methods*, 17(1), pp.69-86.

Ohman, M.D. and Romagnan, J.B., 2016. Nonlinear effects of body size and optical attenuation on Diel Vertical Migration by zooplankton. *Limnology and Oceanography*, *61*(2), pp.765-770.

Ohman, M.D., Frost, B.W. and Cohen, E.B., 1983. Reverse diel vertical migration: an escape from invertebrate predators. *Science*, *220*(4604), pp.1404-1407.

Paffenhöfer, G.A., 2006. Oxygen consumption in relation to motion of marine planktonic copepods. *Marine Ecology Progress Series*, 317, pp.187-192.

Purcell, J.E., 1997. Pelagic cnidarians and ctenophores as predators: selective predation, feeding rates, and effects on prey populations. In *Annales de l'Institut océanographique* (No. 2).

Purcell, J.E., 1980. Influence of siphonophore behavior upon their natural diets: evidence for aggressive mimicry. *Science*, 209(4460), pp.1045-1047.

Saito, H. and Kiørboe, T., 2001. Feeding rates in the chaetognath *Sagitta elegans*: effects of prey size, prey swimming behaviour and small-scale turbulence. *Journal of Plankton Research*, 23(12), pp.1385-1398.

Schuyler, Q. and Sullivan, B.K., 1997. Light responses and diel migration of the scyphomedusa *Chrysaora quinquecirrha* in mesocosms. *Journal of Plankton Research*, *19*(10), pp.1417-1428.

Sheng, J., Malkiel, E. and Katz, J., 2003. Single beam two-views holographic particle image velocimetry. *Applied Optics*, 42(2), pp.235-250.

Sherman, J., Davis, R.E., Owens, W.B. and Valdes, J., 2001. The autonomous underwater glider "Spray". *IEEE Journal of Oceanic Engineering*, 26(4), pp.437-446.

Suchman, C.L. and Sullivan, B.K., 2000. Effect of prey size on vulnerability of copepods to predation by the scyphomedusae *Aurelia aurita* and *Cyanea* sp. *Journal of Plankton Research*, 22(12), pp.2289-2306.

Suchman, C.L., 2000. Escape behavior of *Acartia hudsonica* copepods during interactions with scyphomedusae. *Journal of Plankton Research*, 22(12), pp.2307-2323.

Sullivan, B.K., 1980. In situ feeding behavior of *Sagitta elegans* and *Eukrohnia hamata* (Chaetognatha) in relation to the vertical distribution and abundance of prey at Ocean Station “P”. *Limnology and Oceanography*, *25*(2), pp.317-326.

Sundby, S. and Fossum, P., 1990. Feeding conditions of Arcto-Norwegian cod larvae compared with the Rothschild–Osborn theory on small-scale turbulence and plankton contact rates. *Journal of Plankton Research*, *12*(6), pp.1153-1162.

Swanberg, N., 1974. The feeding behavior of *Beroe ovata*. *Marine Biology*, 24(1), pp.69-76.

Toda, R., Moteki, M., Ono, A., Horimoto, N., Tanaka, Y. and Ishimaru, T., 2010. Structure of the pelagic cnidarian community in Lützow–Holm Bay in the Indian sector of the Southern Ocean. *Polar Science*, 4(2), pp.387-404.

Visser, A.W., 2007. Motility of zooplankton: fitness, foraging and predation. *Journal of Plankton Research*, 29(5), pp.447-461.

Waggett, R. and Costello, J.H., 1999. Capture mechanisms used by the lobate ctenophore, *Mnemiopsis leidyi*, preying on the copepod *Acartia tonsa*. *Journal of Plankton Research*, 21(11), pp.2037-2052.

Whitmore, B.M., Nickels, C.F. and Ohman, M.D., 2019. A comparison between *Zooglider* and shipboard net and acoustic mesozooplankton sensing systems. *Journal of Plankton Research.* DOI 10.1093/plankt/fbz033

Wiebe, P.H., Morton, A.W., Bradley, A.M., Backus, R.H., Craddock, J.E., Barber, V., Cowles, T.J. and Flierl, G.D.1., 1985. New development in the MOCNESS, an apparatus for sampling zooplankton and micronekton. *Marine Biology*, 87(3), pp.313-323.

Wiebe, P.H. and Benfield, M.C., 2003. From the Hensen net toward four-dimensional biological oceanography. *Progress in Oceanography*, 56(1), pp.7-136.

Williamson, C.E. and Stoeckel, M.E., 1990. Estimating predation risk in zooplankton communities: the importance of vertical overlap. *Hydrobiologia*, 198(1), pp.125-131.

Wirtz, K.W., 2012. Who is eating whom? Morphology and feeding type determine the size relation between planktonic predators and their ideal prey. *Marine Ecology Progress Series*, 445, pp.1-12.

Yamaguchi, A., Ikeda, T. and Hirakawa, K., 1999. Diel vertical migration, population structure and life cycle of the copepod *Scolecithricella minor* (Calanoida: Scolecitrichidae) in Toyama Bay, southern Japan Sea. *Plankton Biology and Ecology*, 46(1), pp.54-61.

CHAPTER 5: Conclusion

Questions pertaining to zooplankton ecology cover a broad range of scales. For questions focusing on zooplankton trophic interactions, and specifically the conditions leading to predator-prey encounters, it is necessary to observe zooplankton at scales much less than 1 m. Current zooplankton sampling methods (i.e., acoustic backscatter systems, physical collection, and optical imaging), do not have the resolution or sampling endurance necessary to address zooplankton predator-prey interactions. However, *Zooglider*, a novel acoustic and optical zooplankton-sensing glider, is an exception to these sampling systems.

In this dissertation, I show that *Zooglider* is uniquely capable of studying zooplankton predator-prey interactions at the scales at which interactions occur. First, I validate *Zooglider* against conventional shipboard zooplankton observing systems (vertically stratified nets and acoustics). This comparison addresses the following questions. Do *Zooglider* optics (Zoocam) resolve abundances, vertical distributions, and size-distributions of zooplankton similar to that of conventional net-collection systems? Do *Zooglider* acoustics (Zonar) match ship-based acoustic measurements with respect to magnitude and vertical distributions? Then, after instrument validation, *Zooglider* was deployed seven times from July 2017 to October 2018. These deployments served to address both lower and higher-level zooplankton trophic interactions. Specifically, I address whether predominantly herbivorous/omnivorous zooplankton, (i.e., appendicularia, copepods, and large mineralized protists) overlap to a greater extent with a specific prey source (either chlorophyll-*a* fluorescence, marine snow, or small particles)? Does water column stability have a positive effect on zooplankton and/or prey abundances? Third, Zoocam images allowed for the influence of body size on predator-prey interactions to be examined. Are there size-dependent vertical distributions of zooplankton? Are there size-

dependent DVM behaviors in zooplankton? Does size influence the probability of predator-prey encounter?

In March 2017, *Zooglider's* Zoocam and Zonar systems were compared to samples from a vertically-stratified net collection system (MOCNESS) and ship-mounted Simrad EK80, respectively. *Zooglider* was in close proximity (< 3.3 km) from shipboard operations (on R/V *Sally Ride*) during all sampling events. Vertical profiles of physical (potential density) and biological (chlorophyll-*a* fluorescence) variables measured by both ship- and *Zooglider*-based systems suggest that each instrument sampled similar water parcels. Both Zoocam and MOCNESS observed similar abundances, size distributions, and vertical distributions of chaetognaths, euphausiids, and nauplii. However, Zoocam observed greater vertically integrated abundances of smaller-sized copepods and appendicularians, compared to the MOCNESS. This size discrepancy was primarily attributed to the smaller organisms being extruded through the net mesh. Additionally, greater abundances of larger-sized gelatinous predators and mineralized protists (foraminifera, phaeodaria, and predominately acantharia) were observed by Zoocam. The MOCNESS most likely underestimated these larger, more delicate, zooplankton due to damage induced by net collection or preservations effects resulting in the shrinkage or dissolution of the organism. The ~5 cm vertical resolution of Zoocam revealed high local concentrations of copepods (53,000 organisms m^{-3}) and appendicularians (29,000 organisms m^{-3}) which the MOCNESS did not observe at its coarser vertical resolution (~20 m). Zonar and EK80 agreed in the relative magnitude and vertical distribution of backscatter at 200 kHz, the common frequency of both systems. However, the EK80 only has an effective depth-sampling limit of 200 m, due to a decline in signal-to-noise ratio in deeper depths, whereas the glider-

mounted Zonar allows for effective sampling from the surface to 400 m. Thus, *Zooglider* is comparable to ship-based systems in some respects, but has several distinct sampling advantages.

Zooglider conducted sampling on a 2-3-month interval from July 2017 to October 2018. The goal of these deployments was to observe how lower-level zooplankton trophic interactions varied in different water-column stability conditions. *Zooglider* measured three plausible prey sources for herbivorous/omnivorous zooplankton: chlorophyll-*a* fluorescence (Chl-*a*), marine snow (equivalent circular diameter, ECD > 0.45 mm), and small particles (ECD = 0.25-0.45 mm). The zooplankton examined during this study were appendicularia (*Fritillaria* spp.), appendicularia (other spp.), large protists (i.e., collodaria, foraminifera, Phaeodarea, and mostly acantharia), small copepods (feret diameter, FD ≤ 3 mm), and large copepods (FD > 3 mm). Water column stability was shown to have no significant relationship with zooplankton or prey abundances. I found that, at depths shallower than the Chl-*a* fluorescence maximum, Chl-*a* does not correspond well with marine snow or small particles, whereas there were strong correlations between prey variables below the fluorescence maximum. Similar depth-dependent relationships were observed between Chl-*a* and the abundances of each zooplankton taxon. Specifically, a single Chl-*a* measurement often corresponded with two different concentrations of zooplankton, marine snow, or small particles. In contrast, an index of spatial overlap (Length of the Receiver Operating Characteristic) LROC identified small particles and marine snow to have greater overlap with zooplankton than Chl-*a*, in most cases. GAMs (Generalized Additive Models) revealed that the primary explanatory variable for all zooplankton taxon abundances was either marine snow (*Fritillaria*, appendicularia-others, large protists, and large copepods) or small particles (small copepods). Chl-*a* was either a secondary (small copepods, *Fritillaria*, and both day and night abundances of larger copepods) or an insignificant (large protists and

appendicularia-others) variable in explaining organismal abundances. These results strongly suggest that Chl-*a* alone does not adequately represent the utilized prey field of herbivorous/omnivorous zooplankton and that *in situ* particle distributions have more explanatory power for herbivorous and omnivorous zooplankton than previously thought.

Zooglider also enables the study of higher (carnivorous) planktonic trophic interactions. The Zoocam images enable *in situ* measurements of individual zooplankton sizes, abundances, and carnivorous zooplankton predator-prey encounters. Here, I define a predator-prey encounter as a predatory zooplankton and 'x' prey items cooccurring within a single image (sample volume 250 mL). I categorized prey taxa as *Fritillaria*, appendicularia-others, and copepods, and predatory taxa as chaetognaths, ctenophores, narcomedusae, siphonophores, and trachymedusae. Significant size-dependent vertical distributions were observed for all three prey taxa and five predatory taxa, with the larger animals having deeper weighted mean depths. Additionally, differential size-dependent diel vertical migration (DVM) was observed in copepods and chaetognaths, with only the largest chaetognaths (FD > 16 mm) and smaller copepods (FD ≤ 9 mm) performing DVM.

Spearman rank correlations revealed that the strongest relationships were observed between small predator (chaetognaths, ctenophores, siphonophores, and trachymedusae) and small prey abundances. In contrast, large predators (chaetognaths, ctenophores, siphonophores, and trachymedusae) and all size classes of narcomedusae had more constant intermediate relationships with prey of all sizes, thereby indicating a more size-independent prey field. These ideas of size preferences in predatory taxa were further strengthened by observed probabilities of encounter. Small predators more often encountered smaller prey, compared to larger prey.

Moreover, encounters with multiple small copepods (FD ≤ 3 mm) were more common than encounters with singular medium copepods (FD = 3-9 mm).

In sum, *Zooglider* detects some zooplankton taxa (chaetognaths, euphausiids, nauplii) similar to conventional systems. However, *Zooglider* exceeds the observational capabilities of conventional methods with regards to measurement of heightened local abundances and sampling both small-sized and delicate organisms. *Zooglider* identified that particle distributions have greater overlap and explanatory power (than Chl-*a*) with herbivorous/omnivorous zooplankton abundance distributions. *Zooglider* also revealed the importance of zooplankton body size in predator-prey interactions. These *Zooglider* findings illustrate the need for observed particle distributions and *in situ* sizing of zooplankton to be incorporated more explicitly into the study of zooplankton trophic interactions. Looking forward, it is now possible to address the impacts of storms, bottom topography, and fronts on zooplankton trophic interactions in a way that was previously not possible without the endurance, autonomy, and resolution capabilities of *Zooglider*.